A Steady-State and Hydroelastic Analysis of Towed Line Arrays for ASW Target Applications

APL-UW 8212
February 1983

Contract No. N00024-81-C-6042

A Steady-State and Hydroelastic Analysis of Towed Line Arrays for ASW Target Applications

by D. E. Calkins

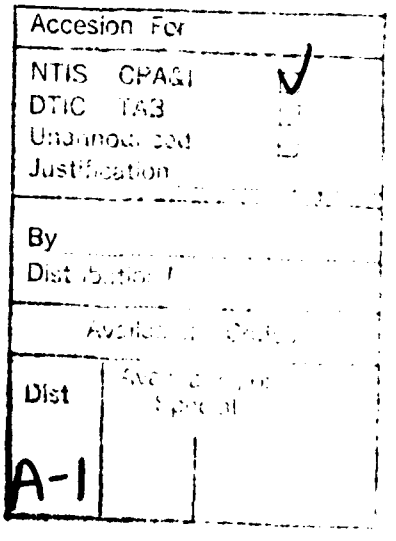

APL-UW 8212
February 1983

Applied Physics Laboratory
University of Washington
Seattle, WA. 98105

UNCLASSIFIED

SECURITY CLASSIFICATION OF THIS PAGE (When Data Entered)

REPORT DOCUMENTATION PAGE

READ INSTRUCTIONS BEFORE COMPLETING FORM

1 REPORT NUMBER	2 GOVT ACCESSION NO. / 3 RECIPIENT'S CATALOG NUMBER
4 TITLE (and Subtitle)	5 TYPE OF REPORT & PERIOD COVERED
A STEADY-STATE AND HYDROELASTIC ANALYSIS OF TOWED LINE ARRAYS FOR ASW TARGET APPLICATIONS	Technical Report
	6 PERFORMING ORG. REPORT NUMBER: APL-UW 8212
7 AUTHOR(s): D.E. Calkins	8 CONTRACT OR GRANT NUMBER(s): N00024-81-C-6042
9 PERFORMING ORGANIZATION NAME AND ADDRESS: Applied Physics Laboratory, University of Washington, 1013 N.E. 40th St., Seattle, WA 98105	10 PROGRAM ELEMENT, PROJECT, TASK AREA & WORK UNIT NUMBERS
11 CONTROLLING OFFICE NAME AND ADDRESS: Naval Sea Systems Command, Department of the Navy, Washington, D.C. 20362	12 REPORT DATE: February 1983 / 13 NUMBER OF PAGES: 174
14 MONITORING AGENCY NAME & ADDRESS (if different from Controlling Office)	15 SECURITY CLASS. (of this report): Unclassified / 15a DECLASSIFICATION DOWNGRADING SCHEDULE

16 DISTRIBUTION STATEMENT (of this Report)

Distribution unlimited

17 DISTRIBUTION STATEMENT (of the abstract entered in Block 20, if different from Report)

18 SUPPLEMENTARY NOTES

19 KEY WORDS (Continue on reverse side if necessary and identify by block number)

towed array hydrodynamics

towed array hydroelasticity

mobile targets

20 ABSTRACT (Continue on reverse side if necessary and identify by block number)

The three-dimensional static and dynamic configurations of towed line arrays such as those used for mobile targets are of extreme importance. It has been found through towing tank tests of a 200-ft array that it assumes a statically deformed shape over its entire length. In addition, under certain conditions dynamic oscillations of the drogue

(cont.)

DD FORM 1 JAN 73 1473 EDITION OF 1 NOV 65 IS OBSOLETE
S/N 0102 LF 014 6601

UNCLASSIFIED

SECURITY CLASSIFICATION OF THIS PAGE (When Data Entered)

20, cont.

end occur. This is in contrast to the design requirement of overall neutral buoyancy, which would result in an essentially straight array under tow.

Three mathematical and numerical computer models have been developed to study and analyze this behavior. These include (1) a three-dimensional steady state model that is sensitive to array weight and/or buoyancy distribution, (2) a two-dimensional (horizontal plane) hydroelastic model that will predict static and dynamic configuration instabilities, and (3) a two-dimensional (horizontal or vertical plane) dynamic response model that will predict response to tow-vehicle maneuvers.

The three computer models have been used to study the characteristics of the 200-ft array tested in the towing tank. It was found that the "as built" nonuniform weight distribution, in conjunction with the uniform buoyancy distribution due to the constant diameter array, results in static deflections. These deflections may in turn initiate hydrostatic instabilities. Dynamic instabilities were found to be confined to the drogue end of the array, where the tension is at a minimum.

TABLE OF CONTENTS

TABLE OF CONTENTS, cont.

LIST OF FIGURES

LIST OF FIGURES, cont.

LIST OF FIGURES, cont.

LIST OF TABLES

NOMENCLATURE

A	strength member area
AR	fin aspect ratio
b	fin span
c	fin chord
C_{D_B}	array base drag coefficient based on upstream body drag
C_{D_o}	drag coefficient of cone drogue
C_{D_o}	drogue body drag coefficient as a function of fineness ratio l/D_b
C_f	array tangential drag coefficient ($\phi = 90°$)
C_f	flat plate friction coefficient
C_n	normal drag coefficient ($\phi = 0°$)
C_{y_b}	fin lift curve slope per degree
d	diameter of blunt base drogue
d	diameter of rope drogue
d_b	diameter of base, fin-stabilized drogue
d_c	diameter of base, cone drogue
ds	array element of unit length
D	array diameter
D_{fore}	nose-piece plus array drag
E	modulus of elasticity
EI	flexural rigidity (array)
F_a	array added mass force/unit length
F_b	array buoyancy/unit length
F_d	drogue end force

F_{d_1}	array base drag
F_{d_2}	cone drogue drag
F_{d_3}	rope drogue drag
F_{d_4}	finned drogue drag
F_i	array inertial force acting on an element of unit length
F_D	array drag/unit length
F_n	array normal forces/unit length at angle ϕ
$F_n(\phi)$	normal loading function
F_L	array lift/unit length
F_s	array side force/unit length
F_t	array tangential forces/unit length at angle ϕ
$F_t(\phi)$	tangential loading function
F_w	weight force acting on element of unit length
k	added mass coefficient (1 for a circular cylinder)
ℓ_1	nose cone length
ℓ_2	drogue length
L	array length
L_{D_4}	tail fin lift (side) force
m	inertial mass/unit length
m_a	hydrodynamic added mass force/unit length
M	virtual array mass/unit length
M	internal bending moment
M_f	added mass of fins
n	number of fins; number of variables
q	dynamic pressure
Q	internal shear force

$\bar{r}$	radius vector to a point P on array
R	turn radius
R_c	Reynolds number based on chord
R_d	Reynolds number based on diameter
R_n	array normal force (ϕ = 90°)
R_t	array tangential force (ϕ = 0°)
s	arc length along array
S	array cross-sectional area
S_B	base area
S_f	fin area
t	time
t/c	fin thickness/chord ratio
T, T(s)	array tension along length
u	dimensionless speed
U	flow velocity (linear)
U	array (system) speed
$U,\bar{U}$	array velocity
y	linear displacement
$\ddot{y}$	linear acceleration
X,Y,Z	stability coordinate system
X_s,Y_s,Z_s	tow velocity coordinate system
X_t,Y_t,Z_t	array coordinate system
α	half-vertex angle of cone drogue
α	ratio of drogue length to nose-cone length
β	dimensionless mass (Paidoussis)

β	relative flow angle, deg
λ	tow-rope-to-length ratio, S/L
$\delta\xi$	array element of unit length
ε	length/diameter ratio
η	dimensionless length (Paidoussis)
η	array kite angle
θ	"float" angle of array
λ_1	ratio of nose length to array length
λ_2	ratio of drogue length to array length
ρ	fluid density
ψ	towline angle relative to flow
τ	dimensionless time (Paidoussis)
$\dot{\psi}$	turn rate
ω	dimensionless eigenfrequency (complex)
$\overline{\omega}$	angular rate vector
Ω	circular frequency (complex), rad/s

1. INTRODUCTION

Artificial, underwater, mobile targets provide a cost effective and highly efficient means of simulating various characteristics of submarines for training U.S. Navy forces and for testing and evaluating underwater weapon and sensor systems. Such targets are utilized in many types of scenarios in a variety of ocean environments. As threat characteristics change and weapon and sensor capabilities improve, the capabilities of these targets must be expanded to keep pace.

The current state of the art in target technology uses towed line arrays containing multiple acoustic transducers to simulate the physical extent of a submarine and its characteristic point echoes. One such system, the Mobile Acoustic Spatial Target (MAST), is currently in use in the Fleet, while others are in the design stage. These arrays are several hundred feet long and include numerous omnidirectional acoustic transducers distributed over their entire length. The MAST, for example, comprises a self-propelled tow-vehicle and a 200 ft acoustic array. The system's configuration is shown in Fig. 1.1. It features three groups of spatial highlights, each highlight being controlled independently by an individual echo-repeat signal processor; two transducers are associated with each highlight group. The tow-vehicle can be programmed to simulate desired submarine maneuvers. Originally developed by the Naval Underwater Systems Center (NUSC), Newport, the MAST has been used for in-water tests of the terminal homing concepts of the Advanced Guidance System developed by the Applied Research Laboratory at Pennsylvania State University.

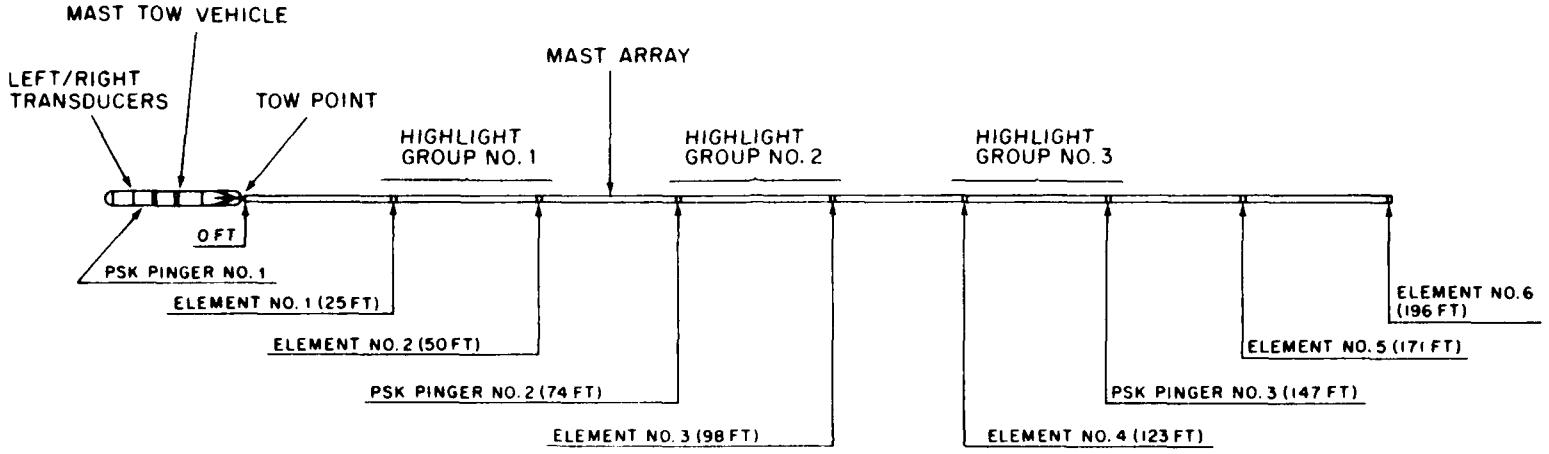

TOW-VEHICLE		ARRAY	
WEIGHT	2380 LB	WEIGHT	445 LB
DIAMETER	19 INCHES	DIAMETER	2.5 INCHES
BUOYANCY	45 LB POSITIVE	BUOYANCY	3-12 LB POSITIVE
LENGTH	22 FEET	LENGTH	200 FEET

Figure 1.1. Mobile Acoustic Spatial Target (MAST) system configuration.

It is expected that in the future torpedo evaluations will be carried out in more complex test environments characterized by the presence of countermeasure devices in shallow water where boundary conditions significantly affect performance, and with the use of more than one torpedo (salvo firings). These conditions will restrict the use of existing artificial targets such as the MAST because (1) the omnidirectional acoustic patterns now used differ greatly from those of a real submarine and (2) the presence of countermeasures can interfere with the ability of a target with omnidirectional receive patterns to recognize the weapon signal, and thus respond.

Real submarines respond to active interrogations with distinctly distributed echoes that are aspect dependent; i.e., when a submarine is ensonified by an acoustic pulse, it reflects or absorbs and reradiates this energy in various directions in a characteristic pattern that depends on the angle at which it is ensonified. To simulate this "total field" scattering characteristic properly, artificial targets should be capable of telling the direction from which a signal is received and thus transmitting a response with the acoustic characteristics that would be emitted by a real target when ensonified at that angle. Such a directional capability must exist for both vertical and azimuthal planes.

In view of these complex requirements, it becomes apparent that to utilize directional receive and transmit acoustic patterns, it is necessary to maintain a stable geometric orientation of the array. As part of the Targets Technology Exploratory Development Block Program, the Applied Physics Laboratory undertook to identify operational problems that might impact the development of artificial targets

capable of simulating total field scattering characteristics.

It was concluded that knowledge of towed target array system dynamics was generally lacking, and that potential hydroelastic instabilities in the arrays existed. There are indications that the array hydroelastic stability may be inadequate to support directional transducers for the following reasons:

(1) There is no provision for quantifying and controlling the roll orientation of the arrays.

(2) Even when configured in flexible tubes, multi-element arrays have not yet been developed that are stable in the pitch and yaw planes. In fact, speed-dependent standing and oscillating waves have been observed in a MAST array being towed past a viewing station in the David Taylor Naval Ship Research and Development Center (DTNSRDC) towing tank.

New technology was therefore necessary in order to develop controlled array orientation for target operations. As a result a task was undertaken, the overall objective of which was to develop this technology through three separate computer programs capable of predicting the spatial orientation, dynamic response, and hydroelastic stability of towed target arrays.

This report presents and describes a parametric computer model of a generic towed target array. This model addresses both the static and dynamic characteristics of the array system. The MAST serves as a baseline for the studies utilizing the model.

2. PROPOSED APPROACH

2.1 Prototype/Model Relationship

The problem may be stated as follows. The motions of a prototype physical system, the towed array of the MAST, must be predicted, analyzed, understood, and perhaps modified through the modeling process.

The model development and analysis strategy is outlined in flowchart form in Fig. 2.1. A mathematical model that describes the behavior and unique conditions of the prototype system is first put in the form of a mathematical relationship among the physical variables. The most general concise characterization of a dynamic system is provided by a system of differential equations reflecting the laws governing its motion. Solution of the system equations establishes an unequivocal relationship among the parameters of the system.

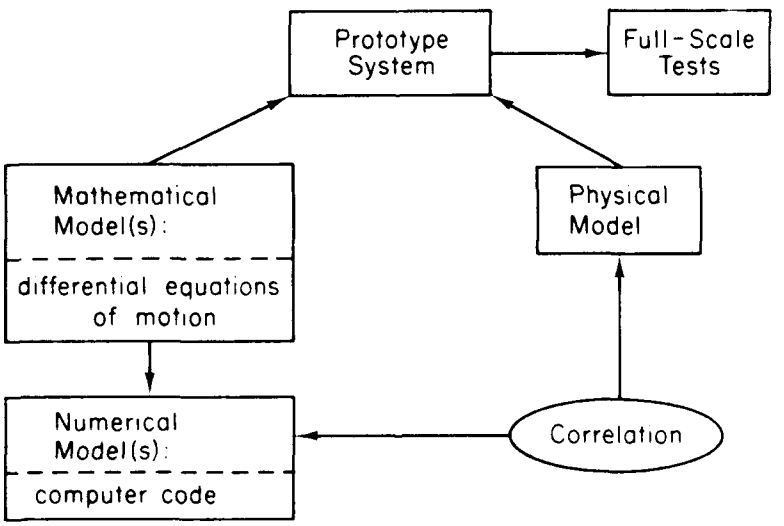

Figure 2.1. Modeling strategy.

Mathematical models of complex phenomena are seldom amenable to rigorous solution. Numerical techniques, coupled with the digital computer, must be used. Thus, the mathematical model is transformed into a numerical model that is a system of algebraic relationships based on the mathematical model. The operations prescribed by the numerical model are then programmed for solution on the computer. This model is used to evaluate the characteristics of the baseline prototype system as well as alternate configurations.

The numerical model must then be verified by correlation with a physical model, i.e., the relationship among system parameters is determined by direct measurements. A physical model of the system is thus built and tested, and the information gained used to infer the behavior of the prototype system in operation. There are so many parameters in any case that the number of combinations to be covered by the measurements is enormous. The tool used to establish the criteria for making a physical model similar to the prototype is "dimensional analysis," or the "similitude method." From these analyses, appropriate configurations are selected for physical modeling. A physical or experimental model is suitable for adjusting and measuring parameters defined by a similitude transformation of the mathematical model. The physical model then provides experimental data for quantitative evaluation and verification of the mathematical and numerical models.

2.2 Mathematical Models

The development of a general mathematical model to describe the motions of a towed array system will, in general, include consideration of the elastic, inertial, and hydrodynamic forces, as well as the tension, weight, and buoyancy forces (Fig. 2.2). This constitutes the general problem of hydroelasticity. Various combinations of these forces form distinct classes of problems. These include, as shown in Fig. 2.2,

(1) Static hydroelasticity (divergence): hydrodynamic + elastic forces

(2) Dynamic hydroelasticity (flutter): hydrodynamic + elastic + inertial forces

(3) Dynamic stability (rigid body): hydrodynamic + inertial forces.

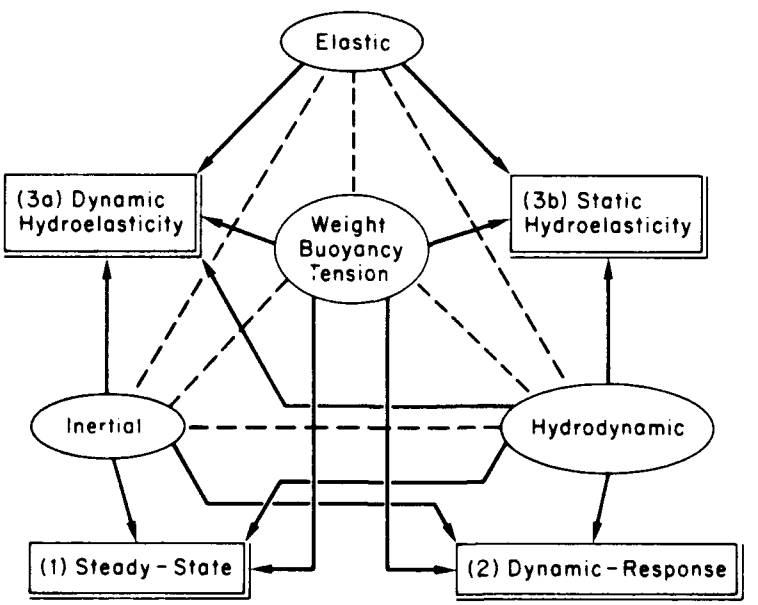

Figure 2.2. Array mathematical models.

To obtain the desired information on towed array motions, and yet avoid undue complexity, more than one mathematical model is necessary.

The arrays are configured such that the weight distribution is not constant along their length, because of the periodic placement of transducers and pingers. This, coupled with the fact that overall neutral buoyancy may not be achievable, will lead to deformed static array configurations; i.e., nonlinear, nonhorizontal configurations. These in turn may generate hydrodynamic forces that lead to hydroelastic or instability problems such as standing or oscillating waves in the array.

Clearly, these hydrodynamic instabilities, as well as the dynamic response of the array to tow-vehicle maneuvers, will impact any directionally sensitive receive and transmit characteristics of the artificial targets.

The total array configuration must then be examined as the sum of the configurations independently developed from models that address each of the three aspects. Three distinct models are necessary:

(1) A steady-state model that is sensitive to the array weight and/or buoyancy distribution

(2) A hydroelastic model that will predict static and dynamic configuration instabilities

(3) A dynamic response model that will predict array response to tow-vehicle maneuvers.

2.2.1 Steady-State Model

The purpose of the steady-state mathematical model is to compute the three-dimensional spatial configuration and tension distribution of the array either for a straight tow or a steady turn. Typically, a steady-state model would include consideration of only the tension, weight/buoyancy, and hydrodynamic forces (Fig. 2.2); however, extension to the three-dimensional steady-turn case requires inclusion of the inertial centrifugal force. The array is modeled as a nonlinear, continuous line structure in three-dimensional space (Table 2.1).

Table 2.1. Array mathematical models.

Type:	Steady-State	Hydroelastic	Dynamic Response
Modeling Technique:	Continuous line structure	Continuous line structure	Finite element
Linearity:	Nonlinear	Linear	Nonlinear
Domain:	Space	Frequency	Time
Forces considered:	Weight Buoyancy Tension Hydrodynamic Inertial	Tension Hydrodynamic Inertial Elastic	Weight Buoyancy Tension Hydrodynamic Inertial
Plane:	X,Y,Z	X,Y	X,Y or X,Z
FORTRAN Name:	ARRAY	SNAKE	FETOW

2.2.2 Hydroelastic Model

The purpose of the hydroelastic model is to determine whether the array is statically and dynamically stable, i.e., to determine the existence of oscillations that would affect its geometry.

Dynamic stability is defined as follows. A linear system initially in a state of static or dynamic equilibrium is subjected to a transient random input disturbance that sets it in motion. If the amplitudes of the motion diminish with time, we have a dynamically stable system; if the amplitudes increase with time, we have a dynamically unstable system. The same disturbance may also result in a statically deformed configuration which is known as a static instability. For the hydroelastic analysis, the array is modeled as a continuous line structure undergoing small motions (Table 2.1).

The stability characteristics of a given system can be determined from the solutions of the governing differential equations of motion by examining the roots of the characteristic (frequency) equation (i.e., the eigenvalues), which are determined in the frequency domain. This is typically done by assuming small motions, and thus linearizing the problem. Once an instability is determined, the motions will increase with time. In fact, nonlinearities present in actual systems will result in limit cycle motions.

2.2.3 Dynamic Response Model

The purpose of the dynamic response model is to examine the response of the array to tow-vehicle maneuvers such as turns or accelerations/decelerations and to study the effect of either random or deterministic motions excited in the array by the tow vehicle.

The time-dependent spatial configuration is important. If the dynamic response motions are assumed to be small, the linear equations of motion can be used to study their characteristics. However, this is typically not true of the array during maneuvers. Angular deflections will be large so that nonlinear motions result. Because of the nonlinearities, these motions are best determined in the time domain rather than the frequency domain. The finite-element technique is therefore used to model the array. Present computing limitations dictate a two-dimensional model in X,Y (constant depth) or X,Z (constant heading) planes (Table 2.1).

3. PHYSICAL MODEL DIMENSIONAL ANALYSIS

Dimensional analysis is a powerful process by which the number of physical parameters that must be considered in a physical problem can be reduced. Dimensional analysis (the similitude method) is a procedural technique whereby the system parameters that are assumed to be significant can be formed into dimensionless groups that are fewer than the number of parameters. These system groups can then be used to both nondimensionalize the mathematical model and help define the physical model in terms of the required test parameters. The technique is useful in that fewer experimental tests are needed to establish a relationship between the groups than between the variables.

Dimensional analysis is based on the following theorems:

(1) Any equation that is dimensionally homogeneous can be put in a form in which the variables enter the equations only through certain dimensionless π groups.

(2) It can be proved that any dimensionless combination is expressible as a product of the powers of the variables.

The variables q_n that enter into a problem can be expressed in terms of basic dimensions which may be chosen as mass M, length L, and time T. Thus, the required response variables can be expressed by the dimensionally homogeneous equation

$$q_1 = \phi(q_2, q_3, q_4 \cdots q_n) \quad . \tag{3.1}$$

Any π product of these variables has the form

$$\pi_{n-m} = q_1^a, q_2^b, q_3^c, q_4^d \cdots q_n \quad , \tag{3.2}$$

where π is a dimensional combination, n is the number of variables,

and m is the number of fundamental dimensions (usually length, mass, and time).

The problem of the hydroelastic motions of an array is one in which the natural frequency Ω and accelerations $\ddot{y}$ are of interest. The array length L and its diameter D describe geometrical properties; the flow velocity is U, and the flexural rigidity EI describes its elastic property.

The accelerated motions of the array will produce a hydrodynamic added mass force per unit length, m_a, where

$$m_a = k\rho S, \tag{3.3}$$

and k = added mass coefficient, which is shape-dependent (1 for circular cylinder)

ρ = fluid density

S = array cross-sectional area.

The virtual mass/unit length M is then

$$M = m + m_a \tag{3.4}$$

$$= m + \rho S$$

where m is the inertial mass/unit length.

Table 3.1 tabulates the ten parameters of interest. Because there are ten variables and three fundamental units, we will have seven π terms. If we choose L, EI, and M as the repeating variables, we obtain the following π terms:

$$\pi_1 = \Omega L^2 \sqrt{\frac{m + \rho S}{EI}} \tag{3.5}$$

$$\pi_2 = \ddot{y} \frac{(m + \rho S) L^3}{EI} \tag{3.6}$$

$$\pi_3 = \frac{y}{L} \tag{3.7}$$

Table 3.1. Array system variables.

Parameter	Symbol	Exponents M	L	T
Natural Frequency	Ω	0	0	-1
Linear Acceleration	$\ddot{y}$	0	1	-2
Linear Displacement	y	0	1	0
Linear Velocity	U	0	1	-1
Length	L	0	1	0
Diameter	D	0	1	0
Flexural Rigidity	EI	1	3	-2
Added Mass/Length	m_a	1	-1	0
Virtual Mass/Length	M	1	-1	0
Time	t	0	0	1

$$\pi_4 = UL\sqrt{\frac{m + \rho S}{EI}} \tag{3.8}$$

$$\pi_5 = \frac{D}{L} \tag{3.9}$$

$$\pi_6 = \frac{\rho S}{m + \rho S} \tag{3.10}$$

$$\pi_7 = \frac{t}{L^2}\sqrt{\frac{EI}{m + \rho S}}\,. \tag{3.11}$$

Note that for the nomenclature of Paidoussis (Ref. 1)

$$\begin{aligned}
\omega &= \pi_1 = \text{dimensionless frequency} \\
\eta &= \pi_3 = \text{dimensionless lengths} \\
u &= \pi_4 = \text{dimensionless speed} \\
\varepsilon &= 1/\pi_5 = \text{dimensionless diameter} \\
\beta &= \pi_6 = \text{dimensionless mass} \\
\tau &= \pi_7 = \text{dimensionless time.}
\end{aligned} \tag{3.12}$$

4. SURVEY OF EXISTING MATHEMATICAL AND PHYSICAL MODELS

4.1 Mathematical Models

4.1.1 Steady-State Model

A general steady-state model of a towed system was previously developed (Ref. 2). This model predicts the steady-state, three-dimensional configuration of a towed system in either a rectangular (straight ahead tow) or a cylindrical (steady turn) coordinate system (Fig. 4.1). The towline, which is modeled by six nonlinear, first-order, ordinary differential equations, is treated as continuous, inextensible, flexible, and uniform in density and geometry along its length. This model has been modified to represent a towline/line array system (Ref. 3). The line array is treated in exactly the same manner as the towline, i.e., as a continuous line structure. This model was modified to represent the target towed array system by first eliminating the tow cable and then removing the uniform density and geometry restriction. The latter modification allows representation of the actual array density distribution so that realistic array configurations can be examined. The input and output parameters are listed in Table 4.1.

4.1.2 Hydroelastic Model

The elastohydrodynamics of towed slender bodies has received extensive theoretical investigation: Paidoussis (Refs. 1 and 4-7), Yu (Ref. 8), and Pao (Refs. 9 and 10). The towed slender body is treated as a continuous beam with discrete nose and tail sections and a towrope, vibrating with infinite degrees of freedom in the lateral (X,Y) plane (Fig. 4.2). The lateral equation of motion is developed

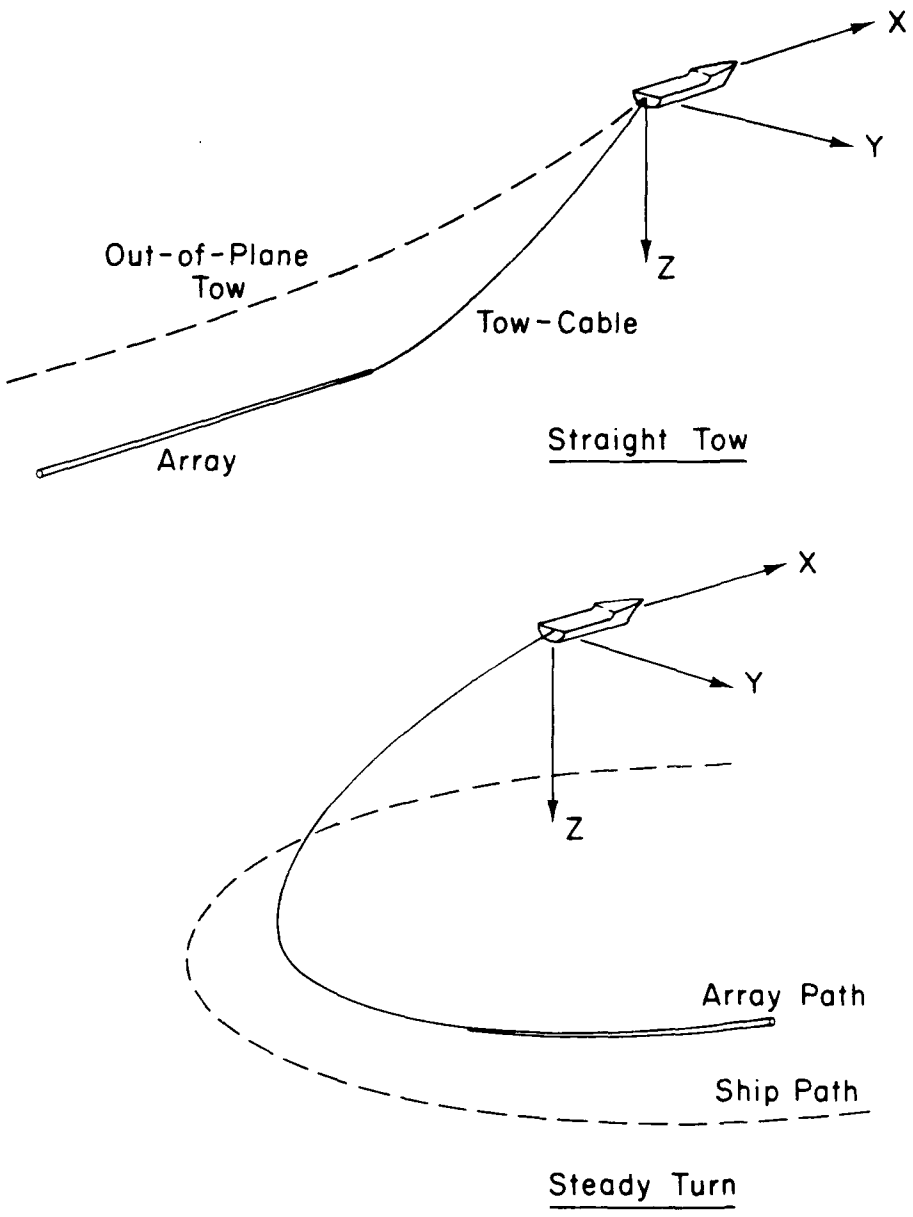

Figure 4.1. Steady-state model.

Table 4.1. Steady-state model: System input/output parameters.

Input				Output	
(1)	U	=	Speed	(1)	Array configuration in X,Y,Z plane
(2)	$\dot{\psi}$	=	Turn rate	(2)	T(s) = array tension along length
(3)	L	=	Length		
(4)	D	=	Diameter		
(5)	C_n	=	Normal drag coefficient		
(6)	C_f	=	Tangential drag coefficient		
(7)	k	=	Added mass coefficient		
(8)	F_w	=	Weight/unit length		
(9)	F_b	=	Buoyancy/unit length		
(10)	F_d	=	Drogue end forces		

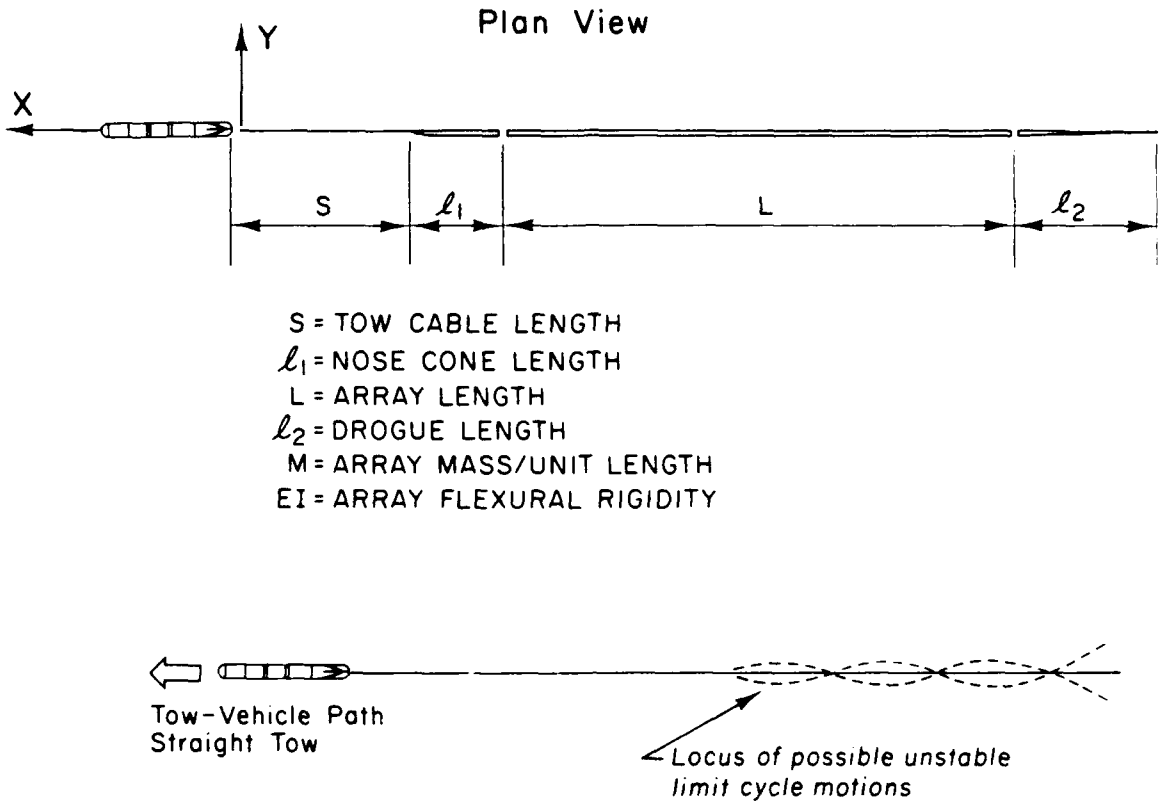

Figure 4.2. Hydroelastic model.

and solved in the frequency domain to obtain the roots of the frequency equation so that dynamic stability can be determined. The system dynamics are determined to be functions of the array's speed, its virtual mass and flexural rigidity, and the lengths of the tow rope, nose, main body, and tail sections. Studies have indicated that speed-dependent instabilities can be controlled by nose and tail section design, as well as by the towline length. It should be emphasized that unstable motions result from the geometrical and structural characteristics of the array and not from motions input to

the system at the towpoint, which is assumed to be traveling on a straight course. The input and output parameters are listed in Table 4.2.

Table 4.2. Hydroelastic model: System input/output parameters.

Input	Output
(1) U = Speed	(1) Eigenfrequencies (stability parameter)
(2) L = Length	(2) Eigenfunctions (mode shapes)
(3) D = Diameter	
(4) C_n = Normal drag coefficient	
(5) C_f = Tangential drag coefficient	
(6) k = Added mass coefficients	
(7) EI = Flexural rigidity	
(8) F_d = Drogue end forces	

4.1.3 Dynamic Response Model

The dynamic response model allows determination of the time-dependent array configurations due to tow-vehicle maneuvers such as turns and accelerations/decelerations.

A nonlinear, time domain, dynamic model of a towed system was developed by the author using the finite-element approach (Ref. 3). The towed system includes the towline and a neutrally buoyant towed array. The model could be either two- or three-dimensional and used to examine the transient and frequency response of the towed cable

system during prescribed tow-vehicle maneuvers. Each axial element was assumed to have one translational and two rotational degrees of freedom (Fig. 4.3). The finite-element approach resulted in three nonlinear, second-order, ordinary differential equations for each element used to simulate either the towline or the array. These equations were integrated using numerical techniques. The model allows for the large, geometric deformation and velocity-squared nonlinearities. The steady-state, three-dimensional continuum model of the towed system (Ref. 2) was used to provide appropriate geometric stiffness and hydrodynamic terms for the dynamic model. This allowed each physical component of the towed system to be represented by a minimum number of elements.

Patel (Ref. 11) has pursued a similar approach to represent a cable. Patel's model has since been combined by McLaughlin (Ref. 12) with a model of the tow-vehicle to provide a complete system simulation. Six elements are used to describe the array in either the X,Y or X,Z planes. Various tow-vehicle maneuvers were simulated to demonstrate the capabilities of the program. The input and output parameters are listed in Table 4.3.

An effort pursued by the Bendix Corporation (Ref. 13) is similar to that described in this report. Programs have been developed to study the steady-state deflections in the vertical plane (buoyancy induced) and the horizontal plane (maneuver induced). In addition, the dynamic characteristics, including both flow and maneuver induced, have been studied.

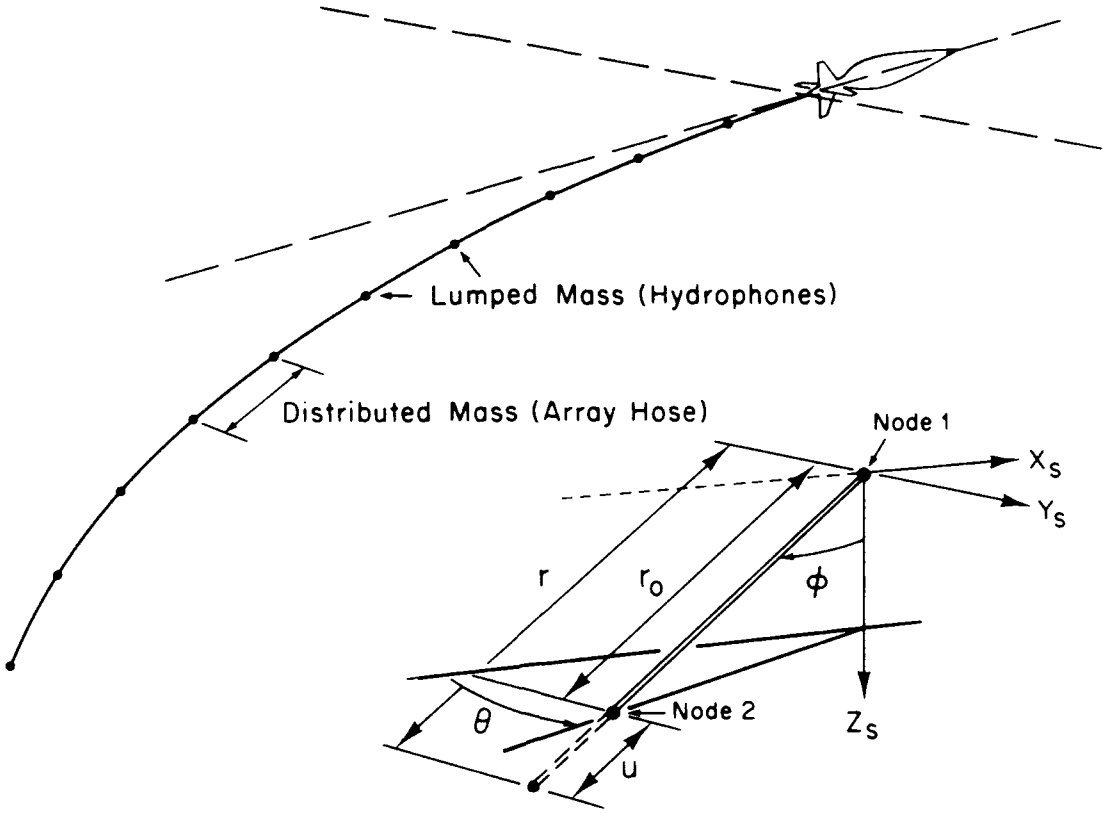

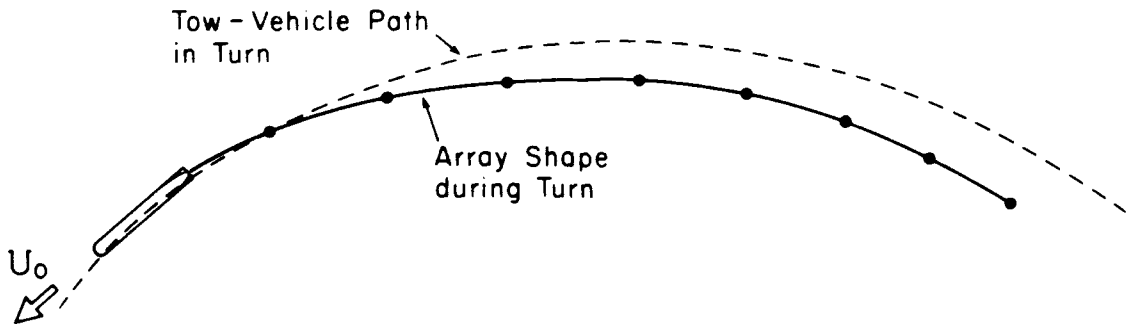

Figure 4.3. Dynamic response model.

Table 4.3. Dynamic response model: System input/output parameters.

Input				Output	
(1)	U	=	Speed	(1)	Two-dimensional, time-dependent array configuration in X,Y or X,Z plane
(2)	$\dot{\psi}$	=	Turn rate		
(3)	L	=	Length		
(4)	D	=	Diameter		
(5)	C_n	=	Normal drag coefficient		
(6)	C_f	=	Tangential drag coefficient		
(7)	F_w	=	Weight/unit length		
(8)	F_b	=	Buoyancy/unit length		
(9)	E	=	Strength member modulus		
(10)	A	=	Strength member area		
(11)	F_d	=	Drogue end forces		

4.2 Physical Model Tests

Paidoussis (Ref. 5), Pao (Ref. 9), and Hansen (Ref. 14) have conducted experimental studies of relatively small-diameter flexible tubes, which may be thought of as physical models of arrays. Table 4.4 lists the range of physical parameters; the nondimensional speed u is shown as a function of nondimensional length ε in Fig. 4.4. The range of ε is from 10 to 500. Kennedy (Ref. 15) has conducted experiments with long, small diameter (16 mm) steel cables (ε = 75,000) to study the horizontal motion of the cable in response to the random cross-track meandering of the tow-vehicle. The cable characteristics are also listed in Table 4.4 and shown in Fig. 4.4. Marine seismic arrays (Ref. 16), some 2 miles in length, are comparable (ε = 20,000 to 30,000). Tests of the MAST array were conducted in the towing tank at the David Taylor Naval Ship Research and Development Center (DTNSRDC). The full 200-ft array was towed at speeds of 5, 7.5, 10, 20, and 25 kn; a 50-ft length was towed at 10 and 20 kn.

Table 4.4. Array physical characteristics.

Reference	Length, ft	Diam, in	Speed, kn
Paidoussis (5)	1.28	0.653	11.7
Pao (9)	0.5-5	0.312	7.7
Hansen (14)	26	0.625	9-13.4
MAST	200	2.5	5-25
Marine Seismic Array (16)	5000	1.95	1.2
Kennedy (15)	3940	0.63	5.9-12.6

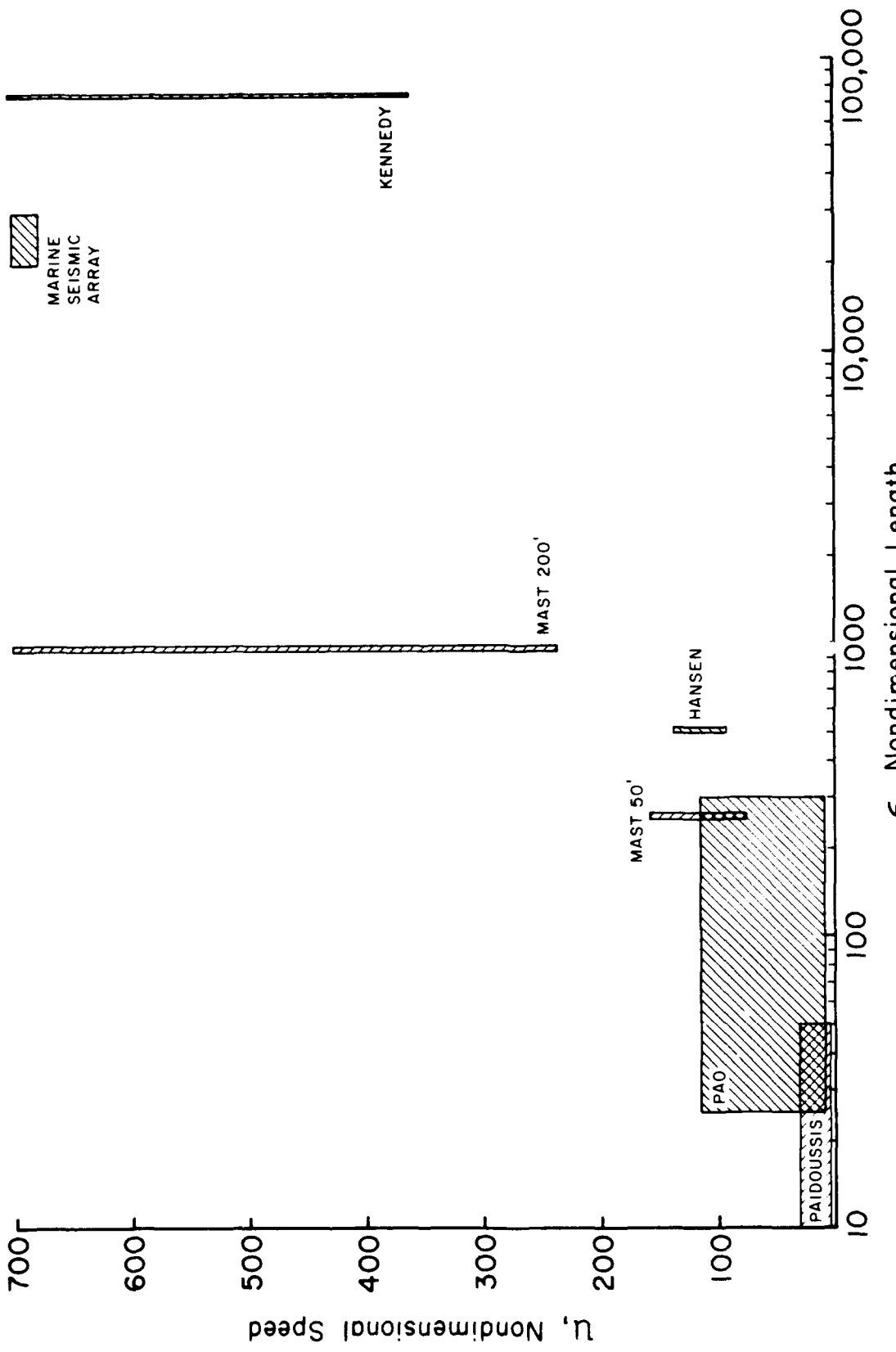

Figure 4.4. Array regimes.

5. HYDRODYNAMICS

5.1 Array

Formulations of the normal F_n and tangential F_t forces per unit length acting on a circular cylinder inclined at an angle ϕ to the flow (Fig. 5.1) have been developed by several sources. For example, Hoerner (Ref. 17) develops a formulation based on components aligned with and normal to the flow:

$$F_D = qD(C_n \sin^3\phi + \pi C_f)$$

$$F_L = qD(C_n \sin^2\phi \cos\phi) \qquad (5.1)$$

where $q = \rho U^2/2$. Now,

$$F_n = F_L \cos\phi + F_D \sin\phi$$

$$F_t = F_D \cos\phi - F_L \sin\phi\,. \qquad (5.2)$$

Substituting (5.1) into (5.2), we have

$$F_n = qD(C_n \sin^2\phi + \pi C_f \sin\phi) = \text{normal force/unit length}$$

$$F_t = qD\pi C_f \cos\phi = \text{tangential force/unit length}, \qquad (5.3)$$

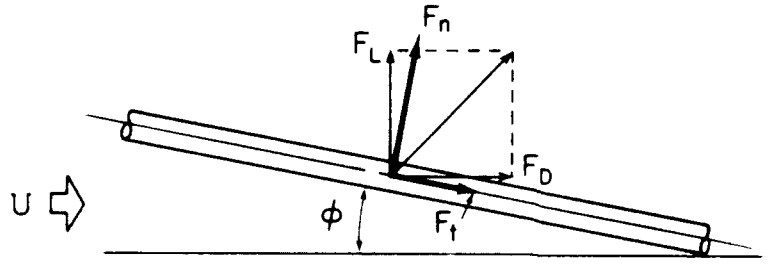

Figure 5-1. Array hydrodynamic forces.

where

C_n = normal drag coefficient ($\phi = 90°$)

C_f = tangential drag coefficient ($\phi = 0°$).

This is the same formulation that Taylor (Ref. 18) proposed for long, slender animals; it was subsequently used by Paidoussis (Ref. 4).

Ramsey (Ref. 19) has developed similar expressions for inclined circular towing cables. The formulation used is based on nondimensional "loading functions." These are defined as

$$f_n(\phi) = B_1\sin\phi + B_3\sin3\phi + B_5 + B_5\sin5\phi + B_7\sin7\phi + B_9\sin9\phi + B_{11}\sin11\phi + B_{13}\sin13\phi + B_{15}\sin15\phi + B_{17}\sin17\phi + B_{19}\sin19\phi$$

$$= \text{normal loading function,} \tag{5.4}$$

where

$B_1 = 0.8755$ $B_7 = -0.0050$ $B_{13} = 0.0017$

$B_3 = -0.1518$ $B_9 = -0.0051$ $B_{15} = 0.0029$

$B_5 = -0.0283$ $B_{11} = -0.0019$ $B_{17} = -0.0039$

$B_{19} = -0.0042,$

and

$$f_t(\phi) = A_1\cos\phi + A_3\cos3\phi + A_5\cos5\phi + A_7\cos7\phi + A_9\cos9\phi \tag{5.5}$$

$$= \text{tangential loading function,}$$

where

$A_1 = 2.2794$ $A_3 = -0.6019$ $A_5 = -0.3772$

$A_7 = -0.1722$ $A_9 = -0.1281.$

These loading functions are shown in Fig. 5.2. The normal force per unit length, as a function of ϕ, is then

$$F_n = R_n[f_n(\phi)], \tag{5.6}$$

where

$$R_n = qC_nD; \ (\phi = 90°). \tag{5.7}$$

The normal drag coefficient, C_n, is shown in Fig. 5.3 for a circular cylinder (Hoerner, Ref. 16) as a function of Reynolds number based on diameter R_d.

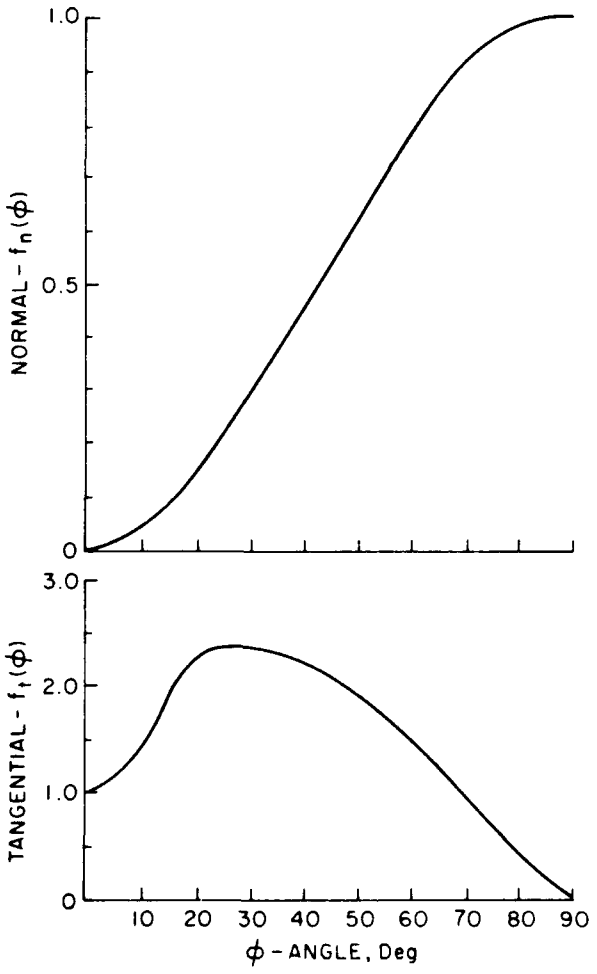

Figure 5.2
Cable loading functions.

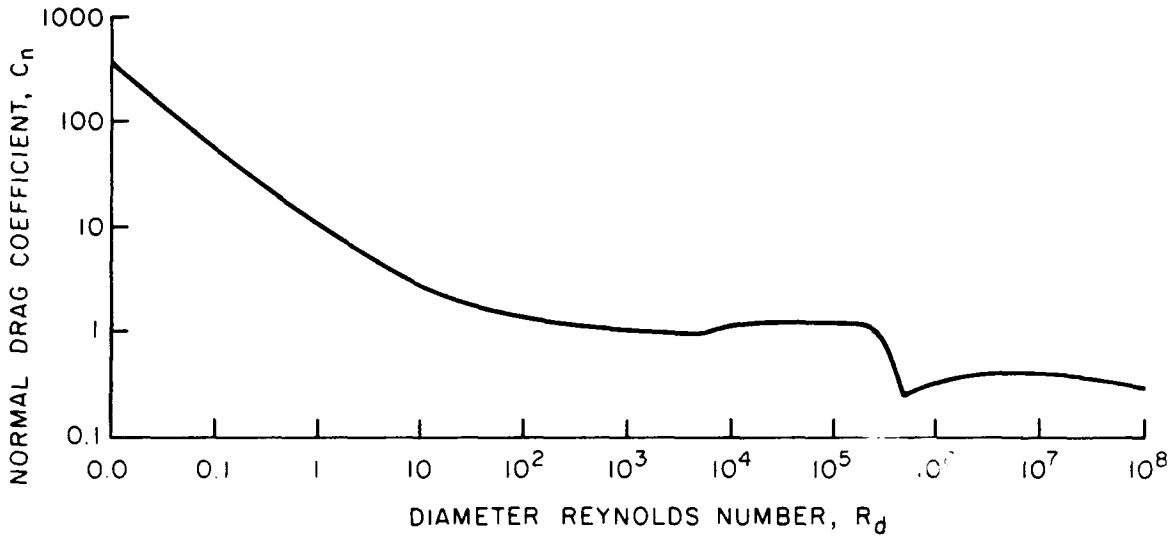

Figure 5.3. Normal drag coefficient for a circular cylinder.

The tangential force per unit length is given by

$$F_t = R_t[f_t(\phi)],$$

where

$$R_t = qC_f\pi D;(\phi = 0°). \tag{5.8}$$

Measured values of C_f, for various diameter arrays [Webster (Ref. 20) and Pao (Ref. 9)] are shown in Fig. 5.4.

For comparison with the Ramsey formulations, we note that for Hoerner

$$f_n(\phi) = \sin^2\phi + \left(\frac{\pi C_f}{C_n}\right)\sin\phi$$

$$f_t(\phi) = \cos\phi. \tag{5.9}$$

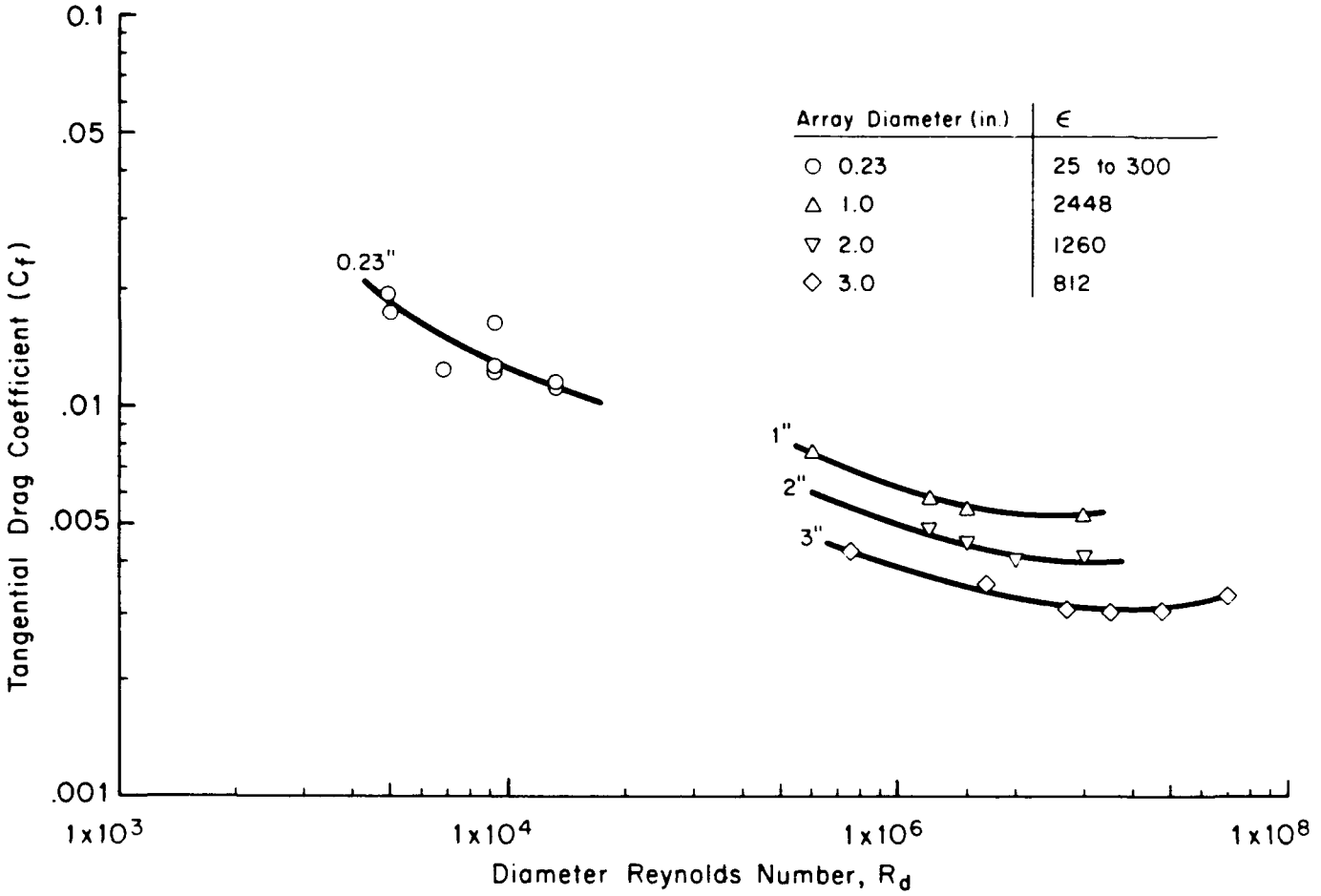

Figure 5.4. Array drag coefficient.

To accelerate a body immersed in a fluid, a certain amount of the surrounding fluid must also be accelerated. The mass of this fluid is termed the "added" (or hydrodynamic) mass. The sum of the body inertial mass and the added mass is termed the virtual mass. The hydrodynamic added mass is a function only of the shape presented to the flow in the direction of motion if the array is deeply immersed. Thus the added mass per unit length of the array is

$$m_a = k\rho S, \tag{5.10}$$

where

k = added mass coefficient = 1 for a circular cylinder

S = array cross-sectional area

$$= \pi D^2/4 \tag{5.11}$$

and

D = array diameter.

5.2 Drogue

The drogue, or array termination, may be one of three types presently in use, or one of two types proposed for future applications (Fig. 5.5). Present configurations include no drogue (i.e., a blunt base), a cone, and a length of rope. The two proposed configurations include a cylindrical body with stabilizing tail fins and a variable-drag drogue. Each of the drogues will have both viscous drag (surface friction) and base drag components.

The base drag of the array alone, configuration 1, is

$$F_{d_1} = qS_B C_{D_B} \tag{5.12}$$

where

$S_B = \pi D^2/4$ = base area

$$C_{D_B} = 0.029/\sqrt{C_{f_B}} \tag{5.13}$$

= base drag coefficient based on the upstream body (array) drag

$C_{f_B} = D_{fore}/qS$

$D_{fore} = q\pi DLC_f$

= array drag.

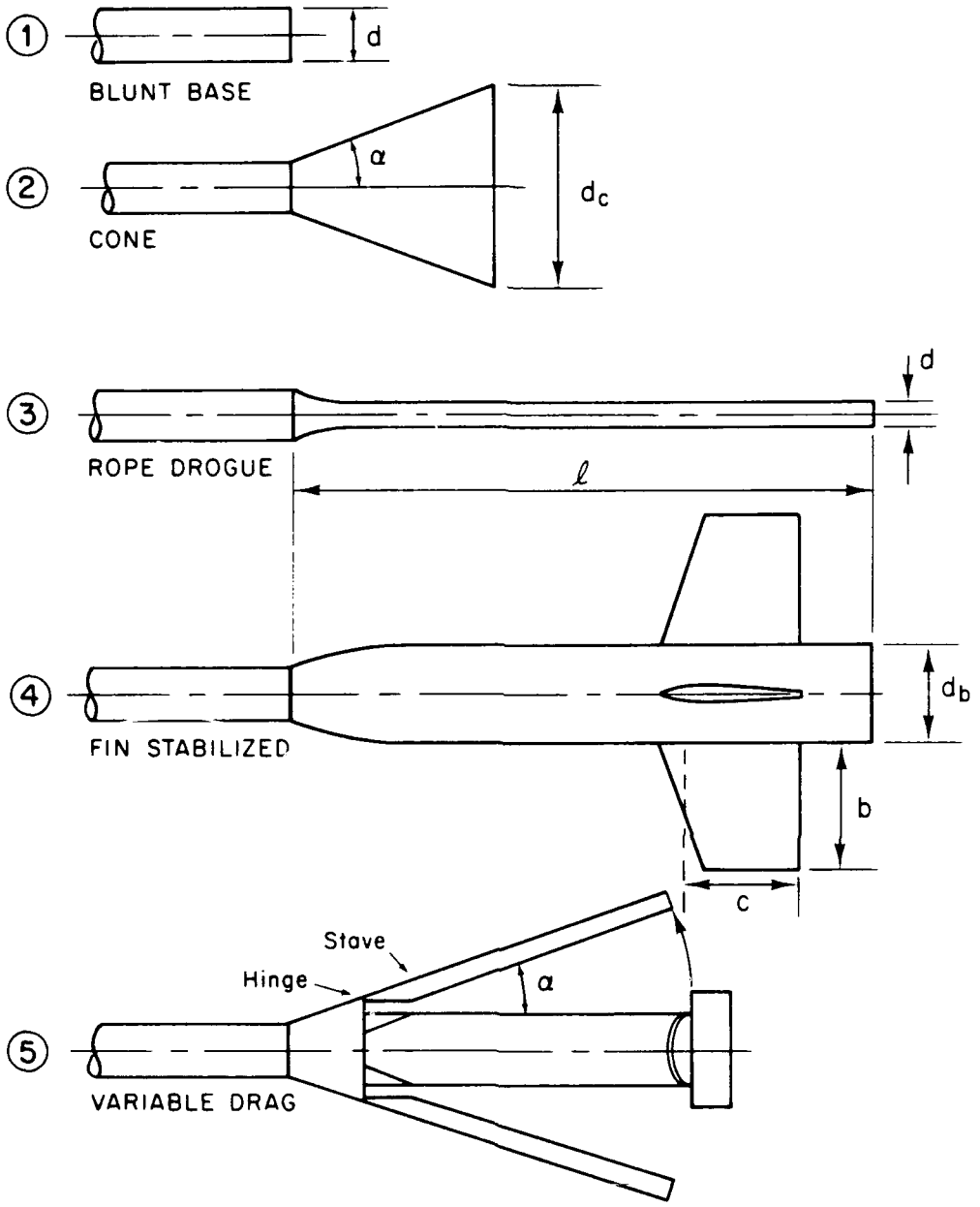

Figure 5.5. Drogue configurations.

Thus,

$$C_{f_B} = 4(L/D)C_f$$

$$= 4\varepsilon C_f$$

and

$$C_{D_B} = 0.029/\sqrt{(4\varepsilon C_f)}. \tag{5.14}$$

The drag coefficient of the cone drogue, configuration 2, is shown as a function of its half-vertex angle α in Fig. 5.6. The total drag is

$$F_{d_2} = qC_{D_o}\pi D_c^2/4, \tag{5.15}$$

where D_c = cone base diameter.

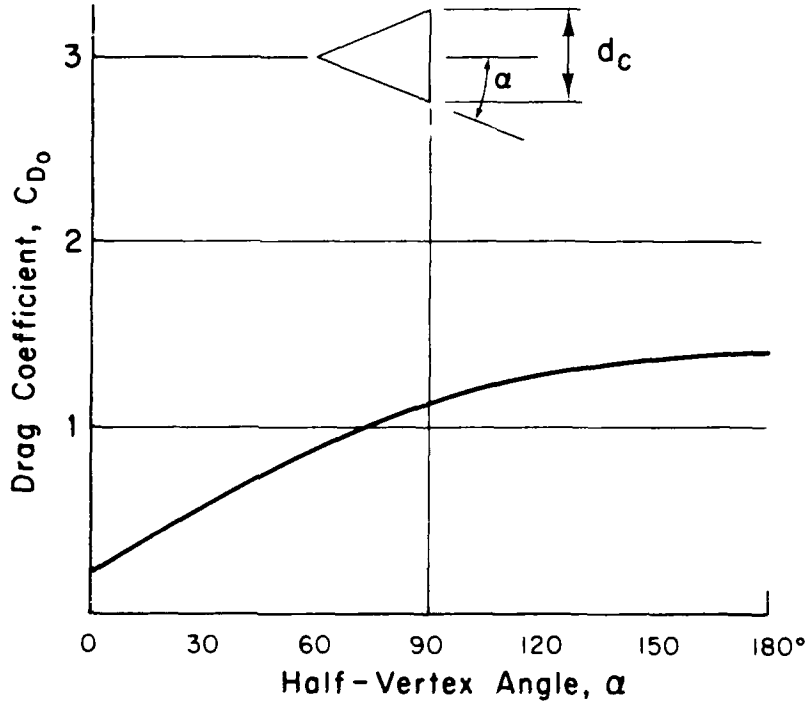

Figure 5.6. Cone drag coefficient.

The drag of a rope drogue, configuration 3, is similar to that of the array.

$$F_{d_3} = qC_f S_{wet}, \tag{5.16}$$

where S_{wet} = drogue wetted area

$= \pi D \ell$.

The drag of the finned, stabilized drogue, configuration 4, will be composed of fin and body viscous, pressure, and base drag components.

$$F_{d_4} = F_f + F_B, \tag{5.17}$$

where

$$F_f = nqC_{D_f} S_f \tag{5.18}$$

$$C_{D_f} = 2C_f\left[1 + 1.2\left(\frac{t}{c}\right) + 60\left(\frac{t}{c}\right)^4\right]$$

C_f = flat plate friction coefficient (Fig. 5.7)

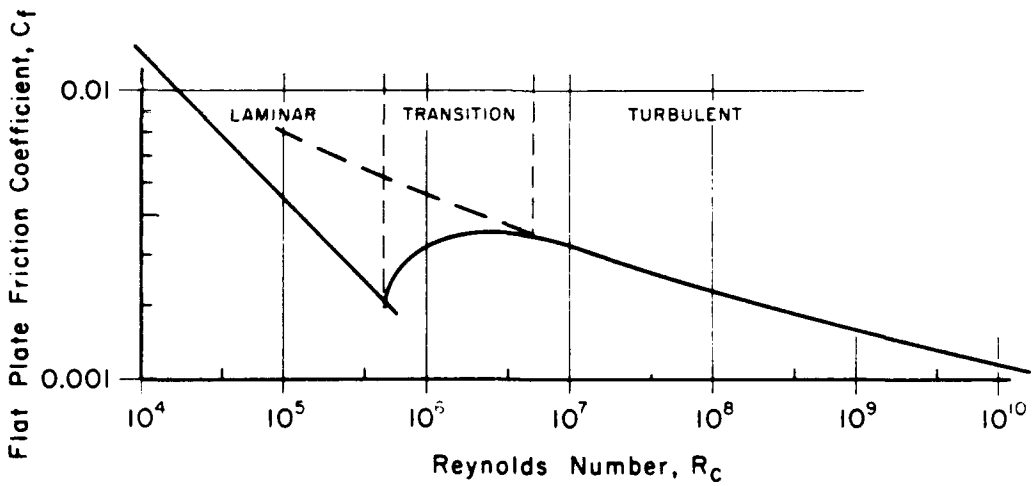

Figure 5.7. Flat plate friction coefficient.

$C_f = 1.328/\sqrt{R_c}$; laminar

$C_f = 0.44/(R_c)^{1/6}$; turbulent

$R_c = Uc/\nu$

t/c = fin thickness/chord

n = number of fins

S_f = fin area = bc

and

$$F_B = C_{D_o} q \left(\frac{\pi D^2 b}{4}\right) \tag{5.19}$$

where C_{D_o} = drogue body drag coefficient as a function of the fineness ratio, ℓD_b, in Fig. 5.8.

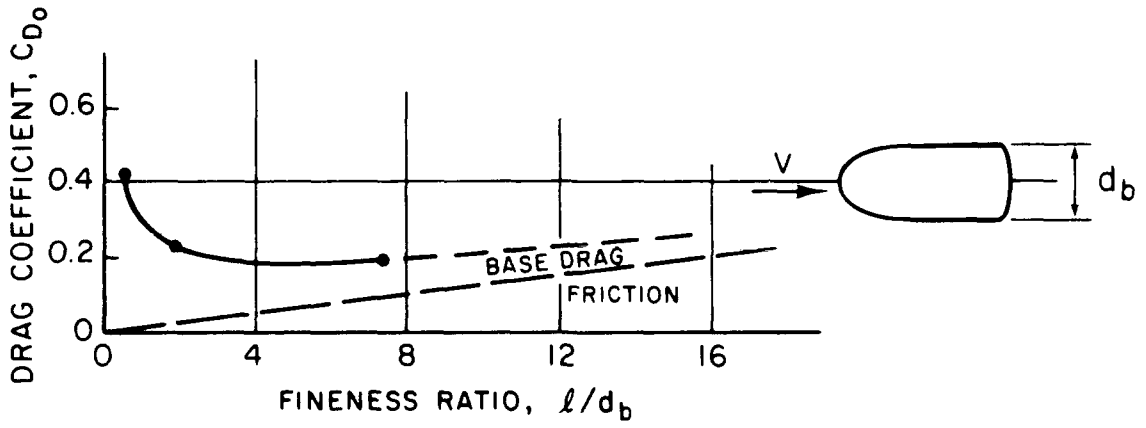

Figure 5.8. Cylindrical body drag coefficient.

The tail fins also produce a hydrodynamic lift (side) force due to the relative angle between the flow vector and the tail drogue body axis. This fin lift is

$$L_{D_4} = nC_{y_\beta} S_f q\beta, \tag{5.20}$$

where

β = relative flow angle, in degrees

C_{y_β} = fin lift curve slope per degree

= $2\pi AR/57.3(AR + 3)$

AR = fin aspect ratio = b/c

b = fin span.

The variable-drag drogue, configuration 5, can be handled by replacing it with a cone with a base area equal to the base area of the cylindrical portion plus the staves. The half-vertex angle α is thus a function of speed.

The added mass of the drogue will be that of a basic cylindrical unit, which is handled in a fashion similar to the array, and that of the fins, if used. The added mass of the fins, for accelerations normal to the fin plane, is

$$M_f = n\rho kV, \tag{5.21}$$

where

n = number of fins

k = 1

V = $(\pi c^2 b)/4$.

6. STEADY-STATE MODEL

6.1 Mathematical Model

The array is assumed to be inextensible and inelastic, with nonuniform density and geometry along its length. A mathematical model of the array capable of handling both straight-tow and steady-turn configurations requires equations of steady motion in both Cartesian and circular cylindrical coordinate systems.

6.1.1 Directional Derivatives

The first coordinate system required is a stability axis (X,Y,Z) system that is fixed in and moving with the drogue and is collinear with a second system (X_S,Y_S,Z_S) that is fixed and moving with the tow-vehicle (Fig. 6.1). For a straight tow, a principal axis system

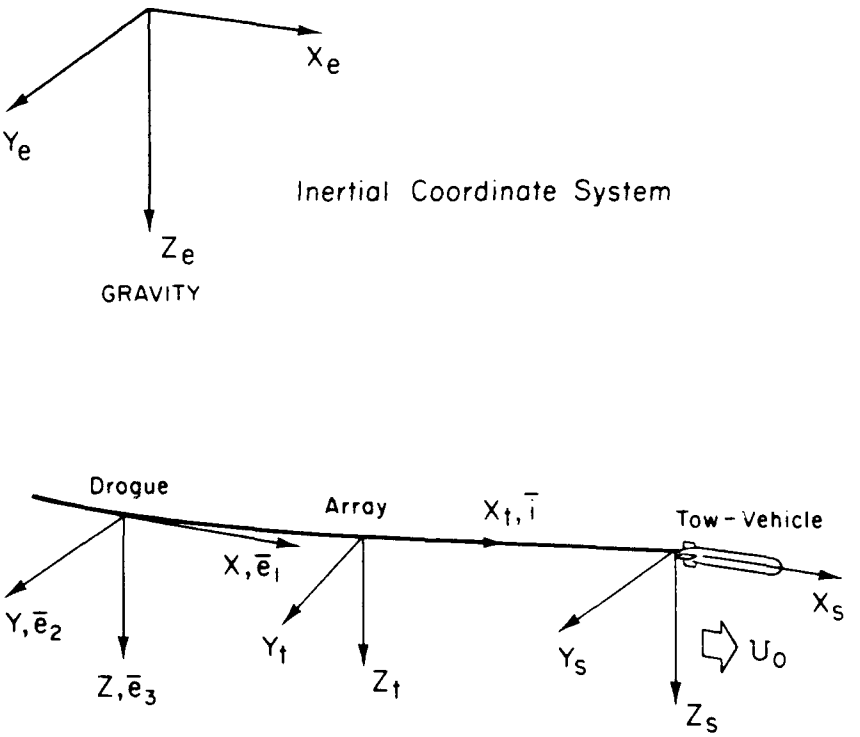

Figure 6.1. Rectangular coordinate system.

(X_t, Y_t, Z_t), Fig. 6.1 is fixed within the array such that the X_t axis is the tangent vector to the array along its length. The radius vector to a point P on the array is

$$\bar{r} = X\bar{e}_1 + Y\bar{e}_2 + Z\bar{e}_3 \ . \tag{6.1}$$

For an inextensible array,

$$\bar{i} = \frac{\partial \bar{r}}{\partial s} = \left(\frac{dX}{ds}\right)\bar{e}_1 + \left(\frac{dY}{ds}\right)\bar{e}_2 + \left(\frac{dZ}{ds}\right)\bar{e}_3 = \frac{d\bar{r}}{ds} \tag{6.2}$$

since

$$\frac{d\bar{e}_1}{ds} \equiv \frac{d\bar{e}_2}{ds} \equiv \frac{d\bar{e}_3}{ds} \equiv 0.$$

The towline angle ϕ (Fig. 6.2) is defined as the angle between the tangent vector $\underline{\bar{i}}$ and the velocity vector $\underline{\bar{U}}$, so that

$$\bar{j} = \bar{U} x \left(\frac{\bar{i}}{U \sin\phi}\right)$$

$$\bar{k} = \bar{j} \times \bar{i}. \tag{6.3}$$

The transformation of a vector in the (X,Y,Z) to the (X_t, Y_t, Z_t) system, for an order of rotation of η, ϕ (Fig. 6.2) is

$$\begin{Bmatrix} \bar{i} \\ \bar{j} \\ \bar{k} \end{Bmatrix} = [A] \begin{Bmatrix} \bar{e}_1 \\ \bar{e}_2 \\ \bar{e}_3 \end{Bmatrix}$$

$$= \begin{bmatrix} \cos\eta\cos\phi & \sin\eta\cos\phi & -\sin\phi \\ -\sin\eta & \cos\eta & 0 \\ \cos\eta\,-\sin\phi & \sin\eta\sin\phi & \cos\phi \end{bmatrix} \begin{Bmatrix} \bar{e}_1 \\ \bar{e}_2 \\ \bar{e}_3 \end{Bmatrix}. \tag{6.4}$$

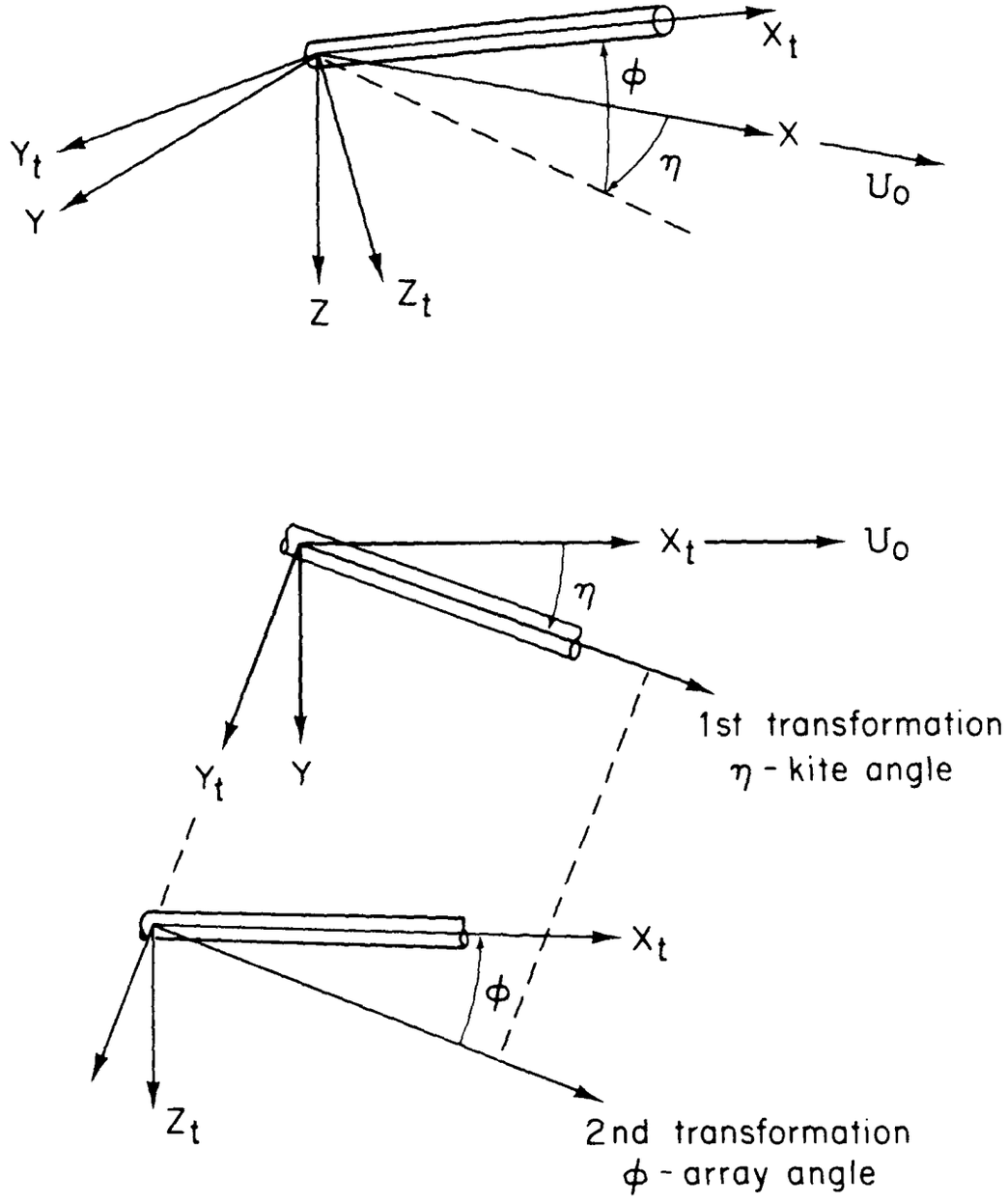

Figure 6.2. Angular transformation.

From Eq. (6.4)

$$\bar{i} = (\eta \cos\phi)\bar{e}_1 + (\sin\eta \cos\phi)\bar{e}_2 + (-\sin\phi)\bar{e}_3,$$

Therefore

$$\frac{dX}{ds} = \cos\eta \cos\phi$$

$$\frac{dY}{ds} = \sin\eta \cos\phi$$

$$\frac{dZ}{ds} = -\sin\phi \qquad (6.5)$$

are the directional derivatives in the rectangular X,Y,Z coordinate system.

The second coordinate system required is a cylindrical system (ψ, R,Z) (Fig. 6.3) that rotates with the tow-vehicle about the Z axis, with unit vectors $\bar{e}_\psi$, $\bar{e}_r$, and $\bar{e}_3$. The orientation of $\bar{e}_\psi$ and $\bar{e}_r$ varies with s along the array so that

$$\frac{d\bar{e}}{d\psi} = \bar{e}_\psi; \quad \frac{d\bar{e}}{d\psi} = -\bar{e}_r. \qquad (6.6)$$

We divide by ds, and

$$\frac{d\bar{e}}{ds} = \bar{e}_\psi \left(\frac{d\psi}{ds}\right); \quad \frac{d\bar{e}_\psi}{ds} = -\bar{e}_r \left(\frac{d\psi}{ds}\right). \qquad (6.7)$$

Also, we have:

Position Vector

$$\bar{r} = -R\bar{e}_r - Z\bar{e}_3 \qquad (6.8)$$

Angular Rate Vector

$$\bar{\omega} = \dot{\psi}\bar{e}_3 \qquad (6.9)$$

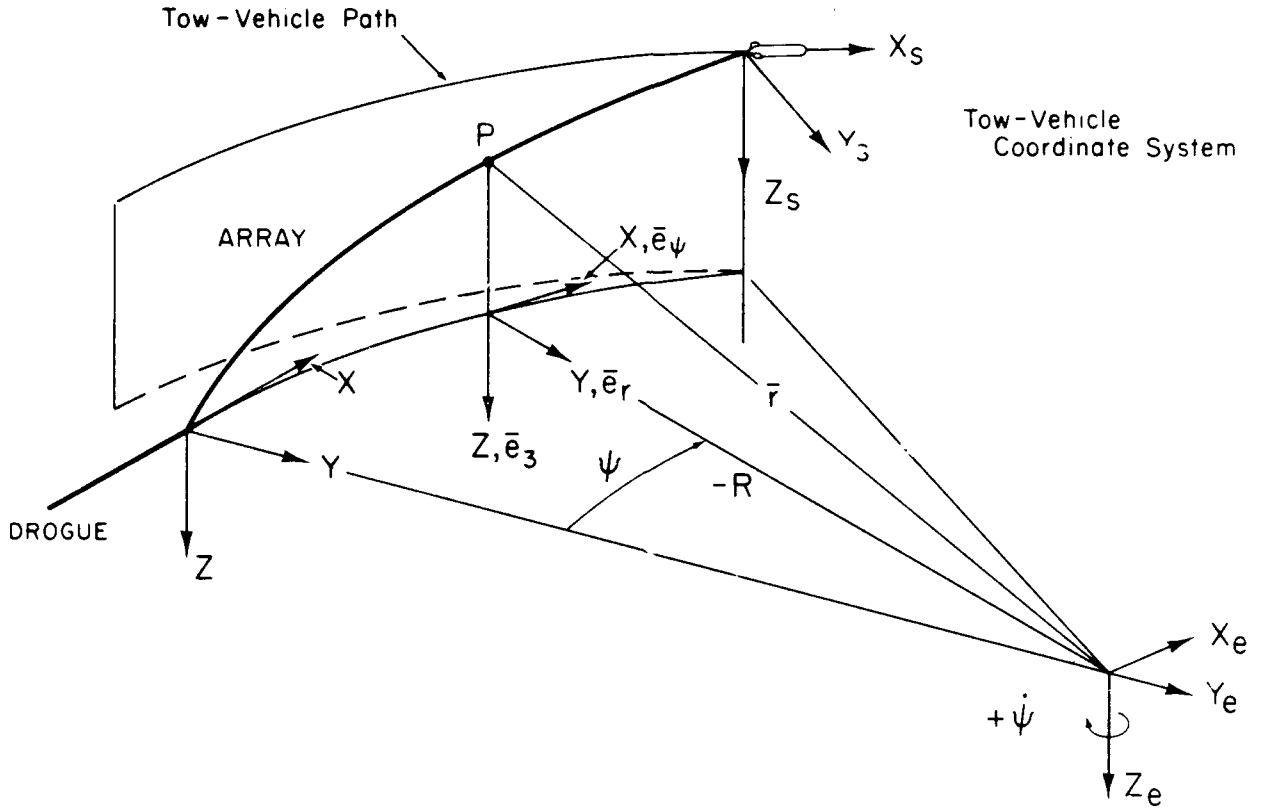

Figure 6.3. Cylindrical coordinate system.

Velocity Vector

$$\bar{U} = \bar{\omega} \times \bar{r} = (R\dot{\psi})\bar{e}_\psi \tag{6.10}$$

Acceleration Vector

$$\frac{\partial \bar{U}}{\partial t} = \bar{U} \times \bar{\omega} = (R\dot{\psi}^2)\bar{e}_r \tag{6.11}$$

Since $\bar{i} = d\bar{r}/ds$, then

$$\bar{i} = (\cos\eta \cos\phi)\bar{e}_\psi + (\sin\eta \cos\phi)\bar{e}_r + (-\sin\phi)\bar{e}_3$$

$$= -R\frac{d\bar{e}_r}{ds} - \bar{e}_r\frac{dR}{ds} - \bar{e}_3\frac{dZ}{ds}. \tag{6.12}$$

If we substitute Eq. (6.6) into Eq. (6.12),

$$\frac{d\psi}{ds} = \frac{\cos\eta \cos\phi}{R}$$

$$\frac{dR}{ds} = -\sin\eta \cos\phi$$

$$\frac{dZ}{ds} = \sin\phi \qquad (6.13)$$

are the directional derivatives in the cylindrical (ψ,R,Z) coordinate system.

6.1.2 Equations of Steady Motion

The forces acting on an element of unit length, ds, of the array are shown in Fig. 6.4. These include:

(1) gravitational, F_w

(2) buoyancy, F_b

(3) inertial, F_i

(4) hydrodynamic, F_a, F_n, F_s, F_t

(5) tension, T,

where

F_w = array weight

F_b = array buoyancy = $\rho g S$

The inertial (centrifugal) force F_i arises because in a steady-state turn the towed array is constantly being accelerated toward the axis of rotation. Thus,

$$F_i = m\left(\frac{\partial \overline{U}}{\partial t}\right)$$

$$= mR\,\dot{\psi}^2, \qquad (6.14)$$

where

R = turn radius

$\dot{\psi}$ = turn rate in radians per second.

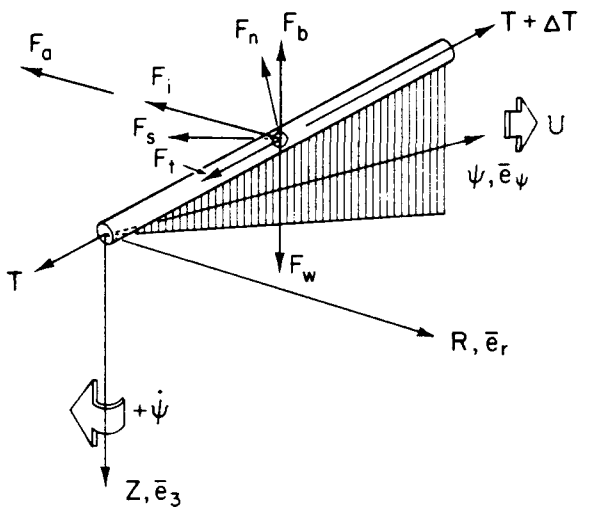

Figure 6.4
Forces acting on an array element.

This acceleration also gives rise to a hydrodynamic force termed the added mass force, F_a, which acts perpendicular to the array longitudinal axis. This term increases the mass of the array by an amount equal to

$$m_a = k\rho S \tag{6.15}$$

where

k = added mass coefficient = 1.0 for circular cylinder.

Thus

$$F_a = k\rho S\frac{\partial \bar{U}}{\partial t} \ . \tag{6.16}$$

Note that $\partial\bar{U}/\partial t$ must be in the towline coordinate system.

The three remaining hydrodynamic forces, due to relative motion through the fluid, are:

F_n = normal force

F_s = side force

F_t = tangential force.

Because of the selection and order of the array angular rotations η and ϕ, F_s is equal to F_n, where $F_n(\phi)$ and $F_t(\phi)$ are computed using Eqs. (5.3) and (5.4).

The array equation of motion in the rectangular coordinate system is

$$m\left(\frac{\partial \bar{U}}{\partial t}\right) = 0 = \left(\frac{\partial T}{\partial s}\right)\bar{i} + F_w\bar{e}_3 - F_t\bar{i} + F_s\bar{j} - F_n\bar{k}, \tag{6.17}$$

where

$$\left(\frac{\partial T}{\partial s}\right)\bar{i} = T\left(\frac{d\bar{i}}{ds}\right) + \bar{i}\left(\frac{dT}{ds}\right)$$

and

$$\left(\frac{d\bar{i}}{ds}\right) = \cos\eta\left(\frac{d\eta}{ds}\right)\bar{j} - \left(\frac{d\phi}{ds}\right)\bar{k}. \tag{6.18}$$

By substituting Eq. (6.18) into Eq. (6.17) and rearranging, we have

$$\frac{dT}{ds} = F_w\sin\phi + F_t$$

$$\frac{d\eta}{ds} = -F_s/T\cos\phi$$

$$\frac{d\phi}{ds} = F_w\cos\phi - F_n/T. \tag{6.19}$$

The equation of motion in the cylindrical coordinate system is modified from Eq. (6.17) by the addition of the added mass term F_a to account for the steady acceleration. Thus,

$$m\frac{\partial \bar{U}}{\partial t} = (mR\dot{\psi}^2)\bar{e}_r = \frac{\partial T\bar{i}}{\partial s} + F_w\bar{e}_3 - F_t\bar{i} + F_s\bar{j} - F_n\bar{k} + F_a\bar{e}_r \tag{6.20}$$

where

$$F_a = -(km)\frac{\partial \bar{U}}{\partial t} = -(kmR\dot{\psi}^2)\bar{e}_r. \tag{6.21}$$

Again, after the proper substitutions,

$$\frac{dT}{ds} = mR\dot{\psi}^2(\sin\eta\cos\phi) + F_w\sin\phi + F_t$$

$$\frac{d\eta}{ds} = [mR\dot{\psi}^2\cos\eta + (T/R)\cos\eta\cos^2\phi - F_s]/T\cos\phi$$

$$\frac{d\phi}{ds} = [-mR\dot{\psi}^2\sin\eta\sin\phi + F_w\cos\phi - F_n]/T. \qquad (6.22)$$

We thus have six simultaneous nonlinear ordinary differential equations, Eqs. (6.5) and (6.19) or Eqs. (6.13) and (6.22), for the array equations of motion.

6.2 Numerical Model

A fourth-order Runge-Kutta numerical method is used to integrate the differential equations. For the turn case, the turn radius of the array drogue tail is not known, since it may follow a path to either the inside or the outside of the tow-vehicle's path. To begin the integration, it is assumed that the drogue's turn radius is equal to the tow-vehicle's turn radius,

$$R_{d_1} = U_s/\dot{\psi} = R_s. \qquad (6.23)$$

After the first pass through the towline program, the drogue's turn radius is adjusted using the turn radius to the last point on the array, R_{t_1}:

$$R_{d_2} = R_s \frac{R_{d_1}}{R_{t_1}}. \qquad (6.24)$$

The speed of the drogue is now

$$U_{d_2} = R_{d_2}\dot{\psi}, \qquad (6.25)$$

which is used to recompute the drogue forces which are in turn used to compute a new array configuration. The corrective procedure

$$R_{d_{n+1}} = R_s \frac{R_{d_n}}{R_{t_n}}$$

$$U_{d_{n+1}} = R_{d_{n+1}} \dot{\psi} \qquad (6.26)$$

is repeated until $R_{d_{n+1}}$ and R_{d_n} are approximately equal within a specified tolerance.

The output of the array program is now transformed into a Cartesian coordinate system aligned with the tow-vehicle velocity vector (Fig. 6.5), with its origin at the tow point. This transformation is especially useful for the steady-state turn case as seen in Fig. 6.5.

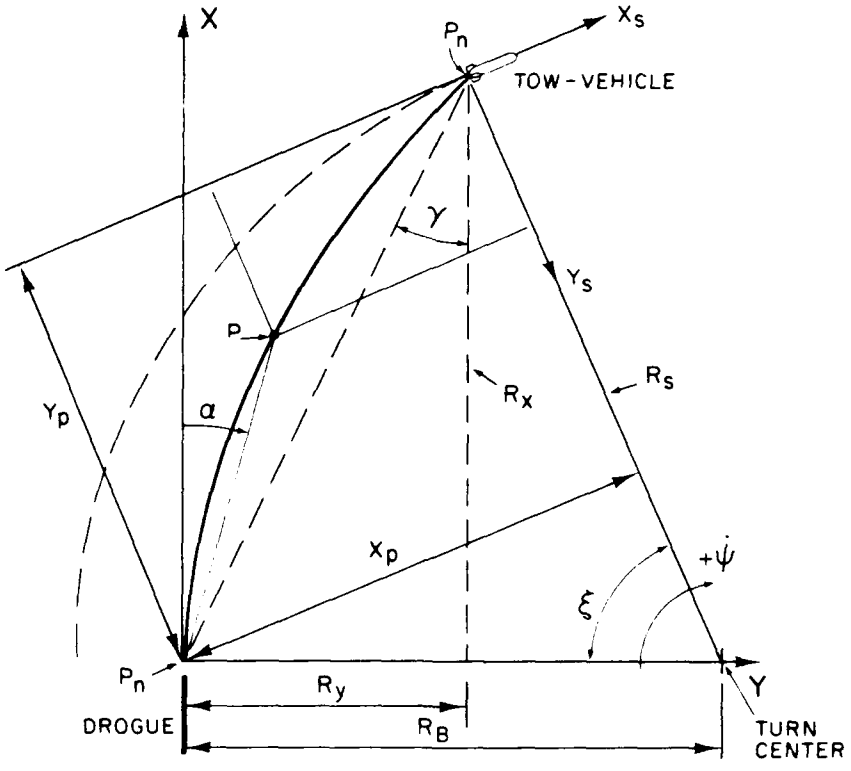

Figure 6.5. Transformation to tow-vehicle coordinate system.

The coordinates of p_n, the termination of the array, are (R_x, R_y, R_z) in the X,Y,Z system. The coordinate transformation is accomplished as follows:

$$\xi = \sin^{-1}(R_x/R_s)$$

$$\gamma = \tan^{-1}(R_y/R_x)$$

$$R_p = \sqrt{R_x^2 + R_y^2}$$

$$\left.\begin{aligned} X_p &= -R_p\cos(\xi - \gamma) \\ Y_p &= R_p\sin(\xi - \gamma) \end{aligned}\right\} \text{ coordinates of } p_n \text{ in tow-vehicle system} \qquad (6.27)$$

The coordinates in the tow-vehicle system of any point, p_{n-1} (X,Y,Z), along the array are

$$R = \sqrt{X^2 + Y^2}$$

$$\gamma = \tan^{-1}(Y/X)$$

$$X_{p_{n-1}} = X_p + R\cos(\xi-\gamma)$$

$$Y_{p_{n-1}} = Y_p - R\sin(\xi-\gamma)$$

$$Z_{p_{n-1}} = Z_p - Z. \qquad (6.28)$$

The description of the computer program ARRAY, including a listing, is contained in Appendix A.

7. HYDROELASTIC MODEL

7.1 Mathematical Model

The array stability problem is one of hydroelasticity, which is a phenomenon involving the mutual interaction of the inertial, hydrodynamic, and elastic forces acting on the towed array. This is classically known as flutter when small disturbances of an arbitrary nature induce more or less violent oscillations. The particular case of oscillation at zero frequency, in which the inertial force may be neglected, is called static hydroelasticity, or divergence.

We will pose the hydroelastic stability problem in the following manner. The array is assumed to be towed along a straight path in the horizontal X,Y plane, and is at rest with no oscillatory motions (Fig. 7.1). The tow-vehicle is assumed to be a fixed (nonoscillatory) rigid body, and the towed array to be a flexible appendage. Initially,

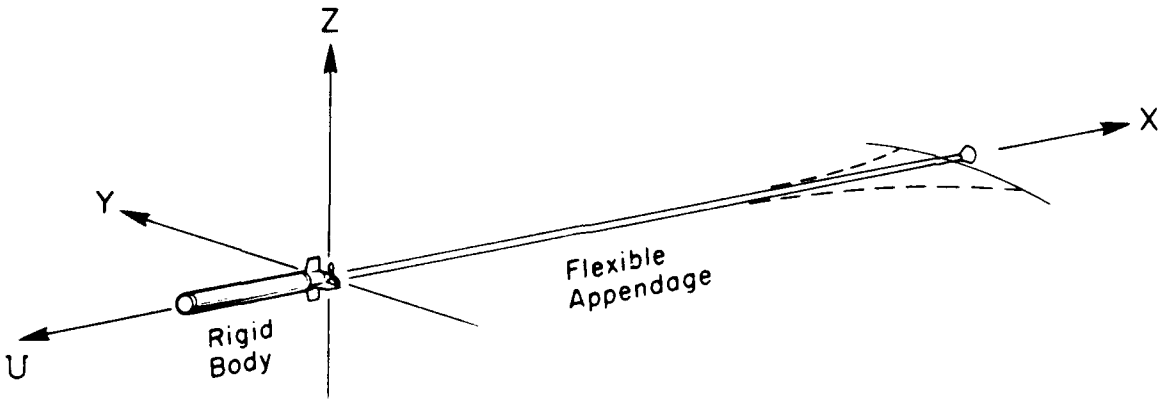

Figure 7.1. Towed array hydroelastic instability.

the system operates in a force-free environment. Random small disturbances then occur, and the existence of dynamic hydroelastic behavior is determined. If unstable motions persist, they are assumed to:

(1) occur only in the lateral plane

(2) be of small magnitude such that a linearity assumption may be made.

Further, the array, Fig. 7.2, is assumed to:

(1) be neutrally buoyant over its length L

(2) have uniform mass density per unit length m and bending rigidity EI along its length

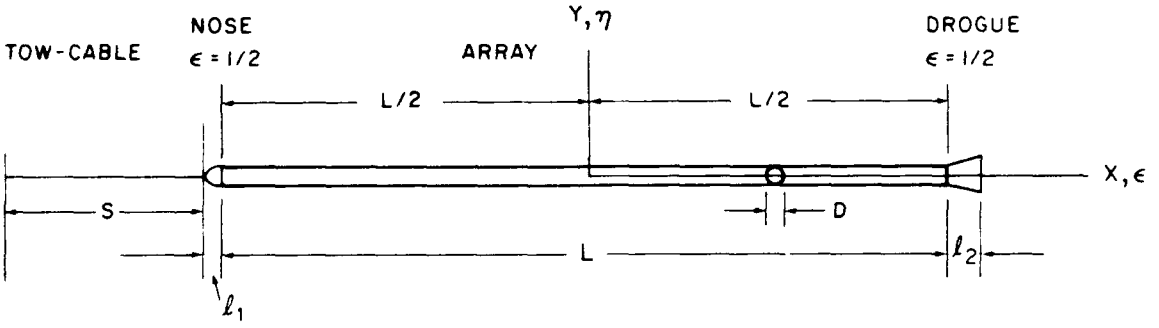

ITEM	NONDIMENSIONAL
$\Lambda = S/L$ $\lambda_1 = \ell_1/L$ $\lambda_2 = \ell_2/L$ $\alpha = \lambda_2/\lambda_1$ $\epsilon = L/D$	GEOMETRY
$u = UL\sqrt{M/EI}$	SPEED
$\omega = \Omega L^2\sqrt{(m+M)/EI}$	FREQUENCY

Figure 7.2. Array nomenclature.

(3) have a uniform circular cross section of diameter D and area S along its length

(4) to be terminated at its free end with a drogue of variable design.

The array is assumed to be towed in an incompressible fluid (water) of density ρ at speed U. The forces and moments per unit length on an element ($\delta\xi$) of the array, Fig. 7.3, include:

(1) tangential viscous hydrodynamic force, F_t

(2) normal viscous hydrodynamic force, F_n

(3) normal inviscid added mass hydrodynamic force, F_a

(4) inertial force, F_i

(5) longitudinal tension, T

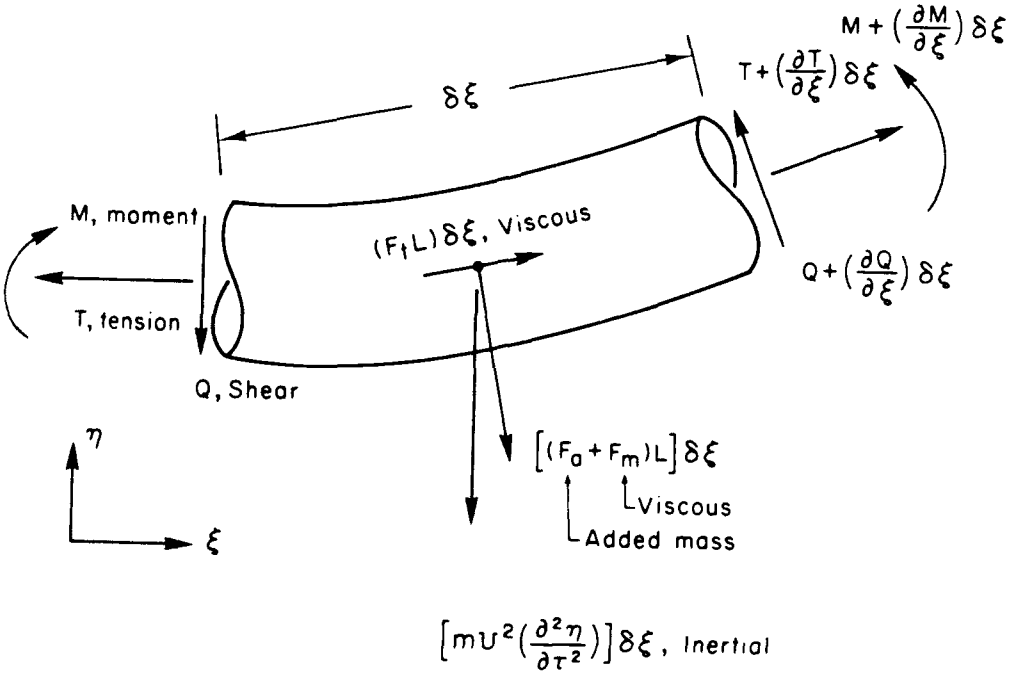

Figure 7.3. Array segment.

(6) internal shear, Q

(7) internal bending moment, M.

The development of the array stability mathematical model follows that of Yu (Ref. 8) and Paidoussis and Yu (Ref. 1). The space parameters x and y and time, t, are first nondimensionalized:

$$\xi = \frac{x}{L}; \quad \eta = \frac{y}{L}$$

$$\tau = Ut/L. \tag{7.1}$$

In addition, the tow point is assumed to be either pinned or clamped, and the array to have a faired nose-piece of length ℓ_1, and a drogue of length ℓ_2. The nondimensional geometry is

$$\lambda_1 = \ell_1/L$$

$$\lambda_2 = \ell_2/L$$

$$\alpha = \lambda_2/\lambda_1$$

$$\varepsilon = L/D. \tag{7.2}$$

The kinematics of the nose-piece and drogue, Figs. 7.4 and 7.5, are

$$\eta(\xi,\tau)_1 = \eta_1(\tau) + (\xi + 1/2)\theta_2(\tau), \tag{7.3}$$

where

$$\eta_1(\tau) = \eta(-1/2,\tau)$$

$$\theta_1(\tau) = \frac{\partial \eta}{\partial \xi}\Big|_{\xi = -1/2},$$

and

$$\eta(\xi,\tau)_2 = \eta_2(\tau) + (\xi - 1/2)\theta_2(\tau), \tag{7.4}$$

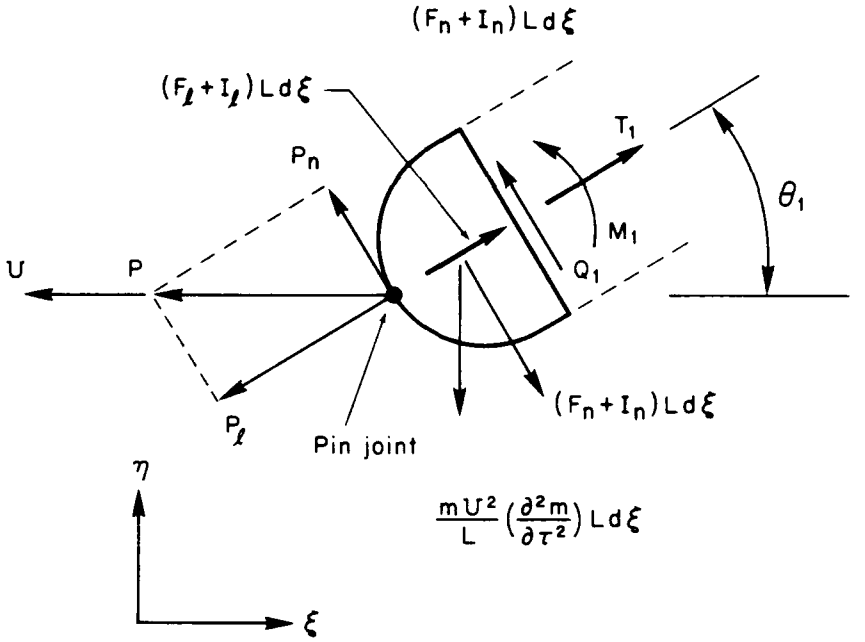

Figure 7.4. Nose-piece.

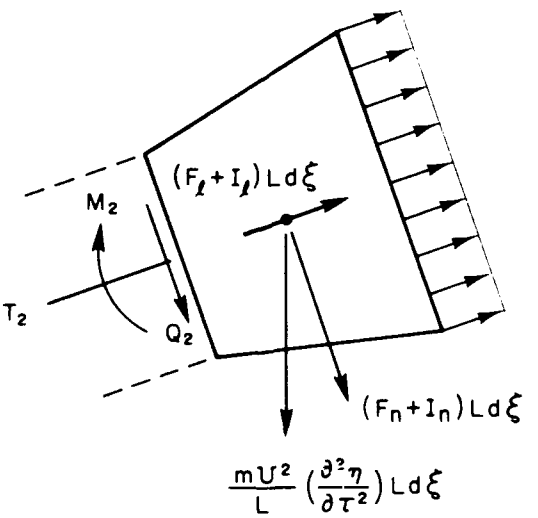

Figure 7.5. Tail drogue.

where

$$\eta_2(\tau) = \eta(1/2,\tau)$$

$$\theta_2(\tau) = \frac{\partial \eta}{\partial \xi} \Big|_{\xi = 1/2}.$$

By making the small angle assumption, we now develop the equations of motion by summing forces in the ξ and η directions and summing moments in the horizontal plane.

$$\Sigma F_\xi = \frac{\partial T}{\partial \xi} + F_t L + (F_n + F_a) L \left(\frac{\partial \eta}{\partial \tau} + \frac{\partial \eta}{\partial \xi}\right) = 0 \qquad (7.5)$$

$$\Sigma F_\eta = \frac{\partial Q}{\partial \xi} - (F_n + F_a) L + \frac{\partial}{\partial \xi}\left(T \frac{\partial \eta}{\partial \xi}\right) + F_t L \frac{\partial \eta}{\partial \xi} - mU^2 \frac{\partial^2 \eta}{\partial \tau^2} = 0 \qquad (7.6)$$

$$\Sigma M = QL + \frac{\partial M}{\partial \xi} = 0. \qquad (7.7)$$

The array viscous hydrodynamic forces are

$$F_n = 1/2 \rho U^2 C_f' \left(\frac{S}{D}\right) \left(\frac{\partial \eta}{\partial \tau} + \frac{\partial \eta}{\partial \xi}\right)$$

$$F_t = 1/2 \rho U^2 C_f' \left(\frac{S}{D}\right), \qquad (7.8)$$

where

$$C_f' = C_f/4 .$$

The inviscid (added mass) hydrodynamic force, if it is assumed that the array has a circular cross section, is

$$F_a = \rho U^2 \frac{S}{L} \left(\frac{\partial}{\partial \tau} + \frac{\partial}{\partial \xi}\right)^2 \eta. \qquad (7.9)$$

By substituting (7.8) and (7.9) into (7.5), ignoring higher-order terms, and integrating from an arbitrary ξ to $\xi = 1/2$, the array tension is

$$T(\xi) = 1/2\rho U^2 C_f' \left(\frac{S}{D}\right) L(1/2 - \xi) + T_2, \tag{7.10}$$

where

T_2 = drogue axial force

$$= \int_{1/2}^{1/2 + \lambda_2} (F_t + F_a) L d\xi + 1/2\rho U^2 S_B C_{D_B} . \tag{7.11}$$

The first term is the sum of viscous and inviscid drogue hydrodynamic forces, whereas the second term is the drogue base drag.

$$F_t = 1/2\rho U^2 C_f' [S(\xi)/D(\xi)]$$

$$F_a = \rho U^2 S_{max} \frac{x^2}{a} \left\{ \frac{(1 + k_1)^2 [1 - (x^2)]^2}{[1 - e^2 (x^2)]^2} - 1 \right\}$$

$$C_{D_B} = 0.029 \left[1/2\rho U^2 \left(\frac{S_B}{D_{fore}} \right) \right]^2 \tag{7.12}$$

D_{fore} = nose-piece plus array drag.

Since

$$M = \frac{EI}{L} \frac{\partial^2 \eta}{\partial \xi^2}, \tag{7.13}$$

then with (7.7)

$$Q = -\frac{1}{L} \frac{\partial M}{\partial \xi}$$

$$= -\frac{EI}{L^2} \frac{\partial^3 \eta}{\partial \xi^3} \tag{7.14}$$

and

$$\frac{\partial Q}{\partial \xi} = -\frac{EI}{L^2}\frac{\partial^4 \eta}{\partial \xi^4} . \tag{7.15}$$

Equation (7.15) along with (7.10), using (7.11) and (7.12), may now be substituted into (7.6) to obtain the lateral equation of motion.

$$\begin{aligned}
&\frac{EI}{L^2}\frac{\partial^4 \eta}{\partial \xi^4} \\
&+ \rho U^2 S\left(\frac{\partial}{\partial \tau} + \frac{\partial}{\partial \xi}\right)^2 \eta \\
&+ 1/2\rho U^2 S\varepsilon C_f'\left(\frac{\partial \eta}{\partial \tau} + \frac{\partial \eta}{\partial \xi}\right) \\
&+ 1/2\rho U S\varepsilon C_f'\left(\frac{\partial \eta}{\partial \xi}\right) \\
&- [T_2 + 1/2\rho U^2 C_f' S\varepsilon(1/2 - \xi)]\frac{\partial^2 \eta}{\partial \xi^2} \\
&+ mU^2\frac{\partial^2 \eta}{\partial \tau^2} = 0.
\end{aligned} \tag{7.16}$$

The boundary conditions for the nose-piece are obtained by summing forces in the transverse direction to obtain the shear force Q, and taking moments about the after end to obtain M_1:

$$Q_1 = -p_n + \left[\int_{-1/2 - \lambda_1}^{-1/2} \left(F_n + F_a + \frac{mU^2}{L}\frac{\partial^2 \eta}{\partial \tau^2}\right) L d\xi\right] \tag{7.17}$$

$$M_1 = \lambda_1 L p_n$$

$$+ \left[\int_{-1/2 - \lambda_1}^{-1/2} L(\xi + 1/2)F_n + F_a + \frac{mU^2}{L}\frac{\partial^2 \eta}{\partial \tau^2}\ L d\xi\right.$$

$$\times \left[\int_{-1/2 - \lambda_1}^{-1/2} \left(\frac{b^2}{a}\right) x^2 F_a L d\xi \right]_{NOSE} , \qquad (7.18)$$

where

$$p_n = \text{tow-vehicle force on nose-piece}$$
$$= p_\ell \theta_1 \quad \text{(towpoint pinned)}$$
$$= 0 \quad \text{(towpoint clamped)} \qquad (7.19)$$

and

$$p_\ell = T_2 + 1/2\rho U^2 \left(\frac{S}{D}\right) L C_f' + \left[\int_{-1/2 - \lambda_1}^{-1/2} (F_t + F_a) L d\xi \right]_{NOSE} , \qquad (7.20)$$

Likewise, the boundary conditions at the drogue are

$$Q_2 = -\left\{ \int_{1/2}^{-1/2 + \lambda_2} \left[F_n + F_a + \frac{mU^2}{L} \left(\frac{\partial^2 \eta}{\partial \xi^2}\right) \right] L d\xi \right\}_{DROGUE} \qquad (7.21)$$

$$M_2 \simeq 0 .$$

Yu (Ref. 8) develops expressions from ideal flow theory for the forces on ellipsoids of revolution which are used to represent the nose-piece and drogue.

7.2 Numerical Model

The motions of the array are assumed to be of the form

$$\eta = [Y(\xi)]e^{i\omega\tau}, \tag{7.22}$$

where

$$Y(\xi) = \sum_{r=0}^{\infty} A_r(\xi + 1/2)^r \tag{7.23}$$

A_r = complex quantities to be determined

$\omega = \left(\sqrt{\frac{m + m_a}{EI}}\right)\Omega L^2$ = dimensionless eigenfrequency (complex)

$u = UL\sqrt{\frac{m_a}{EI}}$ = dimensionless speed

Ω = circular frequency (complex).

The stability of the array is determined by the sign of the imaginary part of the eigenfrequency, $Im(\omega)$. The array is stable if $Im(\omega)$ is positive, unstable if $Im(\omega)$ is negative, and neutrally stable if $Im(\omega)$ is zero. This differs from the conventional use of eigenvalues to determine stability wherein the sign of the real part, $Re(\lambda)$, is used. Since

$$\lambda = i\omega,$$

where

$$\lambda = u_1 + iv_1$$

$$Re(\lambda) = u_1$$

$$Im(\lambda) = v_1$$

and

$$\omega = u_2 + iv_2$$

$$Re(\omega) = u_2$$

$$Im(\omega) = v_2,$$

then

$$\lambda = i(u_2 + iv_2)$$

$$= iu_2 - v_2$$

and

$$Re(\lambda) = u_1 = -v_2$$

$$= -Im(\omega). \qquad (7.24)$$

By substituting (7.22) into (7.16), (7.17), (7.18) and 7.21), we have

(1) Lateral equation of motion

$$g_0 \frac{d^4Y}{d\xi^4} + g_1 \frac{d^2Y}{d\xi^2} + g_2\xi \frac{d^2Y}{d\xi^2} + g_3 \frac{dY}{d\xi} + g_4 Y = 0 \qquad (7.25)$$

(2) Boundary condition at nose ($\xi = -1/2$)

$$g_0 \frac{d^3Y}{d\xi^3} + g_5 \frac{dY}{d\xi} + g_6 Y = 0$$

$$g_0 \frac{d^2Y}{d\xi^2} + g_7 \frac{dY}{d\xi} + g_8 Y = 0 \qquad (7.26)$$

(3) Boundary condition at drogue ($\xi = 1/2$)

$$g_0 \frac{d^2Y}{d\xi^2} + g_9 \frac{dY}{d\xi} + g_{10}Y = 0$$

$$g_0 \frac{d^2Y}{d\xi^2} = 0. \tag{7.27}$$

By substituting (7.23) into (7.25), and collecting terms, we have

(1) Lateral equation of motion

$$24g_0A_4 + 2g_1A_2 + g_3A_1 + g_4A_0 = 0$$

$$120g_0A_5 + 6g_1A_3 + 2(g_2 + g_3)A_2 + g_4A_1 = 0$$

$$360g_0A_6 + 12g_1A_4 + (6g_2 + 3g_3)A_3 + g_4A_2 = 0 \tag{7.28}$$

or

$$n(n-1)(n-2)(n-3)g_0A_n + \left(g_1 - \frac{g_2}{2}\right)(n-2)(n-3)A_{n-2}$$

$$+ (n-3)[g_2(n-4) + g_3]A_{n-3} + g_4A_{n-4} = 0.$$

By substituting (7.23) into (7.26) and (7.27) we have

(2) Boundary condition at nose

$$g_6A_0 + g_5A_1 + 6g_0A_3 = 0$$

$$g_8A_0 + g_7A_1 + 2g_0A_2 = 0 \tag{7.29}$$

(3) Boundary condition at drogue

$$2A_2 + 6A_3 + \sum_{r=4}^{\infty}[4(r-1)]A_r = 0$$

$$g_{10}A_0 + (g_9 + g_{10})A_1 + (2g_9 + g_{10})A_2 + (6g_0 + 3g_9 + g_{10})A_3$$

$$+ \sum_{r=4}^{\infty}[g_0 r(r-1)(r-2) + rg_9 + g_{10}]A_r = 0. \qquad (7.30)$$

From (7.28), we see that the A terms are linear combinations of A_0, A_1, A_2 and A_3. Therefore (7.29) and (7.30) may be expressed as a 4 x 4 determinant which must be equal to zero for a nontrivial solution. In matrix form

$$[G]\begin{Bmatrix} A_0 \\ A_1 \\ A_2 \\ A_3 \end{Bmatrix}^T = \{0\}$$

and

$$DET[G] = 0. \qquad (7.31)$$

The computation procedure is as follows:

(1) At u = 0

Im(ω) = 0

Re(ω) = 3.52, 22.03, 61.7, etc., corresponding to the nondimensional natural frequencies of a cantilever beam.

(2) Then u is increased in small steps, and varied until (7.31) is satisfied. A trace of ω as a function of u is made for each of

the modes from 0 (static instability) through 4 (dynamic instability). The zero crossing points, $Im(\omega) = 0$, are then plotted as a function of the system variables, λ_1, λ_2, ε, C_f, and S_{base}. Thus a stability map showing the effect of changes in system variables can be made.

The description of the computer program SNAKE, including a listing, is contained in Appendix B. The coefficients g_0 ... g_{10} as well as A_0 ... A_3 are contained in the program listing.

8. MAST TOWED ARRAY SYSTEM--PHYSICAL DESCRIPTION

The prototype advanced target system known as the Mobile Acoustic Spatial Target (MAST) was designed and developed by the Naval Underwater Systems Center during 1977 (Ref. 21). The system comprises a self-controlled, preprogrammed tow-vehicle (Fig. 8.1) and a towed array. The tow-vehicle is capable of towing the 2.5-in. diameter 200-ft array at speeds of 8 to 20 kn.

The array is fabricated from polyvinyl chloride (Tygon) hose, and contains two tracking transducers (pingers) and six acoustic transducers (three pairs). Foam spacers are used in sufficient numbers to make the array approximately neutrally buoyant over any 6-ft section. A central member of Kevlar stranded rope is used for strengthening. The hydrodynamic surface friction load is transferred to the central strength member in the following manner. As the load is applied, the hose stretches and thus contracts around the foam spacers which are in turn fixed to the strength member. The hose is

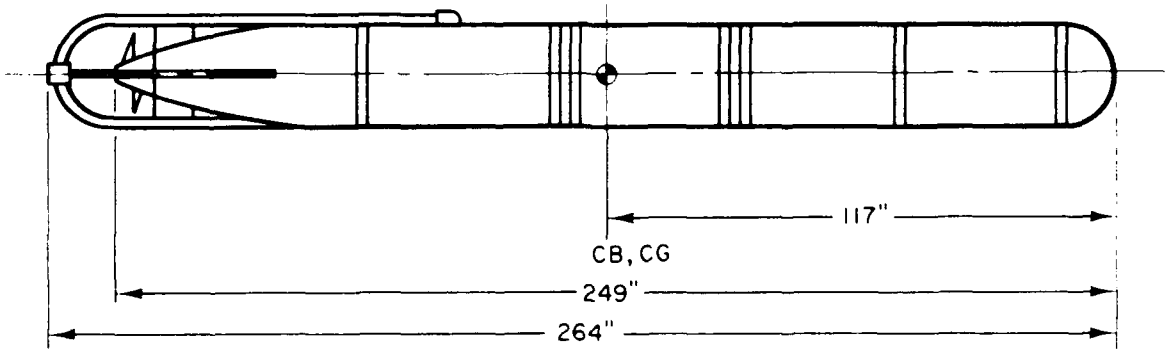

WEIGHT	2380 LB
DIAMETER	19 INCHES
BUOYANCY	45 LB POSITIVE

Figure 8.1. MAST tow-vehicle.

filled with Shellsol oil and pressurized to approximately 7 psi to support the hose shape. Several arrays have been fabricated for the MAST system. Array serial #01 is presently in storage at the Naval Undersea Warfare Engineering Station (NUWES), Keyport. This array has been surveyed to determine its as-built configuration. The results of the survey are shown in Fig. 8.2. Seventy-six foam spacers are used for buoyancy. Details of both array terminations are shown in Fig. 8.3. NUSC supplied the detailed weight figures for this series of arrays, which are tabulated in Table 8.1. This information, along with the results of the survey, allowed the formulation of an idealized "as built" weight model for use in the steady-state array program. The weight model is composed of a "smeared" uniform weight with point loads applied at the transducers, pingers, spacers, and tail connector. For the purpose of the model, the point loads are applied at equidistant spaces of 2.35 ft, thus giving 85 spaces for a 200-ft array length (Fig. 8.4). The exact length of wiring to each of the pingers and transducers was computed (Table 8.1). The total wiring weight was divided by the array length to give a nominal weight per foot of 0.132 for the transducer wire and 0.024 for the pinger wire.

The buoyancy of a 200-ft array is:

Water	Buoyancy, lb	Buoyancy/length, lb/ft
Fresh	425.42	2.12
Salt	436.33	2.18

The array is thus 1.12 lb and 13.7 lb buoyant (light) overall.

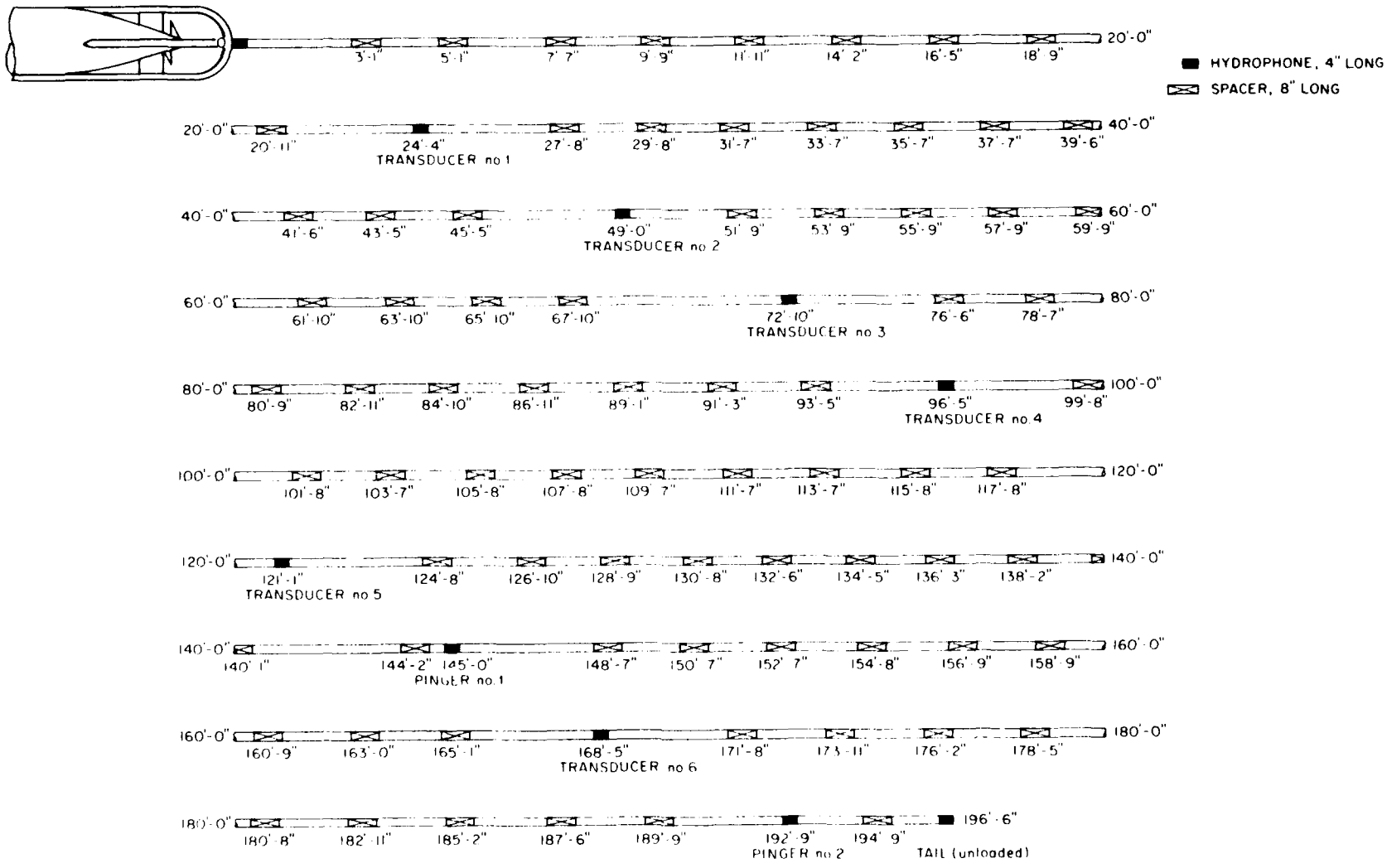

Figure 8.2. MAST array (serial 01).

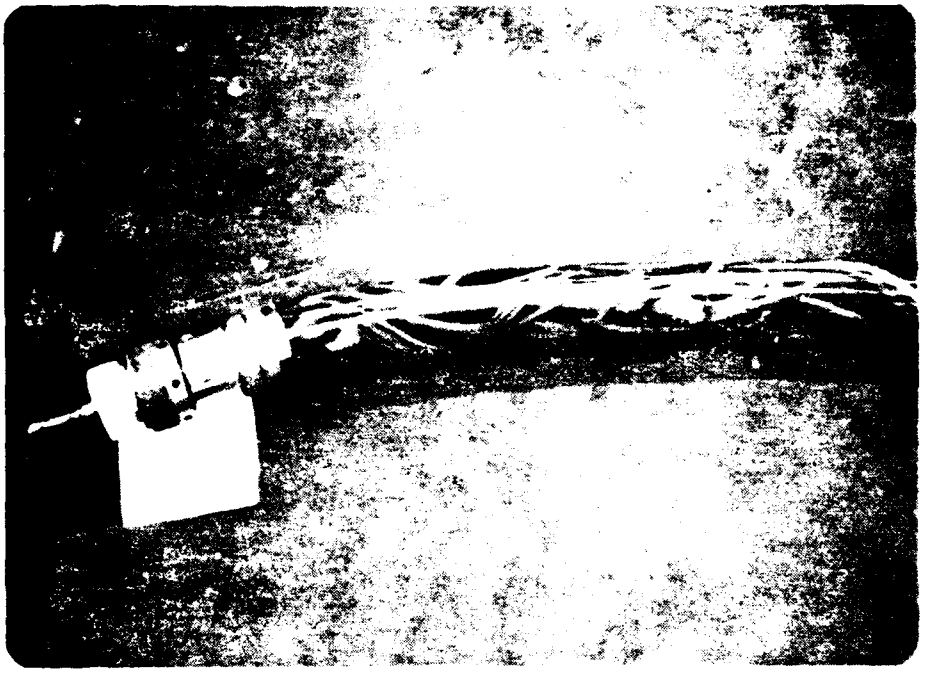

Table 8.1 MAST array weight breakdown.

Uniform Weights

Item	lb/ft	lb per 200 ft length
Kevlar strength member	0.020	4.0
Hose	0.430	86.0
Transducer wire	0.132	25.92
Pinger wire	0.024	3.54
Oil	1.254	250.8
Subtotal	1.86	370.26

Point Weights

Item	Quantity	lb each	lb total
Pingers	2	1.118	2.235
Transducers	6	1.287	7.723
Spacers	76	0.543	41.284
Tail connector (light)	1	1.062	1.062
Subtotal			52.304 lb
Total			422.56 lb
			2.11 lb/ft

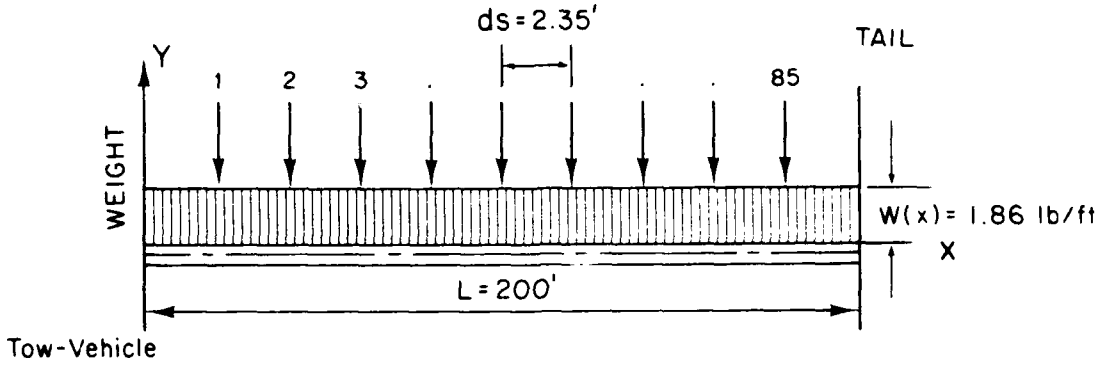

ITEM	NUMBER
Pingers	2
Transducers	6
Spacers	76
End Connector	1

Figure 8.4. Array weight distribution.

9. NUMERICAL AND TEST CORRELATION STUDIES

9.1 MAST Array Towing Tank Tests

Tests of the MAST array were conducted during August 1978 in the David Taylor Naval Ship Research and Development Center's towing tank. The standard, 200-ft length and a short, 50-ft length were towed at speeds from 5 to 25 kn in the approximately 3000-ft long towing basin. During the conduct of these tests, a 16 mm film of the array's behavior underwater was made through a viewport in the side of the basin. A 6-ft to 10-ft length of the array could be seen at any given instant. The test plan corresponding to the film is listed in Table 9.1. The 200-ft length was tested at speeds of 5 to 25 kn; the 50-ft length was tested at speeds of 10 and 20 kn. The array was towed from a vertical surface-piercing strut so that the tow point was at mid-depth. The 200-ft array was tested without a tail drogue (i.e., with a blunt base), and the 50-ft length had a tail-fairing drogue.

The film explicitly showed the existence of what is believed to be static and dynamic instabilities in the array's shape. To study this behavior in detail, two techniques for reconstituting the array's shape were pursued.

The array's shape was first reconstituted photographically by making high-contrast, positive prints directly from the 16 mm movie film. The 4 x 5-in. prints were made from a frame spacing that slightly overlapped the array image approximately every 20th frame. The picture segments were then taped together to form a composite photograph 104 in. long covering the 200-ft array. These composites were then reduced and are shown in Figs. 9.1 and 9.2 for the 200-ft and 50-ft arrays, respectively. The photographs were enhanced by

Table 9.1. DTNSRDC array tow tank tests.

Run No.	Array Length, ft	Speed, kn	End Connector	Drogue	Dynamic Instability	Frame Speed, fr/s	$\varepsilon = L/D$
1*	200	5.0	Light (Alum)	No	No	40	960
2	200	10.0	Light (Alum)	No	No	80	960
3	200	20.0	Light (Alum)	No	No	240	960
4	200	25.0	Light (Alum)	No	Yes	240	960
5	200	7.5	Light (Alum)	No	No	80	960
6	50	10.0	Heavy (Steel)	Yes	Yes	80	240
7	50	20.0	Heavy (Steel)	Yes	Yes	240	240
8	50	10.0	Heavy (Steel)	Yes	Yes	80	240

*data not usable

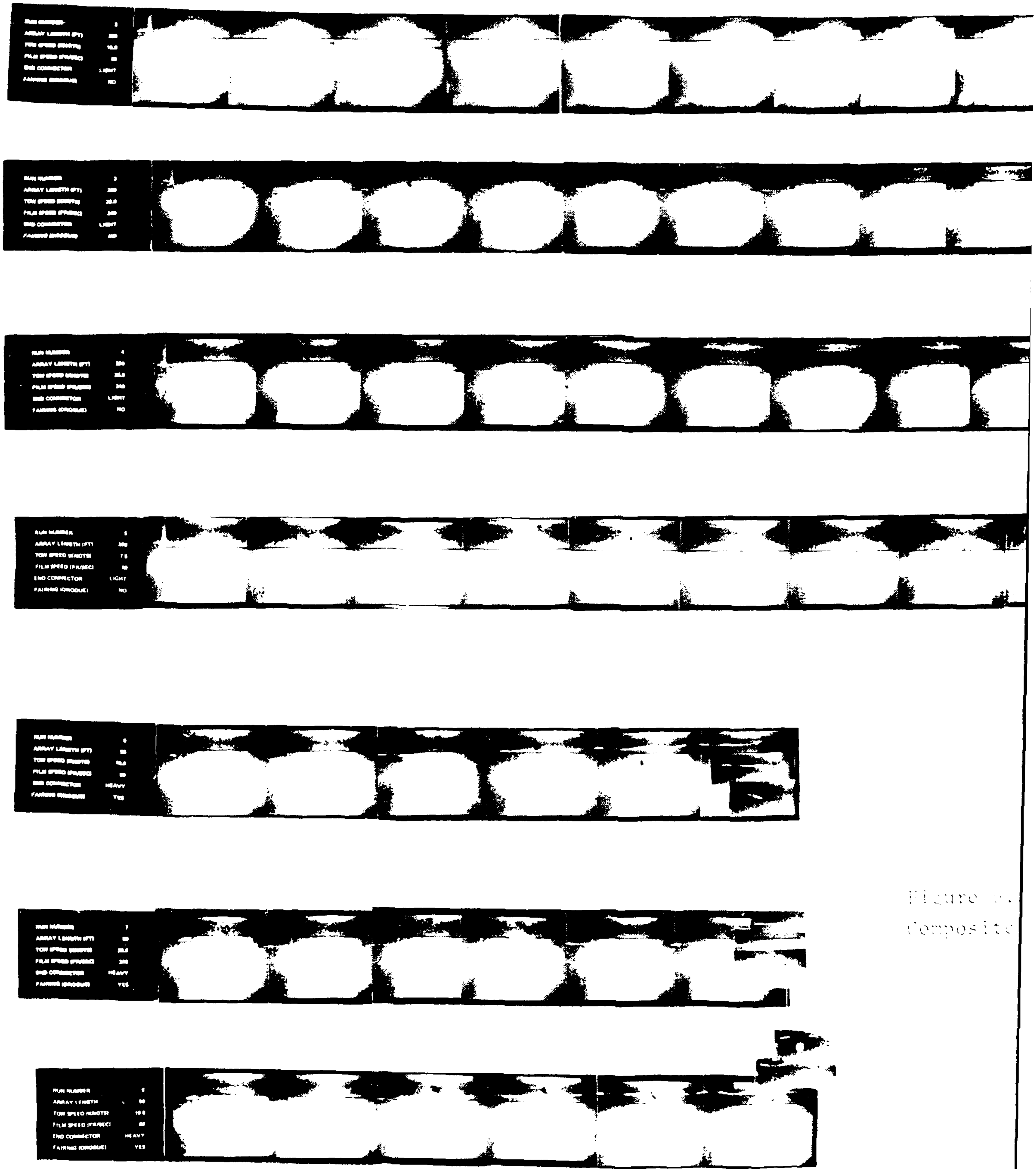

Figure
Composite

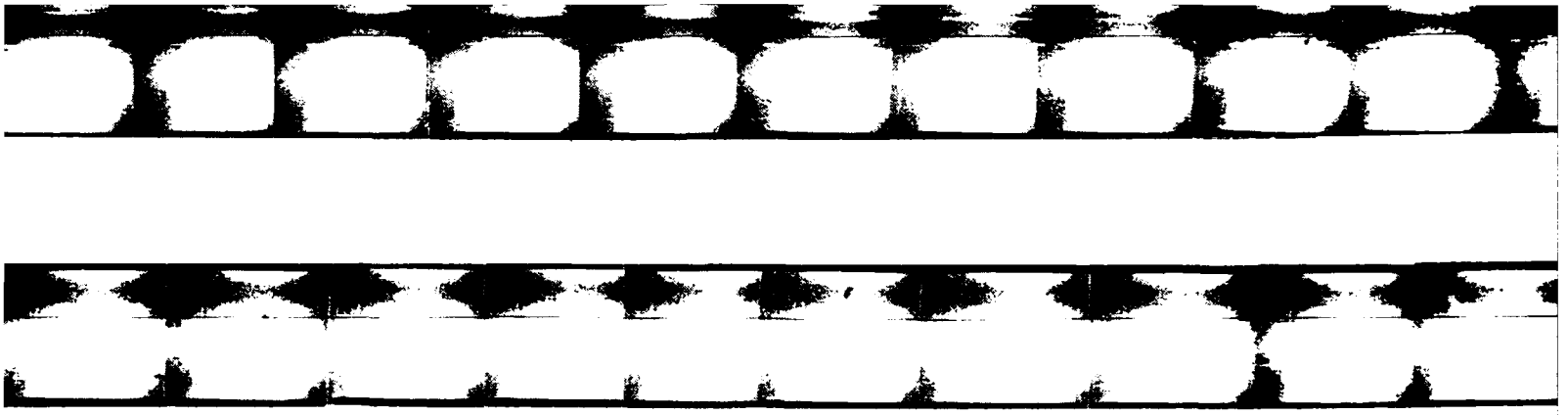

Figure 9.1. Composite photographs of 200-ft array.

Figure 9.2.
Composite photographs of 50-ft array.

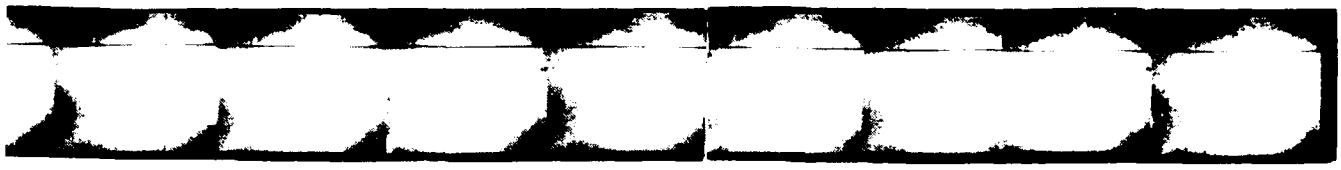

marking in a horizontal reference line corresponding to a fixed background marker. The disadvantage of this technique is the alignment inaccuracies introduced in joining the photographs together. The use of this technique requires that there be no low-frequency oscillations in the vertical plane. This seems to be the case, as determined from an examination of the film. We cannot be certain, however, since the film was not made for this purpose.

A second technique used to reconstitute the array's shape was to digitize the film image by projecting it onto a computer digitizer board. A special motion picture projector (Kodak Analyst II) was used to project the film at slow speed onto a 4-ft x 5-ft digitizer board. While the film was projected at a constant slow speed, the cursor followed the vertical position of the array as it passed a predetermined, vertical reference line on the digitizer board. A sampling program automatically digitized the cursor's position at a preselected rate.

In all, 1390 points were digitized for the 200-ft array and 352 points for the 50-ft array. The digitized points were connected on the computer plot by straight-line segments and a curve fitting routine. The results were identical to the eye. The disadvantage of this technique is the discontinuities or "steps" that appear in the distorted (vertically exaggerated) shape of the array. Once the array configuration was digitized, it was displayed in a format designed to enhance the data. Figure 9.3 shows a composite of four runs of the 200-ft array; Figure 9.4 shows a composite of three runs of the 50-ft array. The vertical and horizontal scales are equal, and hence can be

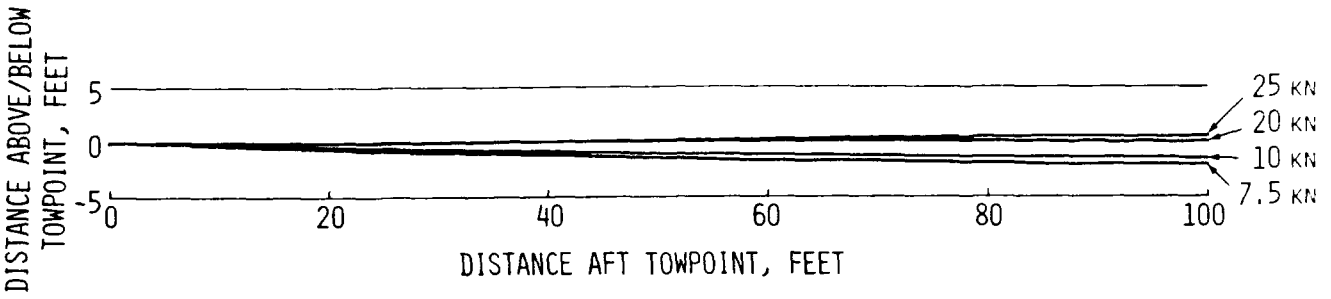

Figure 9.3. Digitized configuration of 200-ft array.

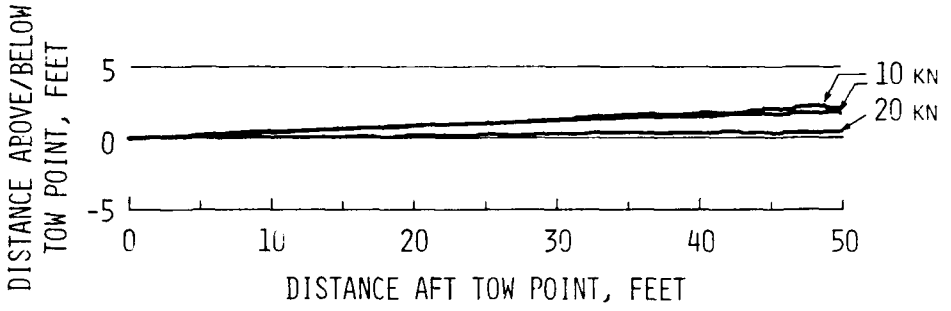

Figure 9.4. Digitized configuration of 50-ft array.

compared directly with the photographs. The vertical scale was then exaggerated by a factor of 20 (Figs. 9.5 and 9.6) to enhance the character of the array's shape.

An examination of the shape from both the photographic and digitized reconstitutions shows that it is the result of three factors:

(1) the weight/buoyancy distribution

(2) a static-instability standing wave

(3) a dynamic instability which manifests itself by a "wagging" of the array tail.

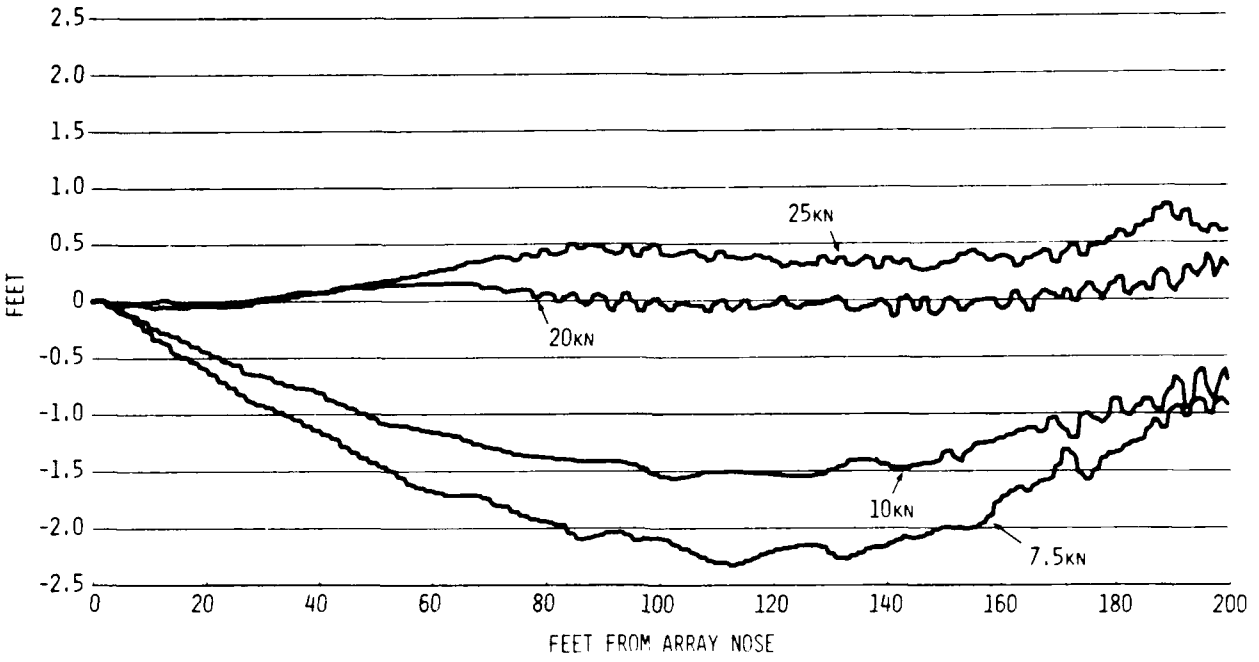

Figure 9.5. Distorted digitized configuration of 200-ft array.

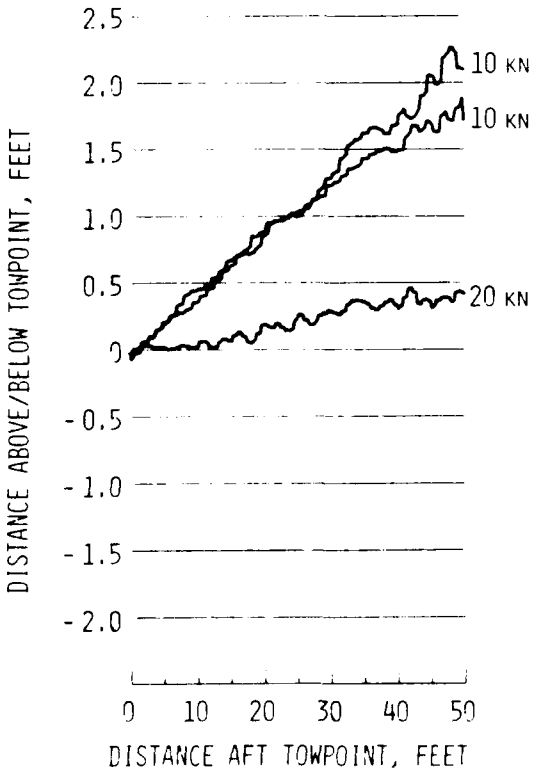

Figure 9.6

Distorted digitized configuration of 50-ft array.

The 50-ft array has a net buoyancy distribution such that it floats at an upward angle. As the speed increases from 10 to 20 kn, the hydrodynamic forces tend to decrease the "float angle" so that the array assumes a more horizontal position. The 200-ft array, on the other hand, has a net weight distribution such that is sinks below the horizontal reference at the lowest speed. As the speed is increased, the hydrodynamic forces tend to straighten out the array so that it approaches the horizontal reference line. It should be noted that the maximum vertical displacement is about 4% of the array's length for the 50-ft array, and about 1.25% for the 200-ft array.

In addition to the effect of the net weight/buoyancy distribution, the reconstituted array exhibits what appears to be a static instability over a significant portion, approximately 75%, of its length. The static instability is characterized by a low-frequency, standing wave shape of wavelength λ_1 over a relatively straight portion of the array beginning at the towpoint and then a high-frequency standing wave of wavelength λ_2 toward the tail. The approximate wavelengths λ and heights h are:

Speed, kn	λ_1, ft	h_1, ft	λ_2, ft	h_2, ft
7.5	30	0.2	5	0.2
10.0	30	0.2	5	0.3
20.0	140	0.3	5	0.2
25.0	100	0.3	5	0.2

It has been determined from the film that high-frequency oscillations (i.e., dynamic instabilities of a short length of the tail of the array) existed. These oscillations occurred over a short enough

segment of the array that the entire length of the oscillating portion was visible in the basin's viewport. The 200-ft array exhibited this behavior at only the highest tow speed of 25 kn. The 50-ft array exhibited the dynamic instability at both the 10 and 20-kn tow speeds. The difference in array length and the drag at the tail has affected this behavior. An examination of the photographs shows that the frequency of oscillation f, in hertz, increased with speed, from about 2.5 at 10 kn to about 8 at 25 kn (Fig. 9.7). Only a relatively short length of the tail (6 diameters) was dynamically unstable; the amplitude of oscillation was about 3 diameters.

A stability map, showing the range of the static and dynamic instabilities, was generated in the nondimensional format of u and ε (Fig. 9.8). The dynamic instability range is seen to be two orders of magnitude away from the static instability range.

9.2 Steady-State Model

9.2.1 Straight Tow Case

Based on the survey of the MAST array discussed in Section 8, a weight file for the 200-ft array was generated for input to the steady-state program, ARRAY. The weight file was based on a segment spacing of 2.35 ft between the discrete weights. The buoyancy was observed to be constant along the length of the array. The net buoyancy was adjusted by varying the quantity of fill oil until a net positive buoyancy of 13 lb was obtained.

The weight and buoyancy distributions along the array's length are shown in Fig. 9.9. The positive values show the buoyancy; the negative ones the weight. The units are pounds per 2.35 ft segment.

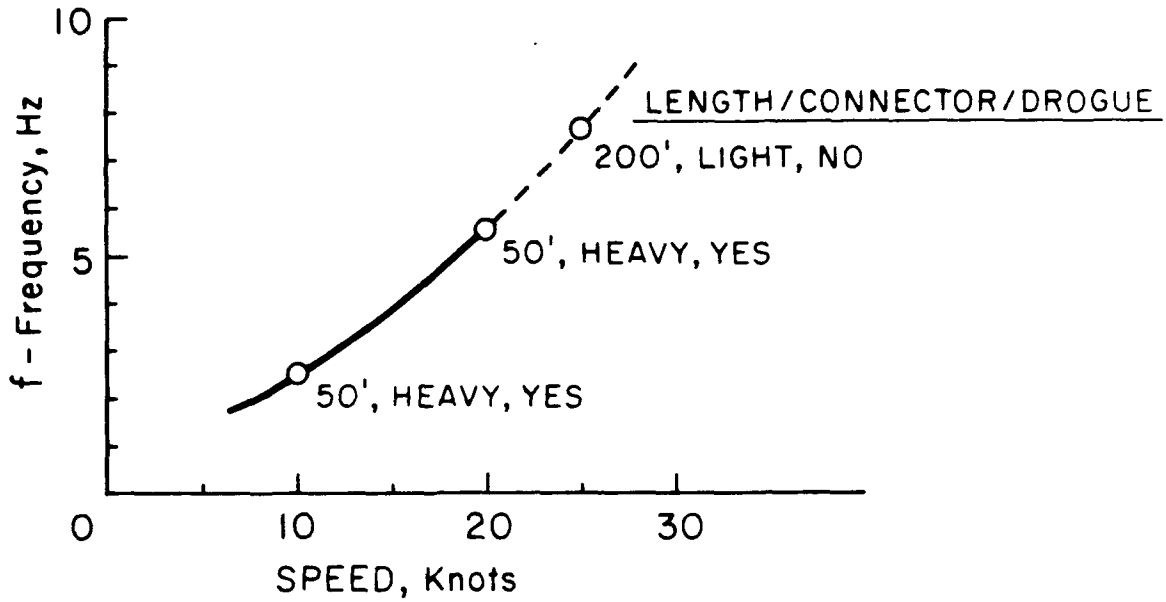

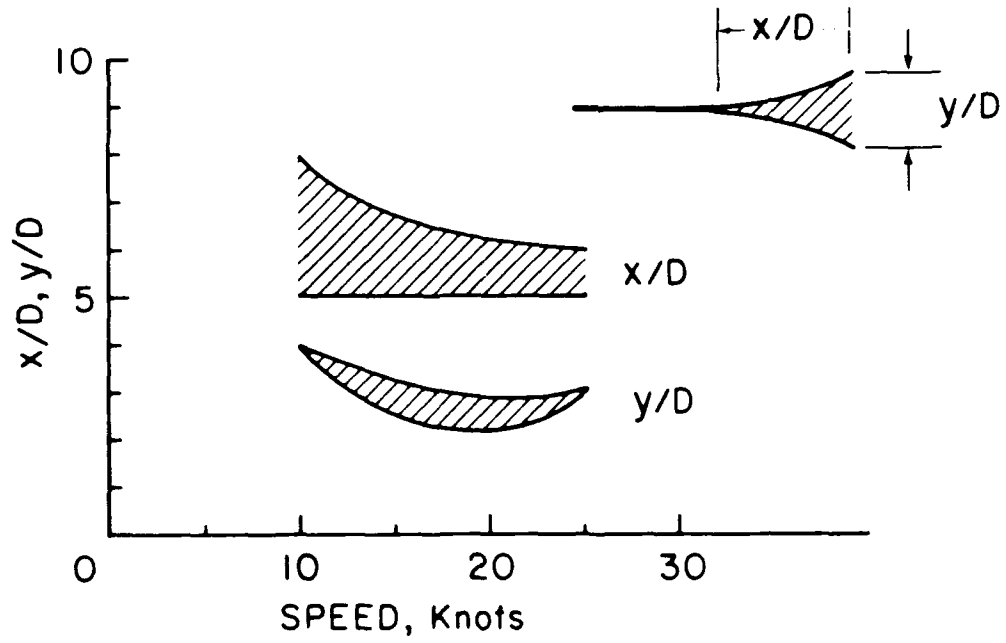

Figure 9.7. Array dynamic instability characteristics.

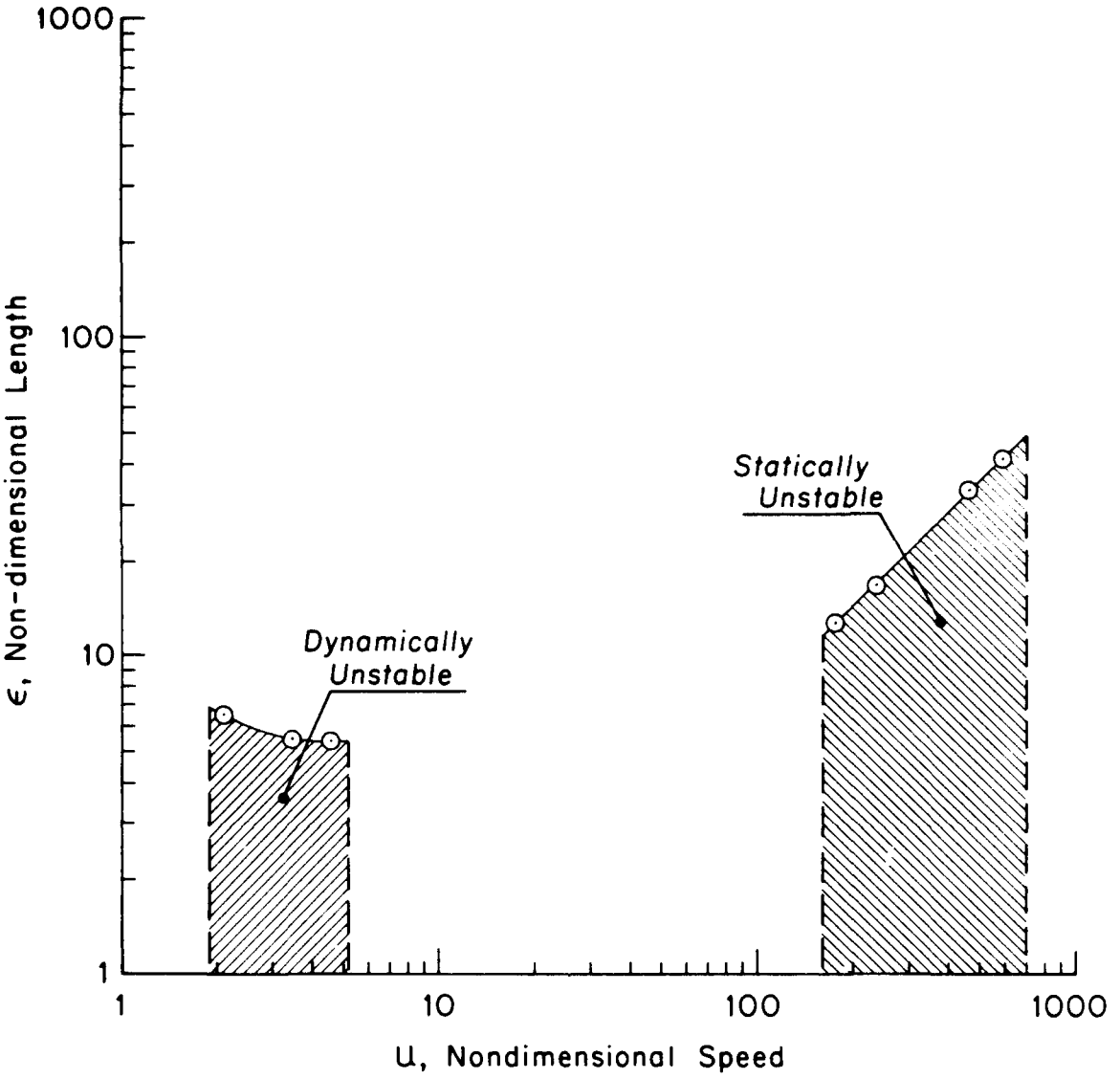

Figure 9.8. Array stability regimes.

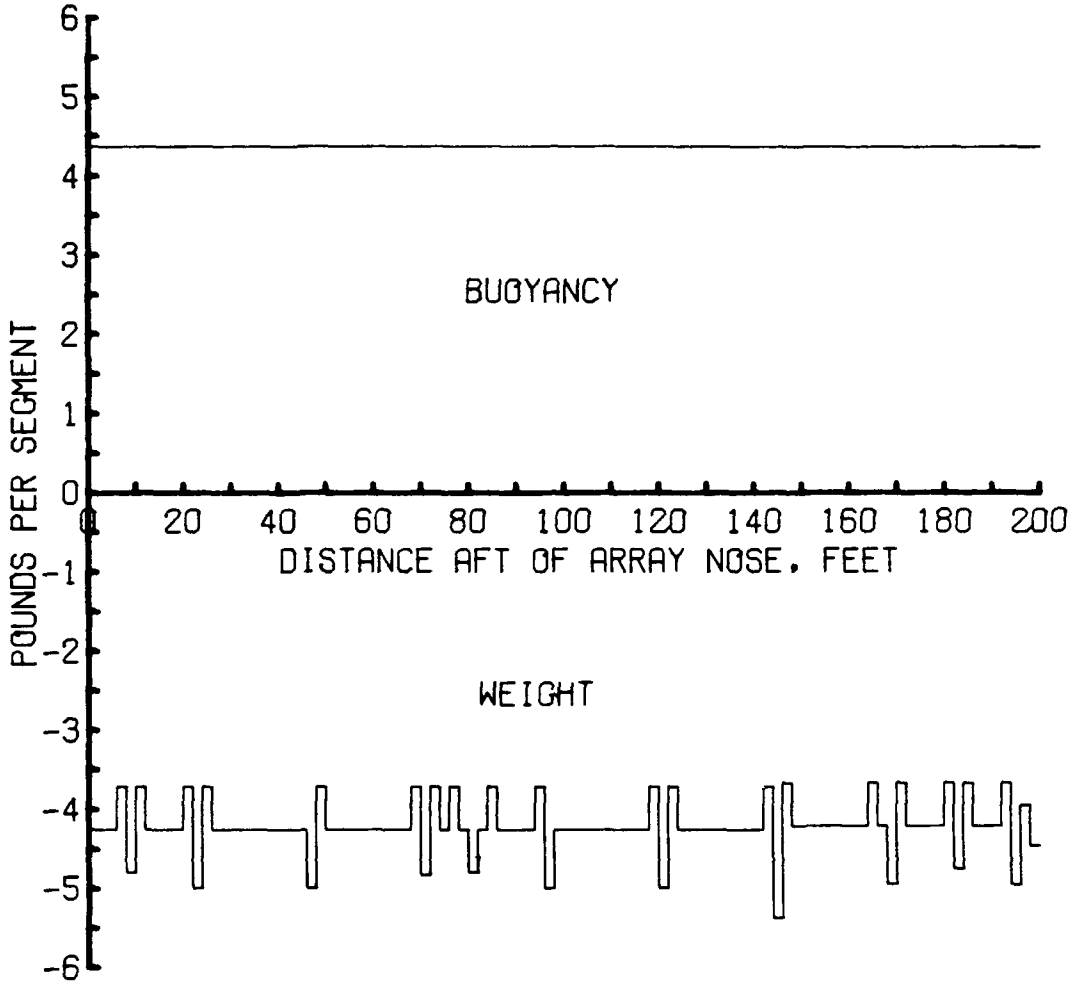

Figure 9.9. MAST array weight and buoyancy distributions. Segment length = 2.35 ft.

Combining the two (Fig. 9.10) shows the net weight/buoyancy distribution. The integral of the area under this curve is the total net buoyancy. A positive buoyancy indicates that the array floats.

The array was assumed to use two types of drogues: (1) a 12.5-in. long, variable-drag cone in which half-angle decreased with speed, and (2) 15 ft of 2.25-in. diameter rope.

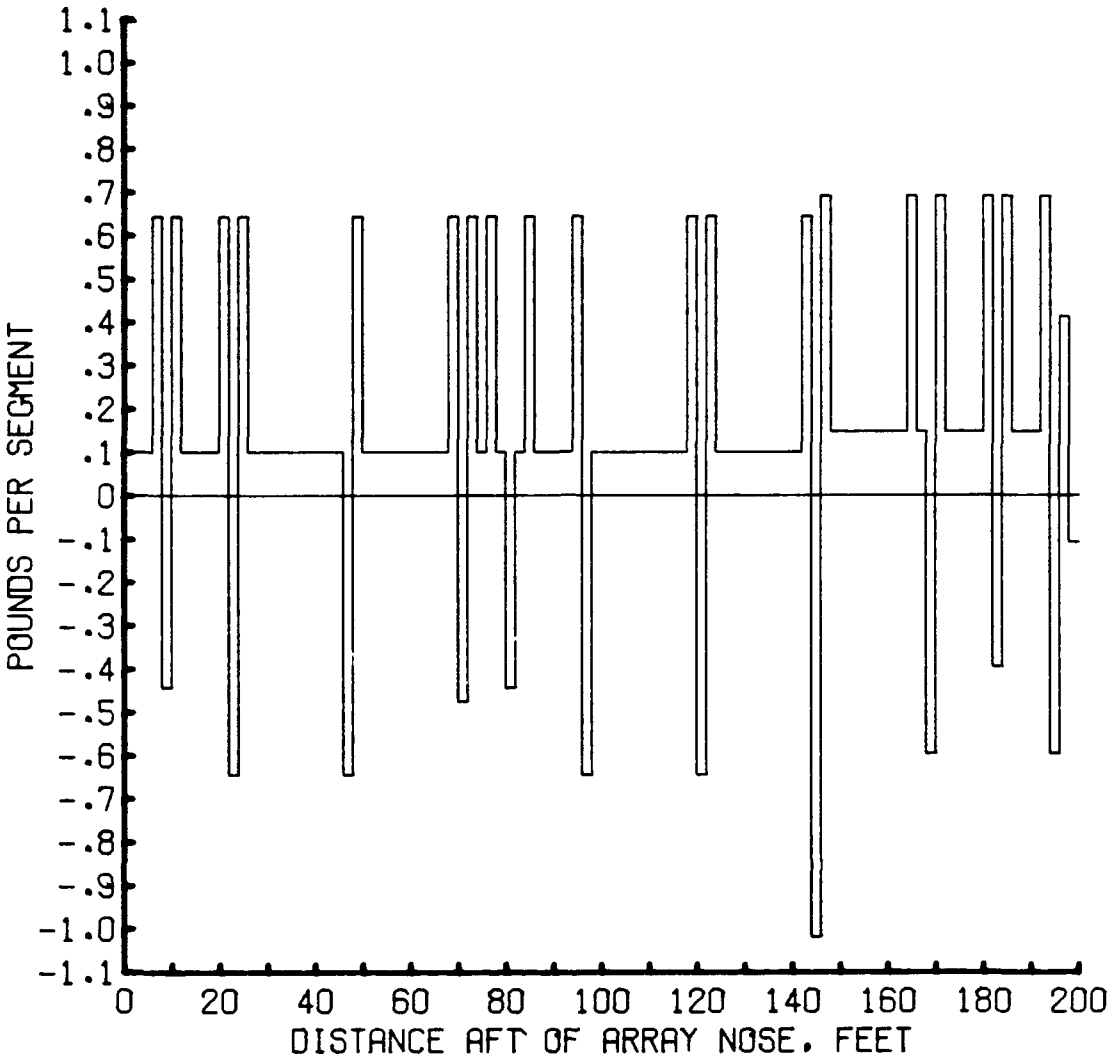

Figure 9.10. MAST array composite distributions. Total net buoyancy is 13 lb positive.

The half-angle of the cone drogue was assumed to vary from 30 degrees at 1 kn to 0 degrees at 10.5 kn. The product of the drag coefficient and the base area is shown in Fig. 9.11. A coefficient of friction of 0.0027 was assumed for the rope drogue; the product of the friction coefficient and wetted area is also shown in Fig. 9.11.

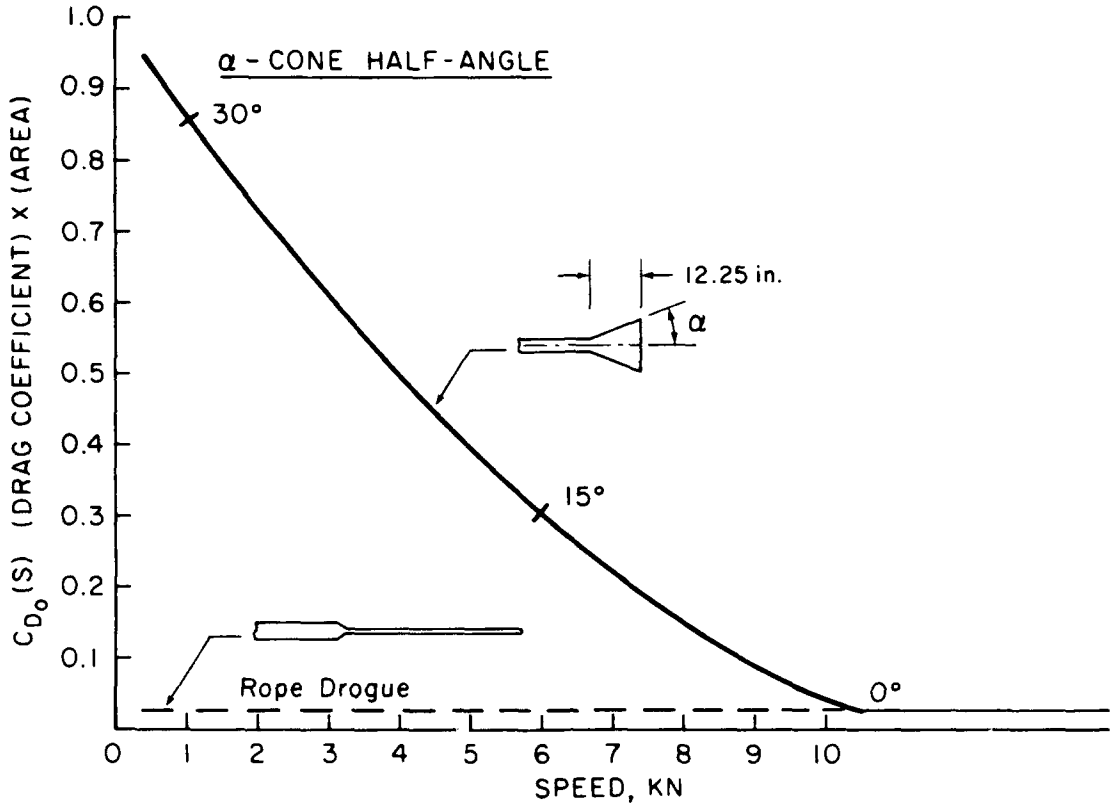

Figure 9.11. Drogue drag characteristics.

The tabular data listing for the ARRAY program output is shown in Fig. 9.12 for a speed of 1 kn. Listings for speeds of 2, 3, 4, 5, 10, 20 and 25 kn are contained in Appendix C.

The tension at the drogue (i.e., the drogue drag) and at the tow-point (drogue plus array drag) as a function of speed is shown in Fig. 9.13. The variable-drag drogue increases the tension at the array tail by a factor of 10 at 5 kn; however, the tow point tension is increased by only a factor of 2.

```
EVENT DESCRIPTION
SHIPS SPEED              1.000  KNOTS
TURN RATE                    0  DEGREES/SEC


ARRAY DIAMETER           2.500  INCHES
ARRAY LENGTH           200.000  FEET
CN=    1.2000  CNN=     1.2000  CF=      .0027

BUOYANCY PER FOOT OF ARRAY                    2.1816  POUNDS PER FOOT
TOTAL BUOYANCY OF ARRAY                     436.3194  POUNDS

500 DISTRIBUTED WEIGHT SEGMENTS ARE GENERATED FROM ARRAY DATA
AVERAGE WEIGHT PER FOOT OF ARRAY              2.1161  POUNDS PER FOOT
TOTAL WEIGHT OF ARRAY                       423.2182  POUNDS

POSITIVE NET BUOYANCY IS LIGHT ARRAY, NEGATIVE IS HEAVY ARRAY
AVERAGE NET BUOYANCY PER FOOT OF ARRAY         .0655  POUNDS PER FOOT (LIGHT)
TOTAL NET BUOYANCY OF ARRAY                  13.1012  POUNDS (LIGHT)

COORDINATE ORIGIN AT TOW VEHICLE
```

SCOPE (FEET)	TENSION (POUNDS)	TRAIL (FEET)	DEPTH (FEET)	SIDE TRAIL (FEET)	TOWLINE ANGLE (DEGREES)	KITE ANGLE (DEGREES)
0	2.430	0	0	0	-14.215	0
.400	2.324	-3.940	-.665	0	-3.984	0
4.000	2.316	-7.841	-1.522	0	-13.196	0
8.000	2.273	-11.758	-2.326	0	-14.519	0
12.000	2.185	-15.678	-3.108	0	-9.885	0
16.000	2.139	-19.592	-3.925	0	-11.356	0
20.000	2.063	-23.521	-4.662	0	-5.881	0
24.000	2.025	-27.471	-5.275	0	-5.403	0
28.000	1.988	-31.398	-5.974	0	-8.234	0
32.000	1.945	-35.328	-6.706	0	-8.916	0
36.000	1.902	-39.260	-7.428	0	-9.539	0
40.000	1.863	-43.204	-8.083	0	-9.492	0
44.000	1.823	-47.148	-8.733	0	-9.395	0
48.000	1.767	-51.108	-9.269	0	-1.071	0
52.000	1.746	-55.040	-9.855	0	-10.124	0
56.000	1.715	-59.006	-10.356	0	-9.950	0
60.000	1.685	-62.974	-10.835	0	-9.595	0
64.000	1.653	-66.931	-11.405	0	-10.072	0
68.000	1.597	-70.888	-11.962	0	-2.358	0
72.000	1.567	-74.853	-12.458	0	-2.087	0
76.000	1.531	-78.788	-13.048	0	-6.389	0
80.000	1.498	-82.744	-13.617	0	-6.857	0
84.000	1.466	-86.702	-14.166	0	-7.148	0
88.000	1.434	-90.659	-14.715	0	-7.480	0
92.000	1.403	-94.623	-15.223	0	-7.342	0
96.000	1.372	-98.588	-15.717	0	-7.060	0
100.000	1.346	-102.530	-16.195	0	-11.342	0
104.000	1.313	-106.473	-16.841	0	-13.089	0
108.000	1.242	-110.404	-17.563	0	-5.395	0
112.000	1.207	-114.355	-18.138	0	-6.270	0
116.000	1.172	-118.303	-18.718	0	-7.384	0
120.000	1.124	-122.184	-19.656	0	-14.675	0
124.000	1.088	-126.093	-20.350	0	-19.360	0
128.000	.960	-129.973	-21.259	0	-.645	0
132.000	.933	-133.944	-21.652	0	.887	0
136.000	.923	-137.915	-22.001	0	-11.978	0
140.000	.891	-141.881	-22.433	0	-11.344	0
144.000	.860	-145.854	-22.773	0	-9.440	0
148.000	.824	-149.770	-23.093	0	-15.060	0
152.000	.762	-153.715	-23.665	0	.475	0
156.000	.730	-157.674	-24.128	0	.872	0
160.000	.699	-161.631	-24.587	0	1.232	0
164.000	.666	-165.585	-25.056	0	1.324	0
168.000	.629	-169.530	-25.587	0	-.008	0
172.000	.619	-173.433	-25.625	0	-22.218	0
176.000	.491	-177.270	-26.588	0	11.860	0
180.000	.463	-181.196	-26.949	0	-19.943	0
184.000	.371	-185.063	-27.788	0	-2.688	0
188.000	.317	-188.956	-28.074	0	.433	0
192.000	.235	-192.760	-28.608	0	-22.482	0
196.000	.093	-196.075	-29.290	0	-36.502	0
200.000	.075	-196.394	-29.532	0	0	0

Figure 9.12. ARRAY program output.

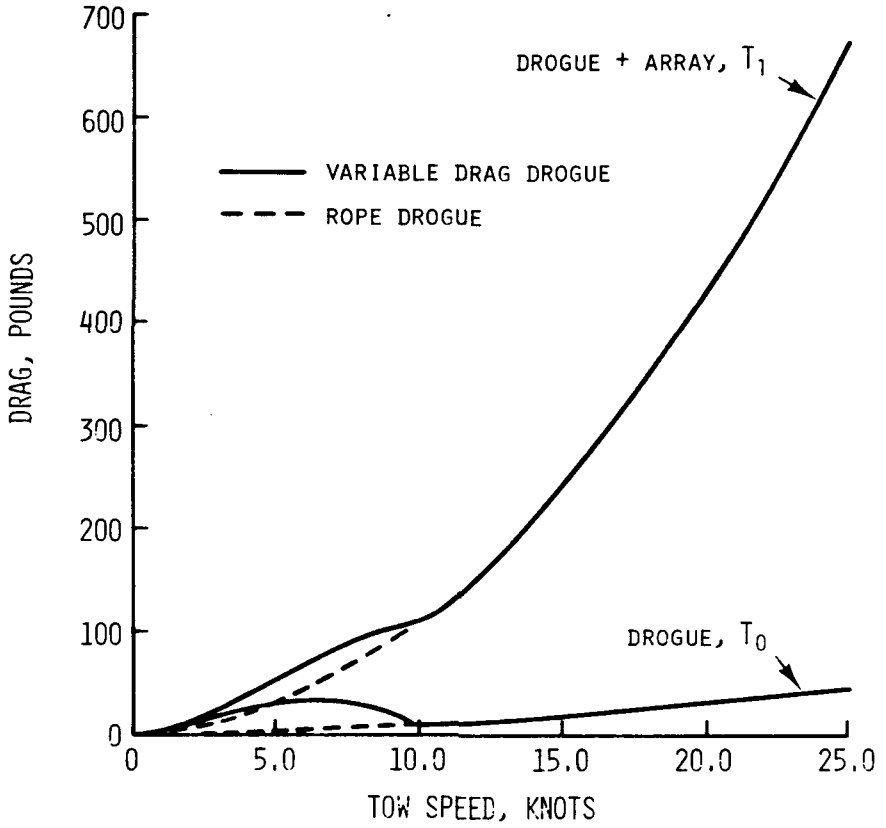

Figure 9.13. Drogue and drogue + array drag versus tow speed.

The array configuration is shown as a function of speed from 1 to 25 kn for the rope drogue and for the variable-drag cone in Figs. 9.14 and 9.15. The vertical scale is exaggerated to show the effect of drogue drag on the distortion due to the weight/buoyancy distribution. The effect of the weight/buoyancy distribution with the lower drogue drag is quite evident at 1 kn. The variable-drag drogue with its higher drag reduces the amount of vertical array distortion over the rope drogue from about 2 ft (0.01 percent length) to 1 ft.

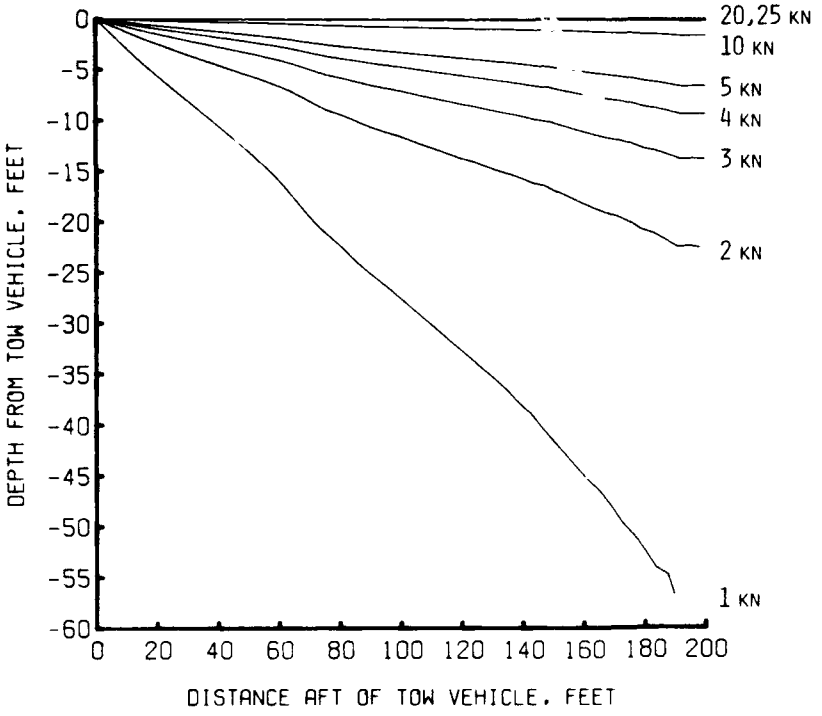

Figure 9.14

Side view of MAST array towed at 1, 2, 3, 4, 5, 10, 20, and 25 kn; NUSC rope drogue configuration.

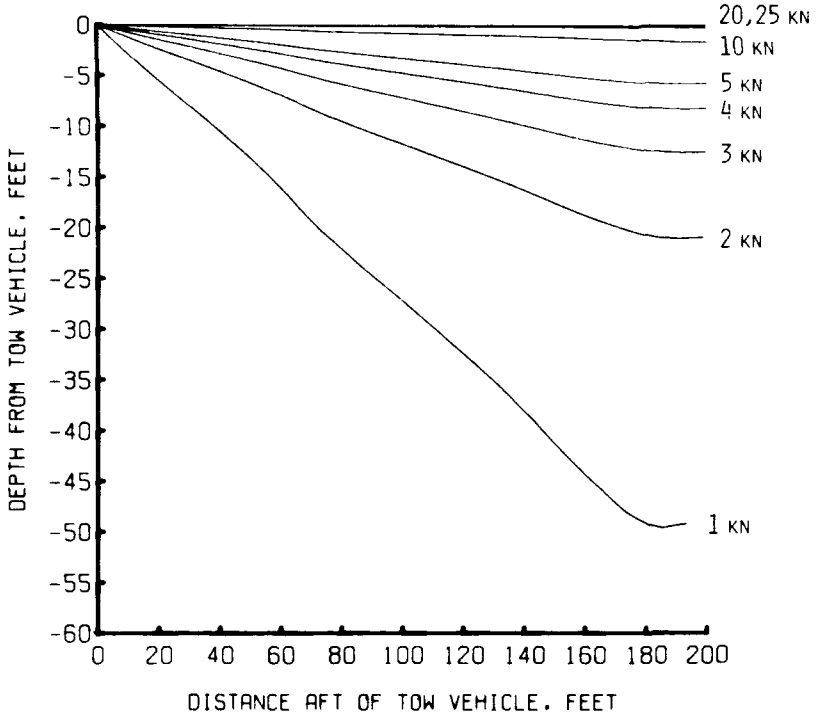

Figure 9.15

Side view of MAST array towed at 1, 2, 3, 4, 5, 10, 20, and 25 kn; variable-drag drogue configuration.

The array is also seen to float upward with the tail about 30 ft (15 percent length) above the tow point. If we define a "float" angle as

$$\theta = \tan^{-1}(y_t/x_t) \tag{9.1}$$

where x_t = array length and y_t = tail vertical displacement, we can see the effect of speed on the array's position relative to the horizontal. The difference between the two drogues is negligible (Fig. 9.16); the float angle quickly decreases from about 8.5° at 1 kn to less than 1° at 5 kn. Thus, we see that the drogue resistance is effective in straightening the array about its mean position but not relative to the horizontal.

This straightening effect is clearly seen if we examine the local array angle relative to the horizontal along the length of the array. These angles are shown in Fig. 9.17 for the rope drogue configuration and Fig. 9.18 for the variable-drag drogue.

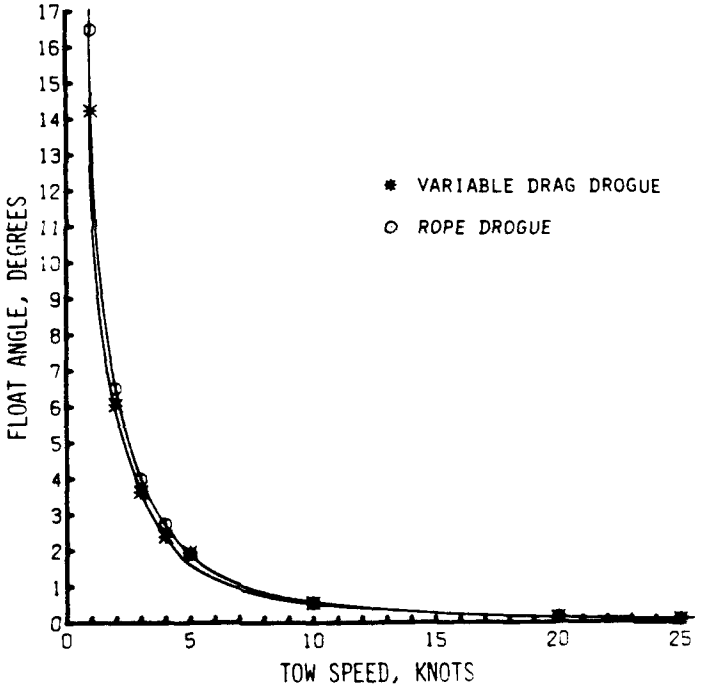

Figure 9.16
Float angle of array tail versus tow speed.

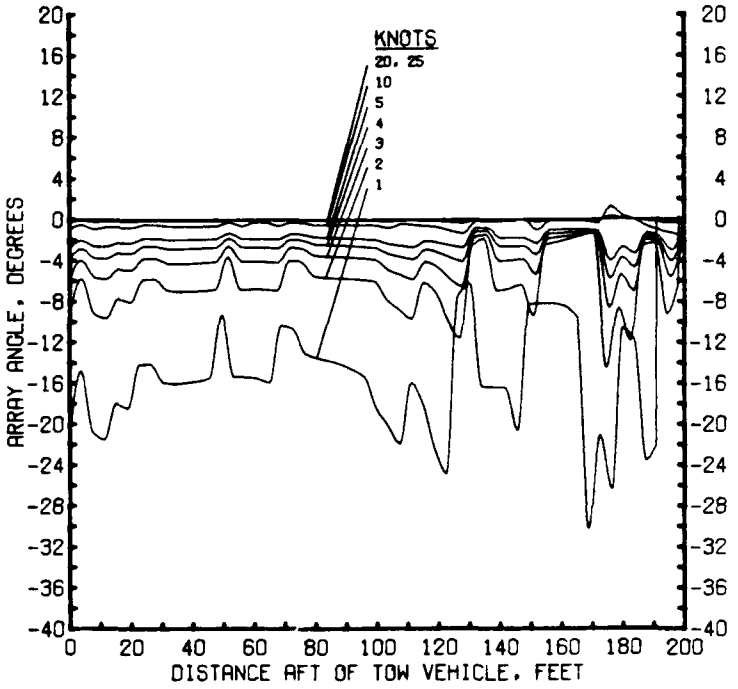

Figure 9.17

Array angle with NUSC rope drogue.

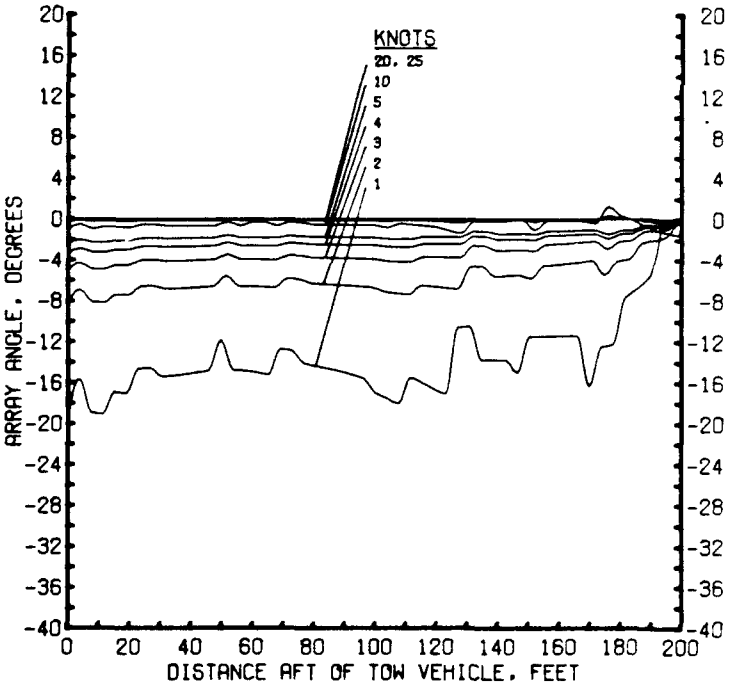

Figure 9.18

Array angle with variable-drag drogue.

9.2.2 Steady-Turn Case

The steady-state model was then exercised in the steady-turn mode. Comparison data were obtained from Ref. 12 for the time domain, finite-length array model. A 90° turn to port was executed with an initial speed of 8.5 ft/s, with a 250-ft turn radius; the turn rate was 1.95°/s.

The finite-length array model consisted of six elements including a 15-ft drogue. The elements were of varying lengths:

Element	Length, ft
1	25
2	42
3	48
4	48
5	42
6	15

The nodes were placed at either projector or hydrophone clusters. The array had an overall length of 205 ft (diameter of 2.25 in.) and was assumed to be neutrally buoyant. These conditions were duplicated in the steady-state model.

The X,Y (plan-view) plot at time 35 s (Fig. 23, Ref. 12) was digitized and enhanced by adding the tow-vehicle path for a steady turn. The array configurations from the steady-state model and the finite-element model can be compared in Figs. 9.19 and 9.20. Two conclusions can be drawn: the array lies slightly to the outside of the tow-vehicle path, and the array configurations are very similar. The last element of the finite-length model represents the drogue, which is not plotted on the steady-state output. The numerical output from the steady-state model is shown in Appendix A.

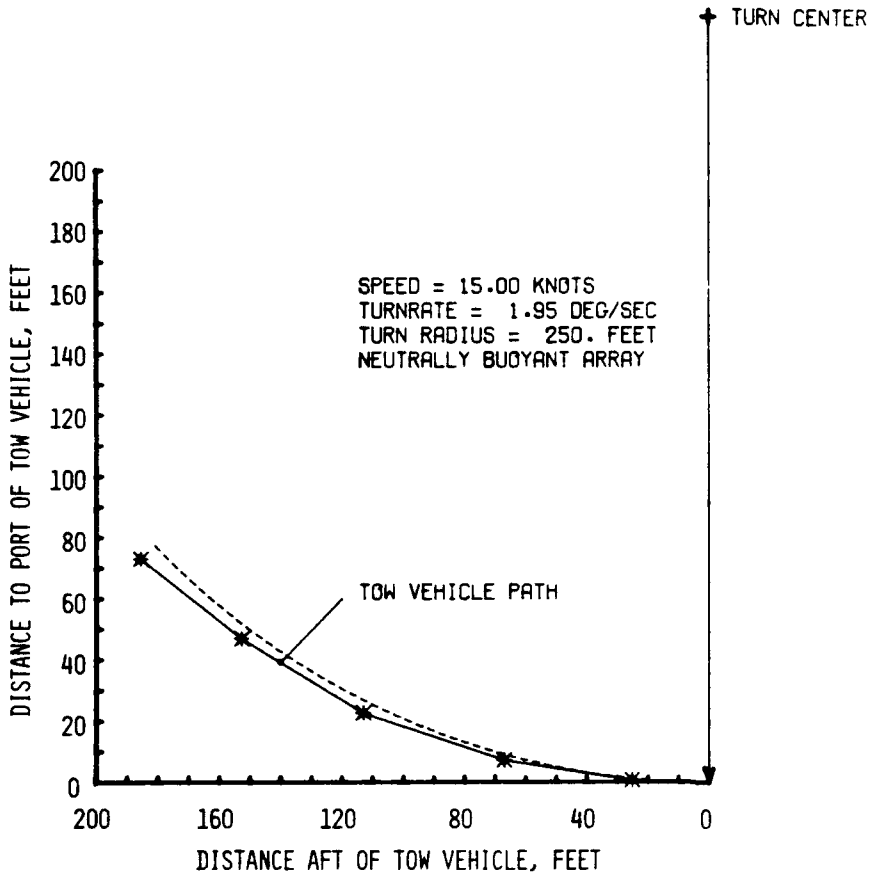

Figure 9.19

Plan view of array at T = 35 seconds (from Ref. 12, Fig. 23).

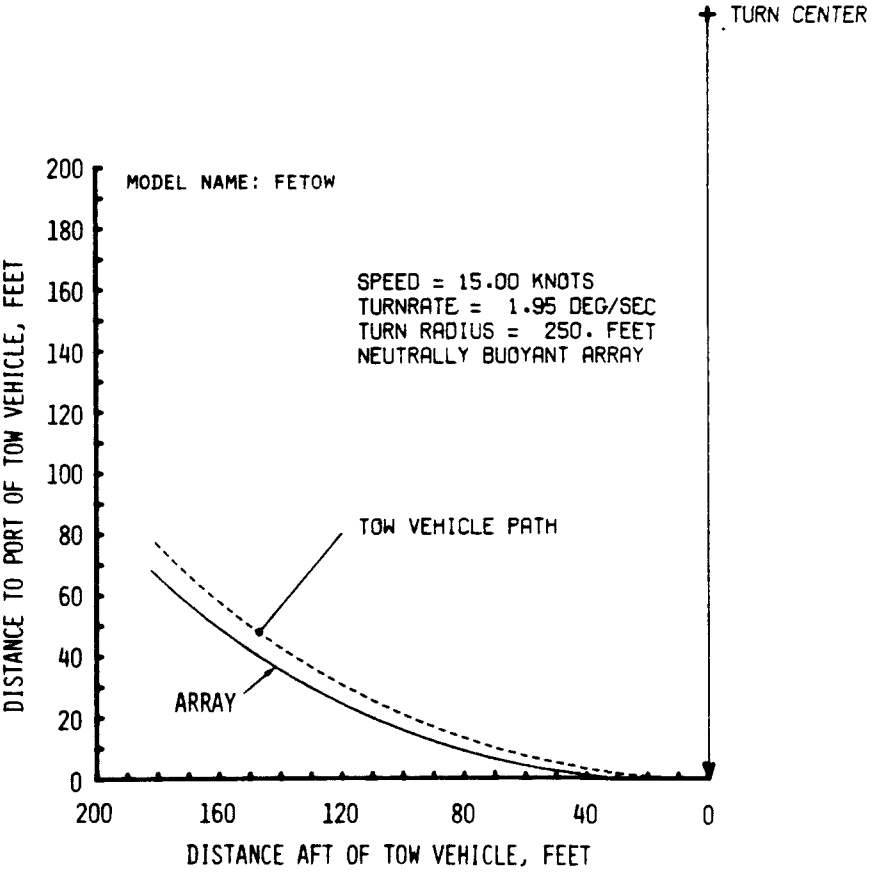

Figure 9.20

NUSC test case.

9.3 Hydroelastic Model

9.3.1 Physics of Instability

The physics of array instability may be best understood by examining the static instability case. If we assume that the array has taken an arbitrarily bowed shape, Fig. 9.21, we see that a hydrodynamic lift or side force exists analogous to that on a cambered airfoil. This lift force acts to increase the camber, while, in contrast, the elastic forces act to restrain this increase in camber.

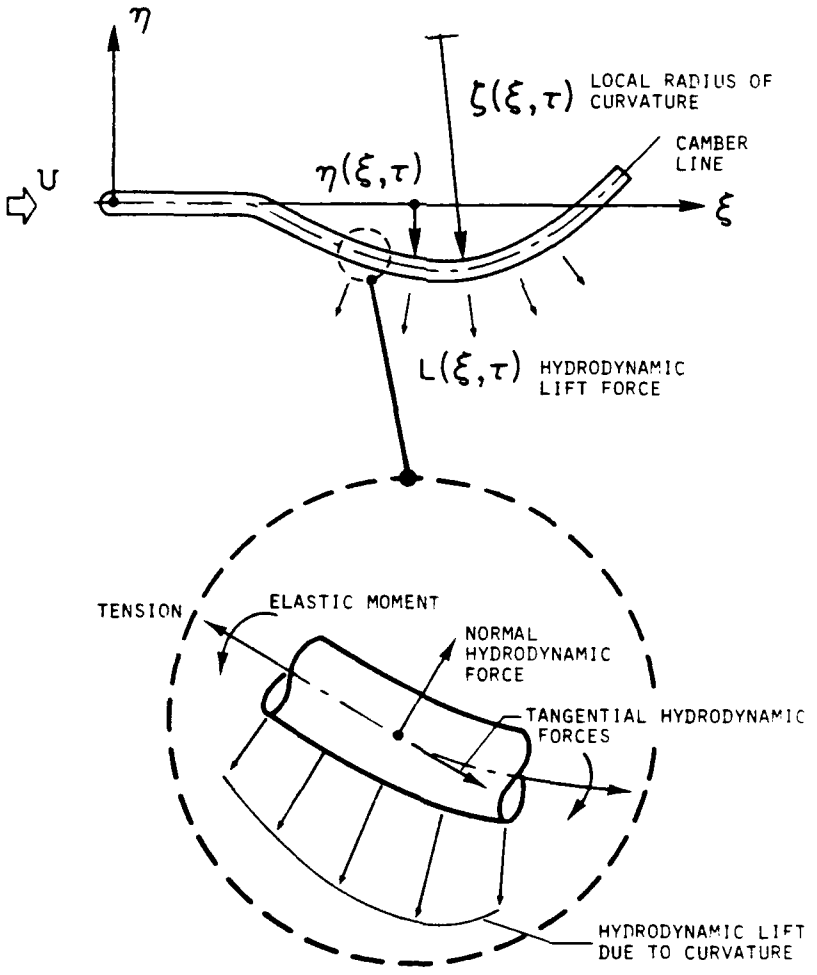

Figure 9.21. Array hydrodynamic lift force due to camber.

The instantaneous lift force per unit length of the array is the inviscid slender body hydrodynamic force whose form was developed by Lighthill (Ref. 22). The lift force is equal and opposite to the rate of change in the momentum of the fluid flowing over the array:

$$L(\xi,\tau) = \rho S[U(\xi,\tau)]\left(\frac{\partial}{\partial\tau} + U\frac{\partial}{\partial\xi}\right) \tag{9.2}$$

where

$$U(\xi,\tau) = \frac{\partial\eta}{\partial\tau} + \frac{U\partial\eta}{\partial\xi}. \tag{9.3}$$

Combining (9.2) and (9.3), we obtain

$$L(\xi,\tau) = \rho S\left(\frac{\partial^2\eta}{\partial\tau^2} + \frac{2U\partial^2\eta}{\partial\xi\partial\tau} + \frac{U^2\partial^2\eta}{\partial\xi^2}\right). \tag{9.4}$$

The steady-state term is simply

$$L(\xi) = \rho SU^2\frac{\partial^2\eta}{\partial\xi^2}, \tag{9.5}$$

where

$$\frac{\partial^2\eta}{\partial\xi^2} = \frac{1}{\rho(\xi)} = 1/\text{local radius of curvature along the array due to the deformed shape.}$$

The array instability may then be examined by eliminating all time-dependent terms in Eq. (7.16), resulting in

$$\frac{EI}{L^2}\frac{\partial^4\eta}{\partial\xi^4} + \rho S\frac{U^2\partial^2\eta}{\partial\xi^2} + 1/2\rho S\varepsilon U^2C_f\frac{\partial\eta}{\partial\xi} - 1/2\rho StU^2C_f(1/2-\xi)\frac{\partial^2\eta}{\partial\xi^2}$$

$$- T_2\frac{\partial^2\eta}{\partial\xi^2} = 0, \tag{9.6}$$

where the first term is the elastic force, the second term is the array lift force, the third and fourth terms are the array viscous normal and tangential forces, and the fifth term is the drogue drag.

An examination of the second term shows that the array lift term contains $\partial^2\eta/\partial\xi^2$, which is equivalent to the reciprocal of the array radius of curvature. The second fact that is important is that this term varies as the square of the velocity. Thus for a sufficiently high velocity, the destabilizing lift force represented by the second term will overcome the stabilizing flexural and tensile restoring forces represented by the first, third, fourth, and fifth terms.

9.3.2 MAST Array Hydroelastic Behavior

The hydroelastic behavior of the MAST array was investigated using program SNAKE. The nose-piece was assumed to be a hemisphere so that ℓ_1 = D/2 and λ_1 =1/2ε. The bending stiffness EI was estimated to be 7.8125 lb-ft, assuming that the hose material (Tygon) had a modulus of elasticity E of 1700 psi and a thickness of 0.126 in. Two array drogue configurations were considered, a blunt base and a cone with a base area 5 times that of the array base. The array tangential drag coefficient was assumed to be $C_f = 0.00375$ ($C_f' = 0.015$).

Solutions for mode 0 (static instability) and mode 1 were not computed by SNAKE. Stability (Argand) plots were computed for modes 2, 3, and 4 for length/diameter ratios ε of 10, 50, 100, 500, and 1000. Mode 2 plots for ε = 10, 100, and 1000 are shown in Figs. 9.22 through 9.24. The critical speeds for instability, Im(ω) =0, were then determined for each mode, and stability maps generated. Stability maps for modes 2, 3, and 4 for the blunt base array are shown in Figs. 9.25 to 9.27. For ε less than 500 the mode 2 array, Fig. 9.25, is stable up to a certain critical speed and then exhibits an unstable region to a second critical speed where it becomes stable again. These critical speeds decrease as ε increases. For ε greater

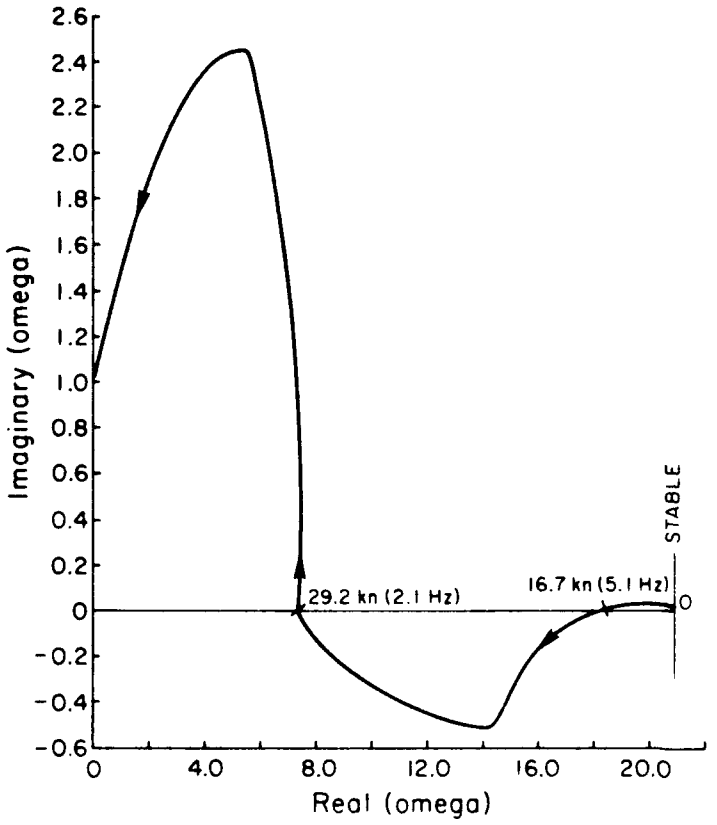

Figure 9.22

Stability plot for mode 2. $\varepsilon = 10$, $\alpha = 0.85$, $C_f' = 0.015$, QD = 1, $\Lambda = 10$.

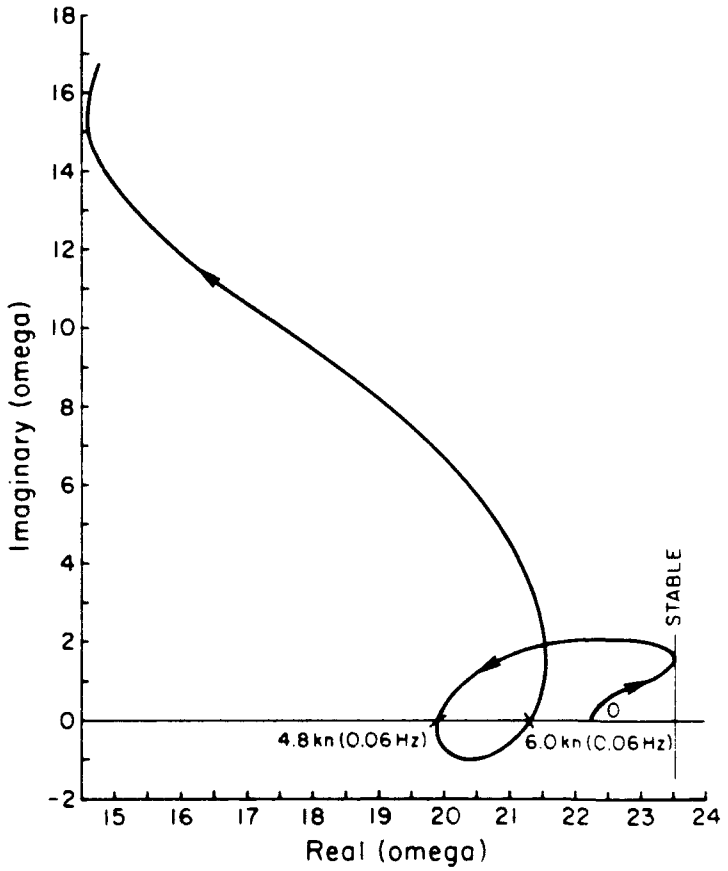

Figure 9.23

Stability plot for mode 2. $\varepsilon = 100$, $\alpha = 0.85$, $C_f' = 0.015$, QD = 1, $\Lambda = 10$.

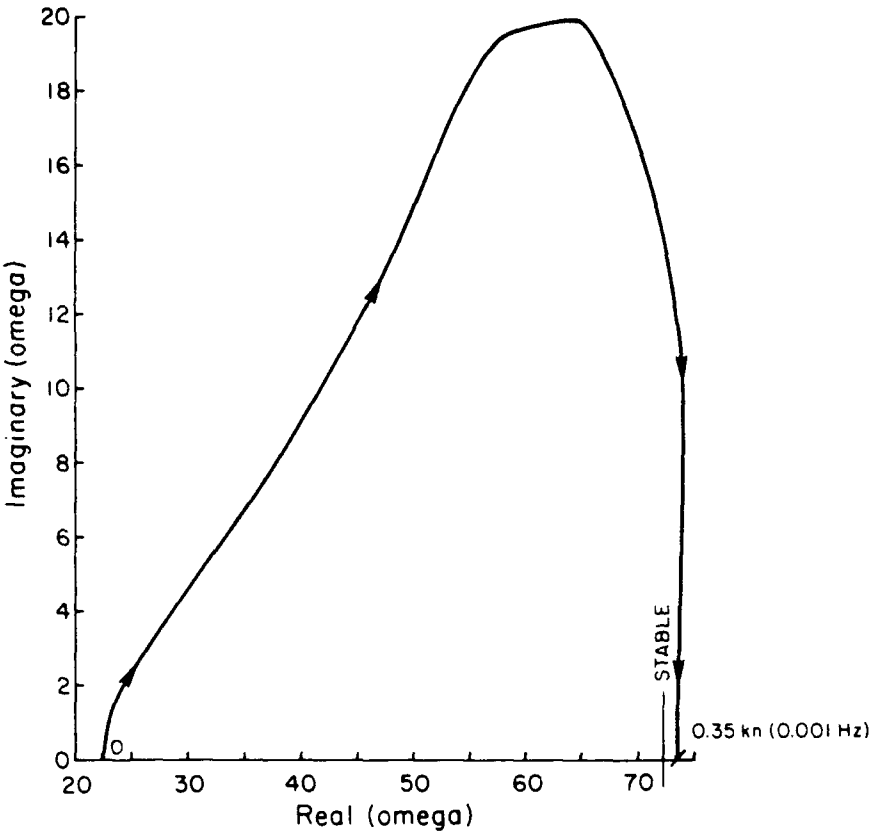

Figure 9.24

Stability plot for mode 2. $\varepsilon = 1000$, $\alpha = 0.85$, $C_f' = 0.015$, QD = 1, $\Lambda = 10$.

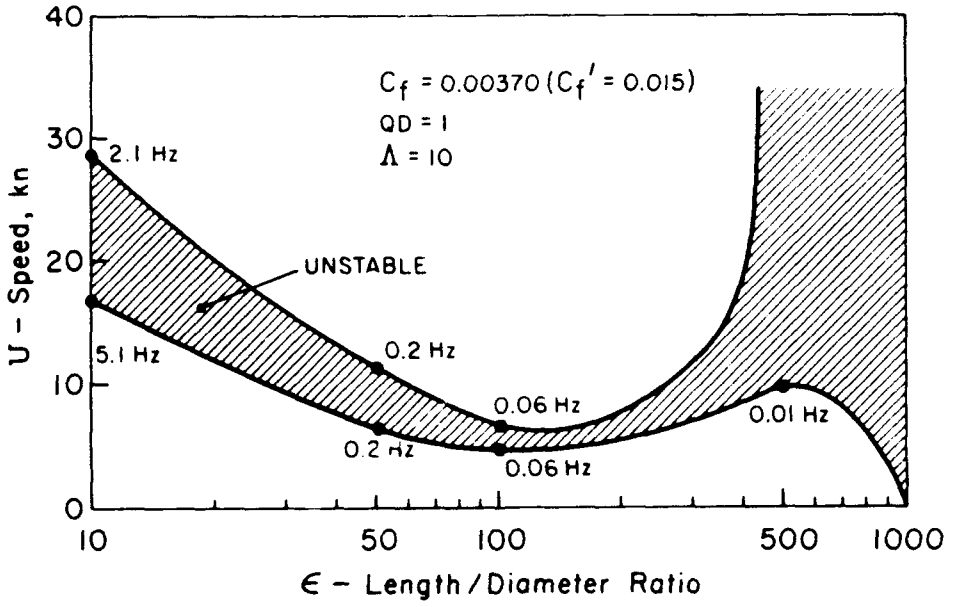

Figure 9.25. Mode 2 stability map (blunt base).

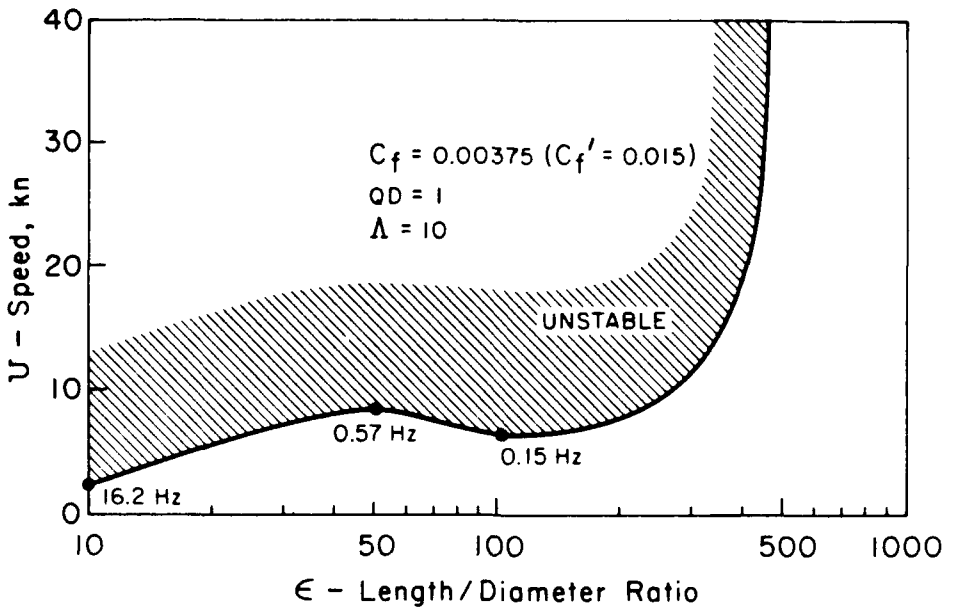

Figure 9.26. Mode 3 stability map (blunt base).

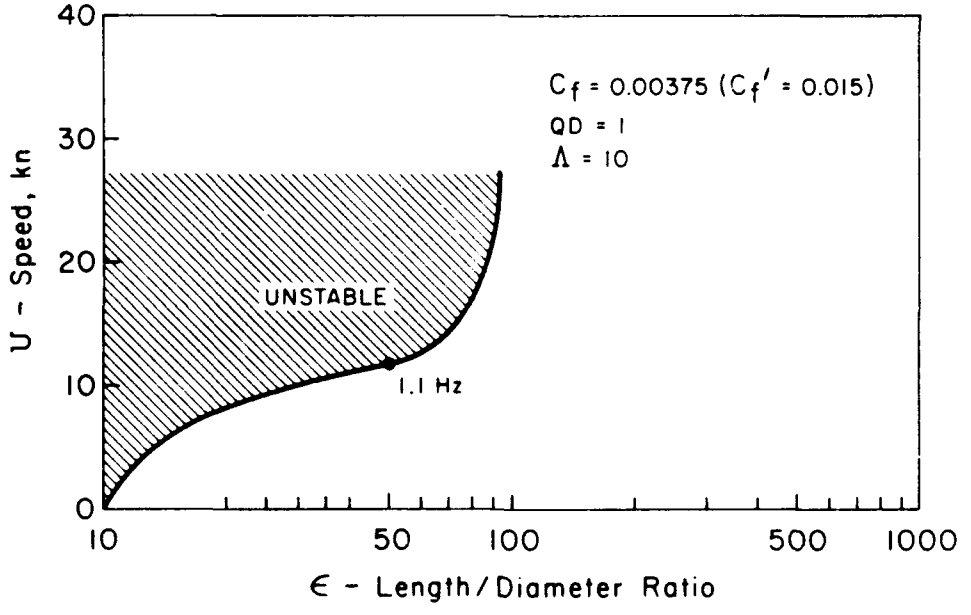

Figure 9.27. Mode 4 stability map (blunt base).

than 1000, the mode 2 array is unstable for all speeds. The mode 3 stability map, Fig. 9.26, shows that the array is always unstable above the critical speed, which increases with ϵ. For ϵ greater than 500, the array is always stable. The mode 4 stability map shows a similar behavior, except that for ϵ greater than 100 the array is always stable.

The stability maps for the array with the cone drogue are shown in Figs. 9.28 to 9.30. The effects of increasing the tension at the tail are evident. In all cases the stable regions are expanded. The mode 2 map, Fig. 9.28, shows that the array is stable for all speeds up to ϵ = 100, after which the critical speed decreases with ϵ. For mode 3, Fig. 9.29, an unstable region exists for ϵ between 10 and 50, after which the array is always stable. Mode 4, Fig. 9.30, shows a small unstable region for ϵ between 10 and 50.

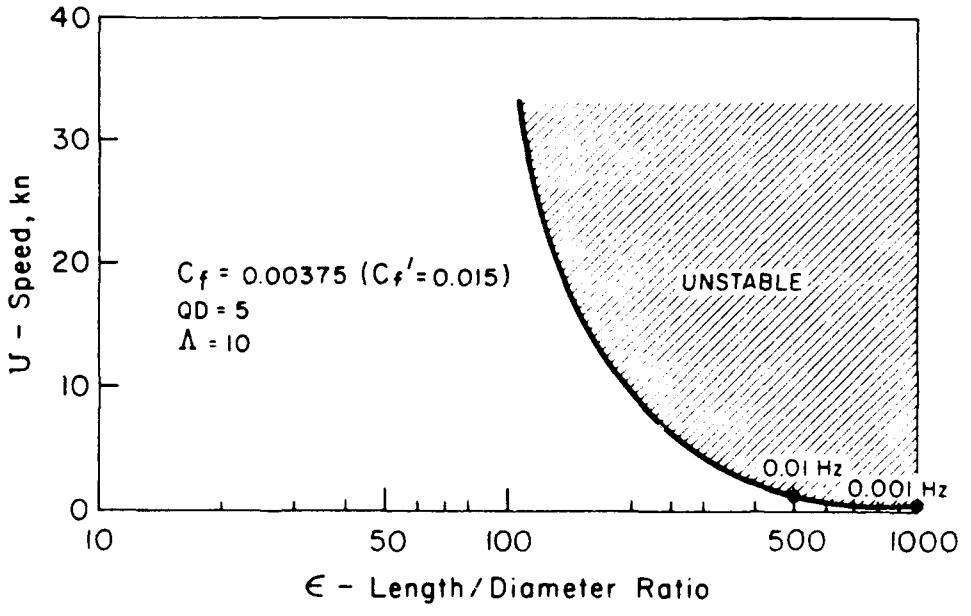

Figure 9.28. Mode 2 stability map (cone drogue).

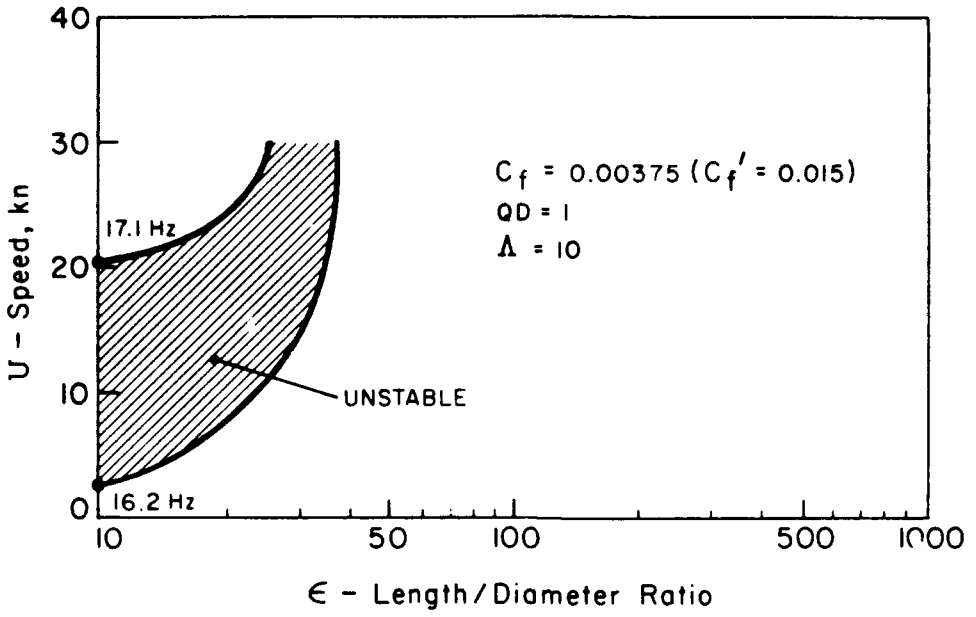

Figure 9.29. Mode 3 stability map (cone drogue).

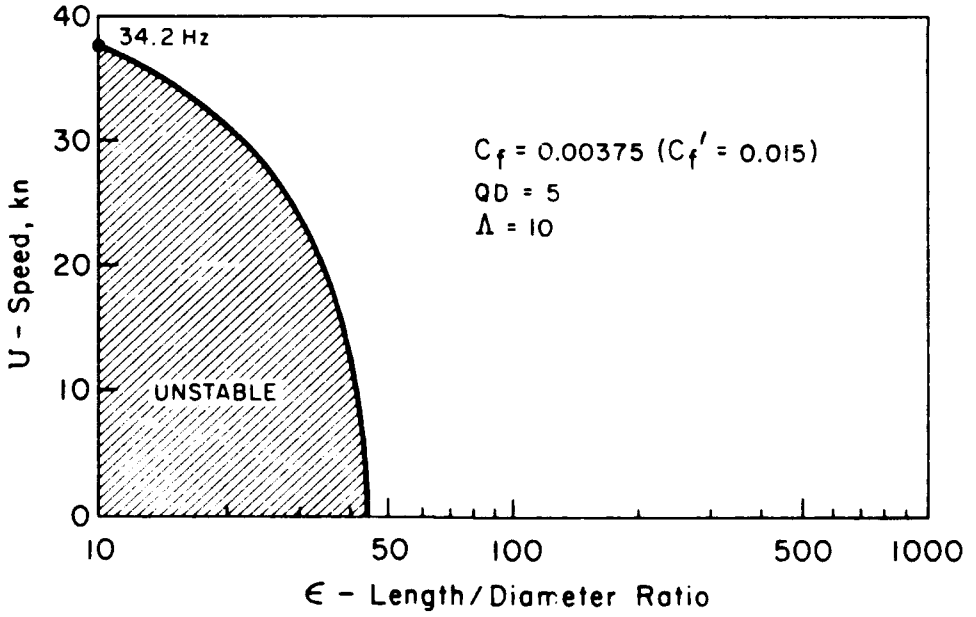

Figure 9.30. Mode 4 stability map (cone drogue).

The frequencies associated with the critical speeds are shown in parentheses in Figs. 9.22 through 9.30. The lower modes of motion (lower frequencies) will be the dominant modes for instability, the higher frequencies being superimposed on the lower ones. The critical speeds (about 5-20 kn) and frequencies (5-16 Hz) for mode 2 instabilities for $\varepsilon = 10$ are in fair agreement with the limited amount of data from the towing tank tests shown in Fig. 9.7. It is interesting to note that only the tail end of the array ($\varepsilon \simeq 6$) exhibits the dynamic instability. This is in agreement with the findings of Pao (Ref. 9) who concluded that the instability is confined to the tail portion up to $\varepsilon \simeq 25$. This makes sense, since the stabilizing effects of the bending rigidity become less important as ε increases. In other words, the beam-like behavior of the array wherein the bending rigidity is stabilizing is superseded by a string-like behavior where the flow induced stabilizing tension is dominant.

The computations in program SNAKE are carried out in nondimensional space. Consequently, the effect of the bending rigidity EI is accounted for simply in the conversion to dimensional space, i.e.,

$$U = u/L\sqrt{M/EI}$$

$$\omega = \omega/L^2\sqrt{(m + M)/EI} \qquad (9.7)$$

Thus the effect of changes in EI on the critical velocities and frequencies is accounted for by

$$U_2 = U_1 \sqrt{\frac{(EI)_2}{(EI)_1}}$$

$$\omega_2 = \omega_1 \sqrt{\frac{(EI)_2}{(EI)_1}} \; . \qquad (9.8)$$

10. CONCLUSIONS AND RECOMMENDATIONS

This report details the development and utilization of two of three computer programs required for the prediction of towed array static and dynamic characteristics. The two programs--ARRAY, which is a three-dimensional, steady-state, space domain model to predict the array shape and tension distribution, and SNAKE, which is a two-dimensional frequency domain model to predict array static and dynamic instability--have been used in a limited number of correlation studies with existing experimental information. Fair agreement has been achieved, but much work remains to be done in extending the model and full-scale array experimental data base. It is recommended that the following tasks be accomplished:

(1) The effort expended in reconstituting the deformed array configurations from the film of the DTNSRDC towing tank tests has emphasized both the importance of this information and the need for further development of the technique. In particular, a micro-computer based video-image processing system should be developed to enhance the present 16 mm film/digitizing board technique. The necessary equipment, based on the Apple computer, is presently on the market. This system should be investigated for its adaptability to the array configuration reconstitution problem.

(2) The development of the two array analysis programs (ARRAY and SNAKE), as well as the implementation of the NUSC finite time domain simulation (FETOW), should be continued.

Further development of the three analytical models should include incorporation of computer-aided engineering (CAE) features to upgrade the programs. Basically, CAE enhancement will result in "conversational" programs with 2-D and 3-D graphics output.

(3) Physical model tests of various array configurations should be conducted in a towing tank. It has been determined that a 1/5-scale model may be towed over a speed range that will scale the dynamic behavior of the full-size array. The use of physical models will allow the investigation of a wide range of advanced target system configurations. The model arrays should be approximately 40 ft in length with a diameter of 0.5 in. This model size would also be useful in that a complete target system could be modeled by utilizing an existing Mk 38 target powered body. This would allow investigation of the effect of propeller wake on array motions.

(4) A comprehensive evaluation of array "lift due to curvature" should also be pursued. A candidate computer program for evaluating this effect is PANAIR, developed by the Boeing Company. This program will be used for an initial estimate. The "lift" term should subsequently be incorporated into the ARRAY model.

11. REFERENCES

1. Paidoussis, M. P., and B. K. Yu, "Elastic Hydrodynamics of Towed Slender Bodies: The Effect of Nose and Tail Shapes on Stability," J. Hydronautics, Vol. 10, Oct. 1976, pp. 127-134.

2. Calkins, D. E., "Hydrodynamic Analysis of a High-Speed Marine Towed System," J. Hydronautics, Vol. 13, Jan. 1979, pp. 10-19.

3. Calkins, D. E., "A Non-Linear, Three-Dimensional Dynamic Towed System Model Based on the Finite Element Method," Dissertation, Department of Naval Architecture, University of California, Berkeley, Dec. 1975.

4. Paidoussis, M. P., "Dynamics of Flexible, Slender Cylinders in Axial Flow, Part 1, Theory," J. Fluid Mech., Vol. 26, 1966, pp. 716-736.

5. Paidoussis, M. P., "Dynamics of Flexible, Slender Cylinders in Axial Flow, Part 2, Experiments," J. Fluid Mech., Vol. 26, 1966, pp. 737-751.

6. Paidoussis, M. P., "Stability of Towed, Totally-Submerged Flexible Cylinders," J. Fluid Mech., Vol. 34, 1968, pp. 273-297.

7. Paidoussis, M. P., "Dynamics of Submerged Towed Cylinders," Proceedings of the 8th Symposium on Naval Hydrodynamics, Office of Naval Research, A.R.C. No. 179, 1970, pp. 981-1016.

8. Yu, B. K., "Elasto-Hydrodynamic Stability of a Towed Slender Body," Master of Engr. Thesis, Department of Mech. Engr., McGill University, May 1975.

9. Pao, H. P., "Dynamical Stability of a Towed Flexible Cylinder," J. Hydronautics, Vol. 4, 1970, pp. 145-150.

10. Pao, H. P., and Q. Tran, "Response of a Towed, Thin, Flexible Cylinder in a Viscous Fluid," J. Acous. Soc. Am., Vol. 53, No. 5, 1973, pp. 1441-1444.

11. Patel, J. S., "Dynamic Response of a Line Cable with Variable Length End Segment due to Time Dependent Kinematic Constraints," Naval Underwater Systems Center, TM No. EM-83-75, 28 Oct. 1975.

12. McLaughlin, E. L., "Dynamic Analysis of the Advanced ASW Target," Naval Underwater Systems Center, TM No. 801130, 13 Aug. 1980.

13. DeMetz, F. C., "Advanced ASW Mobile Target Spatial Array Hydrodynamic Stability Study Report," The Bendix Corporation, Report No. 8-5057, January 1981 (prepared for Naval Undersea Systems Center).

14. Hansen, R. J. and C. C. Ni, "An Experimental Study of the Flow-Induced Motions of a Flexible Cylinder in Axial Flow," J. Fluids Engr., Vol. 100, Dec. 1978, pp. 389-394.

15. Kennedy, R. M., "A Linear Theory of Transverse Cable Dynamics at Low Frequencies," Naval Underwater Systems Center, TR No. 6463, June 1981.

16. Berni, A. J., V. R. Kruka, L. D. Park, Jr., and R. P. McNerney, "Evaluation of a Solid Hydrophone Cable," Proceedings of 12th Annual Offshore Technology Conference, Vol. 3, OTC Paper 38071, 1980.

17. Hoerner, S. F., Fluid Dynamic Drag (published by author) 1965.

18. Taylor, G.I., "Analysis of the Swimming of Long and Narrow Animals," Proc. Royal Society, A21, 1952.

19. Ramsey, J. P., and D. B. Dillon, "Empirical Hydrodynamic Characterization of Two Bare, Double-Armored Towlines," Hydrospace Research Corp., TR No. 29, Nov. 1970.

20. Webster, B., J. Diggs, and P. Rispin, "A Summary of the Hydromechanical Characterization of Various Towed Array Tow Cables," David Taylor Naval Ship Research and Development Center, July 1974.

21. Gomez, D. T., "Launch Handling and Recovery of the Mobile Acoustic Spatial Target (MAST) Array," Naval Underwater Systems Center, TM No. 80-2028, March 1980.

22. Lighthill, M. J., "Note on the Swimming of Slender Fish," J. Fluid Mech., Vol. 97, 1960, pp. 305-317.

APPENDIX A

PROGRAM ARRAY

DESCRIPTION

ARRAY is a steady-state space domain, three-dimensional model of a towed flexible line array.

CAPABILITIES

The program determines the tension and three-dimensional spatial configuration of the line array as a function of distance along its arc length. It is capable of modeling both straight ahead tows and steady-state turns. A variety of drogue configurations is available. A constant weight can be used for each integration element, or an individual weight profile can be input for a specific array.

INPUT

(1) DIARAY - Diameter of array

(2) FLONG - Length of array

(3) USKNOT - Speed of tow-vehicle

(4) SIDDEG - Turn rate

(5) CN - Normal force coefficient

(6) CF - Tangential force coefficient

(7) WA - Weight per foot of array*

(8) MBX - Drogue configuration variable

*Alternately, a weight per element file (up to 1000 elements) may be used instead of a constant weight per foot.

OUTPUT

(1) Three-dimensional spatial coordinates of line angle referenced either to the tow-vehicle or to the tail of the array

(2) Tension as a function of array length

(3) Array angle relative to horizontal as a function of length

MODEL THEORY

A continuous line structure approach is used to model the array, and the resulting differential equations are integrated using the Runge-Kutta technique. The forces resulting from the array drogue are first computed; then, the normal and tangential forces resulting from the line array angle are integrated to yield the spatial coordinates and tension along the array's length.

INPUT DESCRIPTION

Eleven variables are required to run the program, eight of which have already been mentioned. The other three are used for program I/O control and execution. They are input on one card in an 8F8.4, 2I2, F8.4 format:

Column:

1 through 8 DIARAY - Diameter of array in inches.

9 through 16 FLONG - Length of array in feet.

17 through 24 USKNOT - Speed of tow-vehicle in knots.

25 through 32 SIDDEG - Turn rate or turn radius if SIDDEG is less than 10; then the value is assumed to be the turn rate in degrees of turn per second. If SIDDEG is greater than 10, the value is assumed to be the turn radius in feet. Positive values are turns to port; negative values are turns to starboard. For straight tow, use 0.0.

33 through 40 CN - Normal force coefficient for an inclined cylinder in flow.

41 through 48 CF - Tangential force coefficient, function of Reynolds number.

49 through 56 WA - Weight per foot of line array. If WA is equal to zero, a distributed weight profile with *SEG* number of segments is generated from a typical documented line array. If WA is less than zero, a weight file consisting of user-supplied element weights is read in. The number of elements read in must equal the value of *SEG* below.

Eight values are punched per card (Format SF 10.4) starting with the tail of the array. These cards are placed directly behind the first card containing DIARAY, FLONG, etc.

57 through 64 SEG - Number of integration segments used (maximum of 1000). This number determines the accuracy of the output, and generally must be higher if the array is unusually heavy or towed at slow speeds when the array angle becomes large. One hundred segments would be sufficient for an almost neutrally buoyant array; 500 or more may be needed for a heavy array (e.g., where the weight of the array in water exceeds 10% of the weight in air). If *WA* is less than zero, SEG must correspond to the number of elements/weights in the input.

65 through 66 MPRT - Output print control variable. If MPRT = 0, output is printed with coordinate system at tow-vehicle.

If MPRT = 1, output is printed with coordinate system at array tail and at tow-vehicle.

67 through 68 MBX - Drogue configuration control variable. If MBX = 1, a variable-drag drogue is used, with the diameter being inversely proportional to the towing speed up to 10 knots, where the drogue diameter reduces to the array diameter. If MBX = 2, a constant base drogue drag is computed (i.e., no drogue). If MBX = 3, NUSC rope-drag formulation is used (15 ft of rope attached as a drogue). If MBX = 4, a user-supplied value for drogue drag is input in field BXX.

69 through 76 BXX - User-supplied value for drogue drag in pounds, positive, is used with MBX = 4 (left blank otherwise).

Unless a weight file is to be input, this completes the data input. If *WA* is less than zero, then SEG/8 number of cards must follow, each with eight element weights. If there are less than SEG number of element weights, the program prints an error message and aborts.

The output contains the input data values as well as the total and per-foot weights of the array in air and water. Then the array spatial coordinates are printed together with the tension, line array angle, and kite angle as a function of scope or length along the array. Fifty equally-spaced values are printed regardless of the integration length. This may be increased by altering the value of SAVE in the program.

PROGRAM FLOWCHART

The ARRAY program consists of one main program and six subroutines. After the data are read in and printed in the main program, subroutine TURN is called if SIDDEG is not equal to zero; otherwise, subroutine STRATE is called. These two subroutines solve the towline equations using a fourth-order Runge-Kutta technique. The equations are integrated from the tail; in the turn case, the program iterates until the proper turn radius is determined.

Subroutines RECSYS and CYLSYS are used to print the array spatial coordinates, and for transformation from the array tail coordinate system to the tow-vehicle coordinate system. Subroutine WEIGHT computes SEG number of weight elements from a documented, 200-ft hydrophone array. Subroutine DROGUE computes the drogue end conditions for either the variable-base or the rope drogue.

Included is a sample data deck and its associated output. The internal subroutine WEIGHT is used to generate 600 weight elements from the documented array.

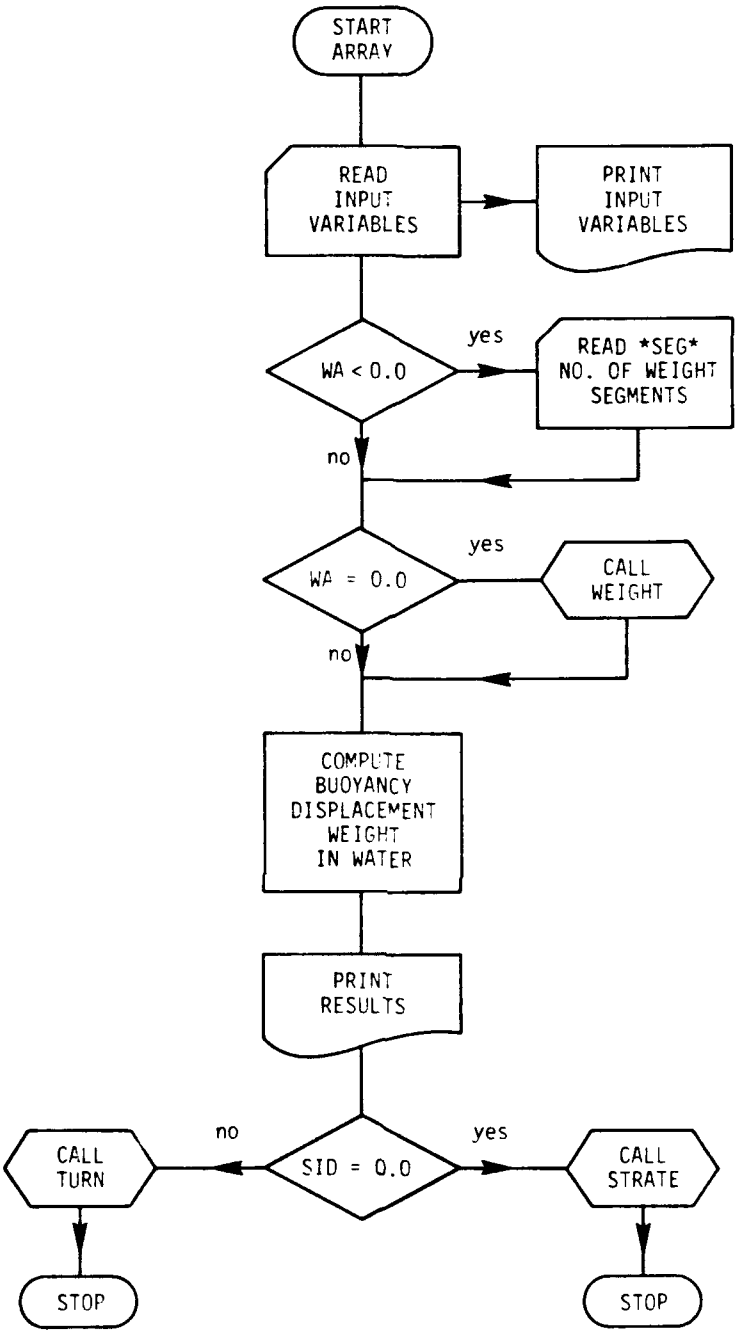
START ARRAY
READ INPUT VARIABLES
PRINT INPUT VARIABLES
WA < 0.0
yes
READ *SEG* NO. OF WEIGHT SEGMENTS
no
WA = 0.0
yes
CALL WEIGHT
no
COMPUTE BUOYANCY DISPLACEMENT WEIGHT IN WATER
PRINT RESULTS
SID = 0.0
no
CALL TURN
yes
CALL STRATE
STOP
STOP

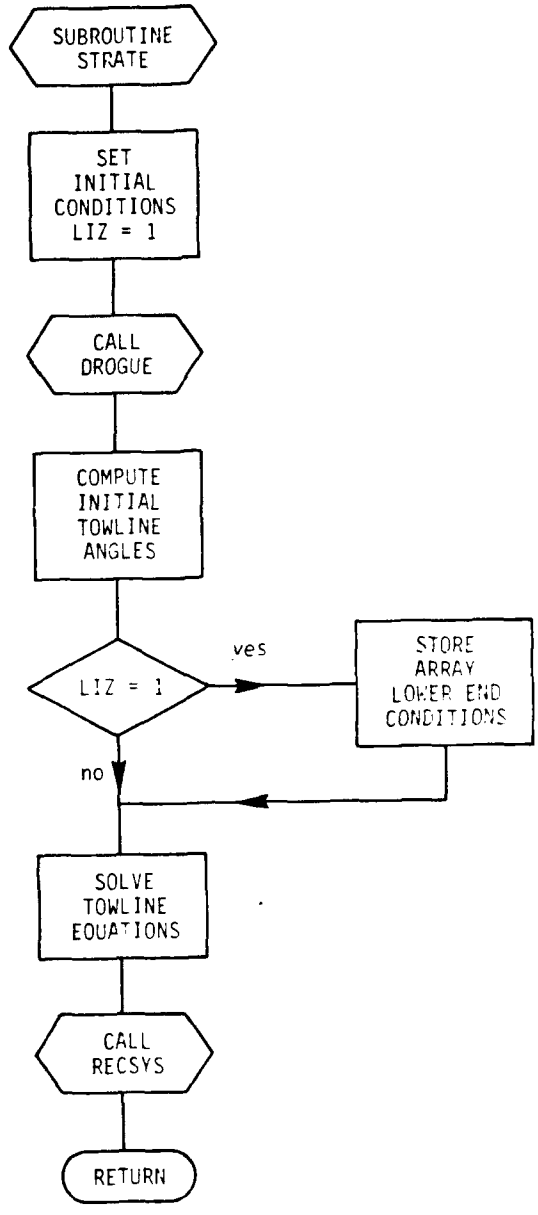
SUBROUTINE STRATE
SET INITIAL CONDITIONS LIZ = 1
CALL DROGUE
COMPUTE INITIAL TOWLINE ANGLES
LIZ = 1
yes
STORE ARRAY LOWER END CONDITIONS
no
SOLVE TOWLINE EQUATIONS
CALL RECSYS
RETURN

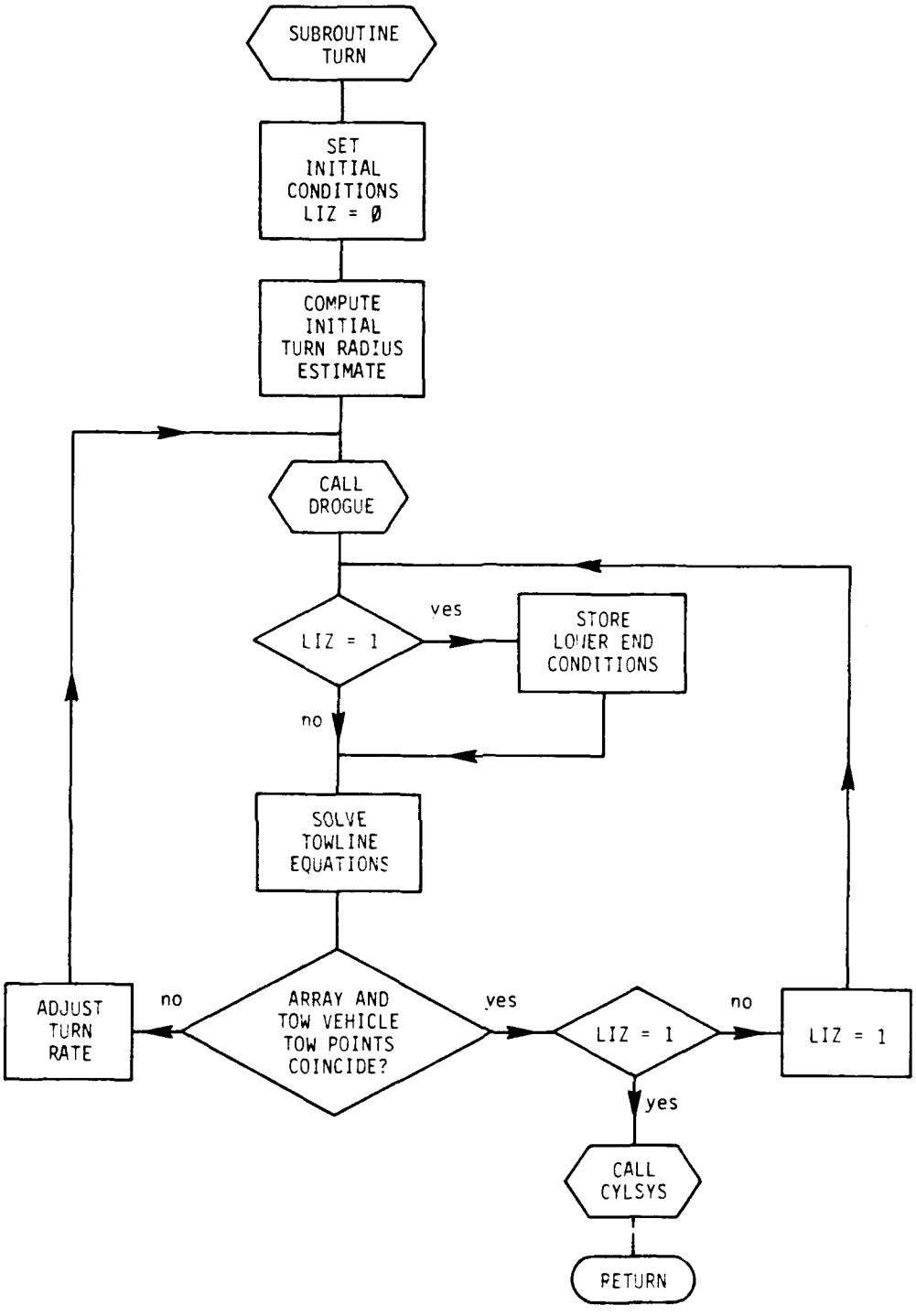
SUBROUTINE TURN
SET INITIAL CONDITIONS LIZ = Ø
COMPUTE INITIAL TURN RADIUS ESTIMATE
CALL DROGUE
LIZ = 1
yes
STORE LOWER END CONDITIONS
no
SOLVE TOWLINE EQUATIONS
ADJUST TURN RATE
no
ARRAY AND TOW VEHICLE TOW POINTS COINCIDE?
yes
LIZ = 1
no
LIZ = 1
yes
CALL CYLSYS
RETURN

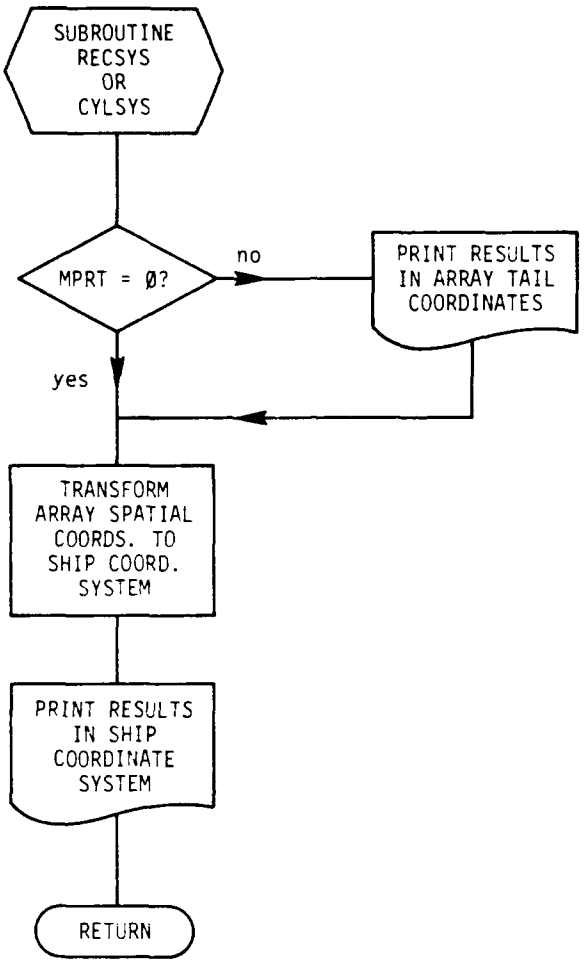
SUBROUTINE
RECSYS
OR
CYLSYS
MPRT = Ø?
no
PRINT RESULTS
IN ARRAY TAIL
COORDINATES
yes
TRANSFORM
ARRAY SPATIAL
COORDS. TO
SHIP COORD.
SYSTEM
PRINT RESULTS
IN SHIP
COORDINATE
SYSTEM
RETURN

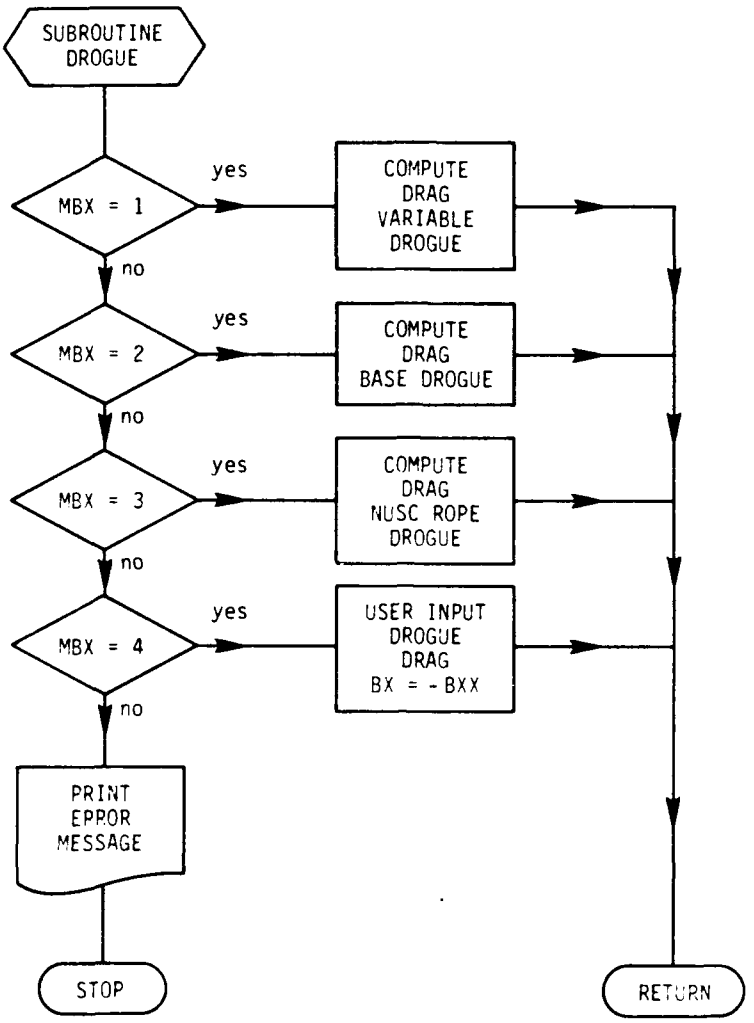
SUBROUTINE DROGUE
MBX = 1
yes
COMPUTE DRAG VARIABLE DROGUE
no
MBX = 2
yes
COMPUTE DRAG BASE DROGUE
no
MBX = 3
yes
COMPUTE DRAG NUSC ROPE DROGUE
no
MBX = 4
yes
USER INPUT DROGUE DRAG BX = - BXX
no
PRINT EPROR MESSAGE
STOP
RETURN

```
      PROGRAM ARRAY(INPUT,OUTPUT,TAPE11,TAPE5=INPUT,TAPE6=OUTPUT)
      COMMON AA(3,3),AF(5),AO(5),AS(3,3),AT(5),ATH(5),C(3)
      COMMON CDKITE(90),CDPH(90),CRX(90),CRY(90),CRZ(90),CT(90)
      COMMON CTXX(90),CTYY(90),CTZZ(90),W(1001)
      COMMON LLL(3),MM(3),RR,SCO(90),SDKITE(90),SDPH(90)
      COMMON SRX(90),SRY(90),SRZ(90),ST(90),STX(90),STXX(90)
      COMMON STY(90),STYY(90),STZZ(90),SXB(90),THK(5),TK(5),OK(5)
      COMMON CN,CF,UD2,US,USKNOT,XNU,WW,WA,DIARAY,LS,KM,BUOY
      COMMON RD,RHO,RN,RO,RX,RY,RZ,SID,SIDDEG,UD,UDDEP,TRAD,MPRT
      COMMON RDO,PPH,UBOD,IEND BX,BY,BZ,RS,CNN FLONG,DS,MBX,BXX
C
C  PROGRAM ARRAY SOVLES THE DIFFERENTIAL EQUATIONS MODELLING
C  A TOWED LINE ARRAY USING A FOURTH ORDER RUNGE KUTTA
C  INTEGRATION TECHNIQUE
C
C  PROGRAMMER, D.E. CALKINS
C  PROGRAM REVISED, FALL 1981, JAMES OSSE
C
C  DEFINE PROGRAM VARIABLE NAMES
C  DIARAY- DIAMETER OF ARRAY IN INCHES
C  FLONG-  LENGTH OF ARRAY IN FEET
C  USKNOT- TOW SPEED OF ARRAY IN KNOTS
C  SIDDEG- TURN RATE OF ARRAY IN DEGREES PER SECOND
C   IF *SIDDEG* .GT.10.0 THEN SIDDEG ASSUMED TO BE TURN RADIUS IN FEET
C   AND SIDDEG COMPUTED FROM TURN RADIUS AND SHIP SPEED
C  CN-     COEFFICIENT OF LIFT
C  CF-     COEFFEICIENT OF FRICTION
C  WA-     WEIGHT OF ARRAY IN AIR, PER FOOT
C    IF *WA* .EQ. 0.0 POUNDS PER FOOT THEN A DISTRIBUTED WEIGHT
C    PROFILE IS GENERATED FROM SUB. WEIGHT WITH *SEG* NO. OF SEGMENTS
C    IF *WA* .LT.0.0 THEN ELEMENT WEIGHTS ARE READ IN FROM FILE *WEIGHT*
C  SEG-    NUMBER OF INTEGRATION SEGMENTS USED (MAX 1000)
C   MPRT=0 OUTPUT PRINTED WITH COORDINATE SYSTEM AT TOW VEHICLE
C   MPRT=1 OUTPUT PRINTED WITH COORDINATE SYSTEM AT ARRAY TAIL AND
C          WITH COORDINATE SYSTEM AT TOW VEHICLE
C  MBX-    DROGUE CONFIGURATION CONTROL
C  MBX=1   VARIABLE DRAG DROGUE
C  MBX=2   CONSTANT DRAG DROGUE, BASE DRAG ONLY, FRON HOERNER
C  MBX=3   NUSC DRAG FORMULATION, 15 FEET OF ROPE
C  MBX=4   USER INPUT BX IN FIELD BXX(POSITIVE VALUE)
C  BXX     DROGUE DRAG OF ARRAY IN POUNDS, USE WITH MBX=4
C
C  READ DATA IN HERE
      READ (5,101)DIARAY,FLONG USKNOT,SIDDEG,CN,CF,WA,SEG,MPRT,MBX,BXX
      IF (ABS(SIDDEG).GT.10.) SIDDEG=USKNOT*1.688*360./(SIDDEG*6.2832)
      IF (ABS(SIDDEG).GT.0.0) TRAD=USKNOT*1.688*360./(SIDDEG*6.2832)
      CNN=CN
      MPRT=MPRT+1
      IF (EOF(5).NE.0) STOP
101   FORMAT(8F8.4,2I2,F8.4)
      WRITE(6,57)        USKNOT,SIDDEG,TRAD
   57 FORMAT(//* EVENT DESCRIPTION*/ * SHIPS SPEED*,T20,F9.3,2X,*KNOTS*/
```

```
     11H ,*TURN RATE*,T20,F9.3,2X,*DEGREES/SEC*/,
     2* TURN RADIUS*,T20,F9.3,*  FEET*/)
      WRITE(6,59) DIARAY,FLONG,CN,CNN,CF
59    FORMAT(/* ARRAY DIAMETER*,T20,F9.3,*  INCHES*,/
     1* ARRAY LENGTH*,T20,F9.3,*  FEET*,/
     2* CN=   *,F7.4,*  CNN=   *,F7.4,*  CF=   *,F7.4/)
C
      IF(MBX.EQ.1.OR.MBX.EQ.2.OR.MBX.EQ.3.OR.MBX.EQ.4) GO TO 13
      WRITE(6,12)
12    FORMAT(* DROGUE DRAG CONTROL VARIABLE MBX NOT PROPERLY SET*)
      STOP
13    GO TO (1,2,3,4) MBX
1     WRITE (6,11)
11    FORMAT(* VARIABLE DRAG DROGUE FORMULATION USED*/)
      GO TO 5
2     WRITE(6,22)
22    FORMAT(* CONSTANT DRAG DROGUE FORMULATION USED*/)
      GO TO 5
3     WRITE(6,33)
33    FORMAT(* NUSC DROGUE DRAG FORMULATION USED*/)
      GO TO 5
4     WRITE(6,44),BXX
44    FORMAT(* USER INPUT DROGUE DRAG OF *,F9.3,* POUNDS*/)
5     CONTINUE
C  INITIAL VALUES
C
      BX=0.0
      BY=0.0
      BZ=0.0
      STXX(1) = 0.0
      STYY(1) = 0.0
      STZZ(1) = 0.0
      RDO=0.0
      RS=0.
      SID = SIDDEG*.01745329
      US=USKNOT*1.688
      UD=US
      UD2=US*US
      UBOD=US
      RHO=1.9875
      RO=RHO/2.
      XNU=.00001233
      DS=FLONG/SEG
      SAVE=FLONG/50.
      XLS=SAVE/DS
      LS=IFIX(XLS)
      XKM=FLONG/DS
      KM=IFIX(XKM)
C  GAMMA IS SPECIFIC WEIGHT
C  BUOYANCY IS BUOYANCY PER FOOT OF ARRAY LENGTH
      GAMMA=64.0
      VOL=(DIARAY**2.0)*3.1415 /576.0
```

```
      BUOY=VOL*GAMMA
      WRITE(6,99) BUOY
 99   FORMAT(* BUOYANCY PER FOOT OF ARRAY  *,T40,F12.4,
     1*  POUNDS PER FOOT*)
      BTOT=BUOY*FLONG
      WRITE(6,98) BTOT
 98   FORMAT(* TOTAL BUOYANCY OF ARRAY *,T40,F12.4,*  POUNDS*)

C  IF WA IS GT 0.0 POUNDS PER FOOT ASSUME CONSTANT WEIGHT DISTRIBUTION
      IF(WA.GT.0.0) GO TO 334
C  IF WA LT 0.0 READ W(K) VALUES FROM INPUT FILE
      IF (WA.LT.0.0) GO TO 444
C  IF WA = 0.0 COMPUTE WEIGHT DISTRIBUTION
C   CALL WEIGHT TO COMPUTE WEIGHT DISTRIBUTION
      WRITE(6,344) KM
344   FORMAT(/I6,* DISTRIBUTED WEIGHT SEGMENTS ARE GENERATED FROM ARRAY
     1DATA*/)
      CALL WEIGHT(W,WTOT,DS,FLONG)
      GO TO 335
334   CONTINUE
      BPFT=BUOY-WA
      WTOT=WA* FLONG
      GO TO 335
444   DO 445 I=1,KM
      READ(5,446) W(I)
      IF (EOF(5).NE.0.0) GO TO 450
445   WTOT=WTOT+W(I)
      GO TO 335
446   FORMAT(F10.4)
450   WRITE(6,455) SEG
455   FORMAT (* INCORRECT NUMBER OF WEIGHT ELEMENTS ,*,
     1*MUST BE EXACTLY *,F9.3,* VALUES*)
      STOP
335   CONTINUE
      AVWT=WTOT/FLONG
      BPFT=BUOY-AVWT
      WRITE(6,230) AVWT
230   FORMAT(* AVERAGE WEIGHT PER FOOT OF ARRAY*,T40,F12.4,
     1*  POUNDS PER FOOT*)
      WRITE(6,232) WTOT
232   FORMAT(* TOTAL WEIGHT OF ARRAY*,T40,F12.4,*  POUNDS*)
      BARR=BTOT-WTOT
      WRITE(6,237)
237   FORMAT(/* POSITIVE NET BUOYANCY IS LIGHT ARRAY, NEGATIVE IS HEAVY
     1ARRAY*)
      IF(BPFT.GT.0.0) GO TO 240
      WRITE(6,234) BPFT
234   FORMAT(* AVERAGE NET BUOYANCY PER FOOT OF ARRAY*,T40,F12.4,
     1*  POUNDS PER FOOT (HEAVY)*)
      WRITE(6,235) BARR
235   FORMAT(* TOTAL NET BUOYANCY OF ARRAY*,T40,F12.4,
     1*  POUNDS (HEAVY)*)
```

```
      GO TO 250
 240  WRITE(6,244) BPFT
244   FORMAT(* AVERAGE NET BUOYANCY PER FOOT OF ARRAY*,T40,F12.4,
     1*  POUNDS PER FOOT (LIGHT)*)
      WRITE(6,245) BARR
245   FORMAT(* TOTAL NET BUOYANCY OF ARRAY*,T40,F12.4,
     1*  POUNDS (LIGHT)*)
250   CONTINUE
C
C  CALL STRATE FOR ZERO TURN CASE, WHICH CALLS RECSYS
C  CALL TURN FOR TURN CASE, WHICH CALLS CYLSYS
C
      IF (SID.EQ.0.0) CALL STRATE
      IF(SID.NE.0.0) CALL TURN
      STOP
      END

      SUBROUTINE CYLSYS
C  PRINTS TOW BODY AND SHIP COORDINATES SYSTEMS FOR TURN CASE
C
      REAL K1,K2
      COMMON AA(3,3),AF(5),AO(5),AS(3,3),AT(5),ATH(5),C(3)
      COMMON CDKITE(90),CDPH(90),CRX(90),CRY(90),CRZ(90),CT(90)
      COMMON CTXX(90),CTYY(90),CTZZ(90),W(1001)
      COMMON LLL(3),MM(3),RR,SCO(90),SDKITE(90),SDPH(90)
      COMMON SRX(90),SRY(90),SRZ(90),ST(90),STX(90),STXX(90)
      COMMON STY(90),STYY(90),STZZ(90),SXB(90),THK(5),TK(5),OK(5)
      COMMON CN,CF,UD2,US,USKNOT,XNU,WW,WA,DIARAY,LS,KM,BUOY
      COMMON RD,RHO,RN,RO.RX,RY,RZ,SID SIDDEG,UD,UDDEP,TRAD,MPRT
      COMMON RDO,PPH,UBOD IEND,BX,BY,BZ,RS,CNN,FLONG.DS,MBX,BXX
      GO TO (500,1000) MPRT
1000  CONTINUE
C      BODY COORDINATE SYSTEM
      PRINT 400
      PRINT 200,TRAD
200   FORMAT(/* COORDINATE ORIGIN AT ARRAY TAIL, TURN RADIUS IS *,F9.3,
     1*  FEET*/)
      PRINT 108, STXX(1),STYY(1),STZZ(1)
      PRINT 47
      DO 54 I=1,IEND
 54   PRINT 17, SCO(I),ST(I),SRX(I),SRZ(I),SRY(I),SDPH(I),
     1SDKITE(I)
      PRINT 107,STXX(IEND),STYY(IEND),STZZ(IEND)
      PRINT 400

500   CONTINUE

C   TRANSFORMATION TO SHIP COORDINATE SYSTEM
C   XS=POSITIVE FORWARD
C   YS=POSITIVE STARBOARD
C   ZS=POSITIVE DOWN
      RX=SRX(IEND)
```

```
      RY=SRY(IEND)
      ZETA=ASIN(RX/RS)
      GAMMA=ATAN(RY/RX)
      RDIF=SQRT((RX*RX)+(RY*RY))
      XDIF=-COS(ZETA-GAMMA)*RDIF
      YDIF=SIN(ZETA-GAMMA)*RDIF
C
C  TURN CASE
C
      DO 90 IC=1,IEND
      K=IEND+1-IC
      CT(IC)=ST(K)
      IF(IC.EQ.IEND) GO TO 906
      R=SQRT((SRX(K)*SRX(K))+(SRY(K)*SRY(K)))
      ALPHA=ATAN(SRY(K)/SRX(K))
      ETA=ZETA-ALPHA
      CRX(IC)=XDIF+R*COS(ETA)
      CRY(IC)=YDIF-R*SIN(ETA)
      CRZ(IC)=SRZ(IEND)-SRZ(K)
      XX=CRX(IC)
      YY=CRY(IC)
      ZZ=CRZ(IC)
      ICC=IEND-1
      IF(IC.EQ.ICC) GO TO 1700
      IC1=IC+1
      K=IEND+1-IC1
      R=SQRT((SRX(K)*SRX(K))+(SRY(K)*SRY(K)))
      ALPHA=ATAN(SRY(K)/SRX(K))
      ETA=ZETA-ALPHA
      CRX(IC1)=XDIF+R*COS(ETA)
      CRY(IC1)=YDIF-R*SIN(ETA)
      CRZ(IC1)=SRZ(IEND)-SRZ(K)
      EX=CRX(IC1)-XX
      EY=CRY(IC1)-YY
      EZ=CRZ(IC1)-ZZ
      RDPH=ATAN(-EZ/EX)
      RDKIT=ATAN(EY/EX)
      CDPH(IC)=RDPH*57.296
      CDKITE(IC)=RDKIT*57.296
      IF(IC.GT.1) GO TO 1702
      RR=SQRT(EX*EX+EY*EY)
      BETA=ATAN(EZ/RR)
      CTXX(IC)=-CT(IC)*COS(BETA)*COS(RDKIT)
      CTYY(IC)=-CT(IC)*COS(BETA)*SIN(RDKIT)
      CTZZ(IC)=CT(IC)*SIN(BETA)
 1702 CONTINUE
      GO TO 907
 1700 EX=XDIF-XX
      EY=YDIF-YY
      EZ=SRZ(IEND)-CRZ(IC)
      RDPH=ATAN(-EZ/EX)
      RDKIT=ATAN(EY/EX)
```

```
      CDPH(IC)=RDPH*57.296
      CDKITE(IC)=RDKIT*57.296
      GO TO 907
  906 RDKIT=-ZETA
      SD=SDPH(K)/57.296
      RDPH=ATAN(TAN(SD)/COS(ZETA))
      CDKITE(IC)=RDKIT*57.296
      CDPH(IC)=RDPH*57.296
      CRX(IC)=XDIF
      CRY(IC)=YDIF
      CRZ(IC)=SRZ(IEND)-SRZ(K)
      CTXX(IC)=-CT(IC)*COS(PPH)*COS(RDKIT)
      CTYY(IC)=-CT(IC)*COS(PPH)*SIN(RDKIT)
      CTZZ(IC)=CT(IC)*SIN(PPH)
  907 CONTINUE
   90 CONTINUE
      PRINT 300,TRAD
300   FORMAT(/* COORDINATE ORIGIN AT TOW VEHICLE, TURN RADIUS OF*,F9.3,
     1* FEET*/)
      PRINT 107,CTXX(1),CTYY(1),CTZZ(1)
      PRINT 47
      DO 55 IC=1,IEND
   55 PRINT 17, SCO(IC),CT(IC),CRX(IC),CRZ(IC),CRY(IC),CDPH(IC),
     1CDKITE(IC)
      PRINT 108,CTXX(IEND),CTYY(IEND),CTZZ(IEND)
C  PRINT TO TAPE 11 FOR PLOTTING
C  PRINT TURN RADIUS OFFSETS FOR PLOTTING
      TRAD2=TRAD*TRAD
      DO 60 I=1,IEND
      TY=TRAD-SQRT(TRAD2-CRX(I)*CRX(I))
60    WRITE(11,19) SCO(I),CT(I),ABS(CRX(I)),CRZ(I),CRY(I),CDPH(I)
     1,CDKITE(I),TY
19    FORMAT(8F10.3)
C
  108 FORMAT(1HO,*LOWER TENSION COMPONENTS*,/1H ,*TX= *,F10.4,2X,
     C*TY= *,F10.4,2X,*TZ= *,F10.4)
47    FORMAT(1HO,5X,*SCOPE    TENSION    TRAIL      DEPTH   SIDE TRL*,
     1*   LINE ANGL  KITE ANGL*,/6X,*(FEET)   (POUNDS)   (FEET)*,
     2*      (FEET)   (FEET)    (DEGREES)  (DEGREES)*)
   17 FORMAT(3X,7F10.3)
  107 FORMAT(1HO,*UPPER TENSION COMPONENTS*,/1H ,*TX= *,F10.4,2X,*TY= *,
     1F10.4,2X,*TZ= *,F10.4)
  400 FORMAT(1HO)

      END
      SUBROUTINE RECSYS
C  PRINT BODY AND SHIP COORDINATE SYSTEMS FOR ZERO TURN CASE
C
      COMMON AA(3,3),AF(5),AO(5),AS(3,3),AT(5),ATH(5),C(3)
      COMMON CDKITE(90),CDPH(90),CRX(90),CRY(90),CRZ(90),CT(90)
      COMMON CTXX(90),CTYY(90),CTZZ(90),W(1001)
      COMMON LLL(3),MM(3),RR,SCO(90),SDKITE(90),SDPH(90)
```

```
      COMMON SRX(90),SRY(90),SRZ(90),ST(90),STX(90),STXX(90)
      COMMON STY(90),STYY(90),STZZ(90),SXB(90),THK(5),TK(5),OK(5)
      COMMON CN,CF,UD2,US,USKNOT,XNU,WW,WA,DIARAY,LS,KM,BUOY
      COMMON RD,RHO,RN,RO,RX,RY,RZ,SID,SIDDEG,UD,UDDEP,TRAD,MPRT
      COMMON RDO,PPH,UBOD,IEND,BX,BY,BZ,RS,CNN,FLONG,DS,MBX,BXX
      GO TO (500,1000) MPRT
1000  PRINT 400
      PRINT 200
200   FORMAT(/* COORDINATE ORIGIN AT ARRAY TAIL*/)
      PRINT 108, STXX(1),STYY(1),STZZ(1)
      PRINT 47
      DO 54 I=1,IEND
 54   PRINT 17, SCO(I),ST(I),SRX(I),SRZ(I),SRY(I),SDPH(I),
     1SDKITE(I)
      PRINT 107,STXX(IEND),STYY(IEND),STZZ(IEND)
      PRINT 400
500   CONTINUE

C     TRANSFORMATION TO SHIP COORDINATE SYSTEM
C     XS=POSITIVE FORWARD
C     YS=POSITIVE STARBOARD
C     ZS=POSITIVE DOWN
C
C     TOW VEHICLE RECTANGULAR SYSTEM  PRINTED

C       TURNRATE=ZERO
        DO 91 IC=1,IEND
        K=IEND+1-IC
        CT(IC)=ST(K)
        CRX(IC)=-SRX(IEND)+SRX(K)
        CRY(IC)=-SRY(IEND)+SRY(K)
        CRZ(IC)=SRZ(IEND)-SRZ(K)
        CDPH(IC)=SDPH(K)
        CDKITE(IC)=SDKITE(K)
        IF(IC.EQ.IEND) GO TO 1703
        IF(IC.GT.1) GO TO 91
 1703   CONTINUE
        CTXX(IC)=STXX(K)
        CTYY(IC)=STYY(K)
        CTZZ(IC)=-STZZ(K)
   91   CONTINUE

        PRINT 300
 300    FORMAT(/* COORDINATE ORIGIN AT TOW VEHICLE*/)
        PRINT 107,CTXX(1),CTYY(1),CTZZ(1)
        PRINT 47
        DO 55 IC=1,IEND
        WRITE(11,44) SCO(IC),CT(IC),CRX(IC),CRZ(IC),CRY(IC),
       1CDPH(IC),CDKITE(IC)
   55   PRINT 17, SCO(IC),CT(IC),CRX(IC),CRZ(IC),CRY(IC),CDPH(IC),
       1CDKITE(IC)
        PRINT 108,CTXX(IEND),CTYY(IEND),CTZZ(IEND)
```

```
44    FORMAT(7F10.3)
  108 FORMAT(1HO,*LOWER TENSION COMPONENTS*,/1H ,*TX= *,F10.4,2X,
     C*TY= *,F10.4,2X,*TZ= *,F10.4)
47    FORMAT(1HO,5X,*SCOPE    TENSION    TRAIL      DEPTH   SIDE TRL*,
     1*   LINE ANGL  KITE ANGL*,/6X,*(FEET)  (POUNDS)    (FEET)*,
     2*    (FEET)    (FEET)    (DEGREES)    (DEGREES)*)
   17 FORMAT(3X,7F10.3)
  107 FORMAT(1HO,*UPPER TENSION COMPONENTS*,/1H ,*TX= *,F10.4,2X,*TY= *,
     1F10.4,2X,*TZ= *,F10.4)
 400  FORMAT(1HO)
      RETURN
      END

      SUBROUTINE STRATE
C  ZERO TURN CASE
C
      COMMON AA(3,3),AF(5),AO(5),AS(3,3),AT(5),ATH(5),C(3)
      COMMON CDKITE(90),CDPH(90),CRX(90),CRY(90),CRZ(90),CT(90)
      COMMON CTXX(90),CTYY(90),CTZZ(90),W(1001)
      COMMON LLL(3),MM(3),RR,SCO(90),SDKITE(90),SDPH(90)
      COMMON SRX(90),SRY(90),SRZ(90),ST(90),STX(90),STXX(90)
      COMMON STY(90),STYY(90),STZZ(90),SXB(90),THK(5),TK(5),OK(5)
      COMMON CN,CF,UD2,US,USKNOT,XNU,WW,WA,DIARAY,LS,KM,BUOY
      COMMON RD,RHO,RN,RO,RX,RY,RZ,SID,SIDDEG,UD,UDDEP,TRAD,MPRT
      COMMON RDO,PPH,UBOD,IEND,BX,BY,BZ,RS,CNN,FLONG,DS,MBX,BXX
      DIMENSION FR(4),FH(4)
      REAL K1,K2
C BEGIN TOWLINE CALCULATIONS
      K=0
      RD=0.0
      LIZ=1
C
C  CALL DROGUE TO SET DROGUE DRAG
      CALL DROGUE(BX,BY,BZ,DIARAY,FLONG,CF,RO,UD2,MBX,BXX)

C     PRINT CONTROL
      RX=0.0
      RY=0.0
      RZ=0.0
      SCOPE=0.0
      LBM=0
      LSM=0
      UD=UBOD
      UD2=UD*UD
      IC=0
      TT=BX*BX+BY*BY+BZ*BZ
      T=SQRT(TT)
      PPH=BZ/((BX*BX+BY*BY)**0.5)
      PI=ATAN(PPH)
      TTH=-BY/BX
      TH=ATAN(TTH)
      DTH=TH*57.296
```

```
      DPH=PI*57.29
C
      IF (LIZ) 76,76,74
 74   CONTINUE

C STORE LOWER END CONDITION VALUES
      IC=IC+1
      SCO(IC)=SCOPE
      ST(IC)=T
      SRX(IC)=RX
      SRZ(IC)=RZ
      SRY(IC)=RY
      SDPH(IC)=DPH
      SDKITE(IC)=DTH
      STXX(IC)=BX
      STYY(IC)=BY
      STZZ(IC)=BZ
   76 SC=0.0
C  LOOP TO SOLVE TOWLINE EQUATIONS

      DO 16 K=1,KM
      SC=SC+1.0
      I=1
      AT(I)=SIN(PI)
      AO(I)=COS(PI)
      AF(I)=SIN(TH)
      ATH(I)=COS(TH)


C    WT IS WEIGHT MINUS BUOYANCY OF EACH SEGMENT
      WT=W(K)-BUOY*DS
      IF(WA.GT.0.0) WT=(WA-BUOY)*DS


      B1=.8755
      B3=-.1518
      B5=-.028298
      B7=-.00503798
      B9=-.00506455
      B11=-.00190368
      B13=.00172655
      B15=.002913
      B17=-.0039122
      B19=-.00423226
      UD2=UD*UD
      RT=RO*UD2*DIARAY/12.

      FH(1)=B1*SIN(TH)+B3*SIN(3.*TH)+B5*SIN(5.*TH)+B7*SIN(7.*TH)
     1+B9*SIN(9.*TH)+    *SIN(11.*TH)+B13*SIN(13.*TH)
     2+B15*SIN(15.*TH)+B17*SIN(17.*TH)+B19*SIN(19.*TH)

      FR(1)=B1*SIN(PI)+B3*SIN(3.*PI)+B5*SIN(5.*PI)+B7*SIN(7.*PI)
```

```
     1+B9*SIN(9.*PI)+B11*SIN(11.*PI)+B13*SIN(13.*PI)+B15*SIN(15.*PI)
     2+B17*SIN(17.*PI)+B19*SIN(19.*PI)

11     CONTINUE
       FH(I)=FH(I)*RT*CNN*DS
       FR(I)=FR(I)*RT*CN*DS
       FG=RT*AO(I)*3.1416*CF
C
C RECTANGULAR COORDINATE SYSTEM

C   ETA/PHI ROTATION
       TK(I)=-FH(I)/T*AO(I)
       OK(I)=(WT*AO(I)-FR(I))/T
       THK(I)=FG+WT*AT(I)

C  FORTH ORDER RUNGE KUTTA INTEGRATION
       IQ=I-3
       IF(IQ) 41,42,43
41     DC=.5
       GO TO 44
42     DC=1.0
44     PII=PI+DS*DC*OK(I)
       AO(I+1)=COS(PII)
       AT(I+1)=SIN(PII)
       FR(I+1)=B1*SIN(PII)+B3*SIN(3.*PII)+B5*SIN(5.*PII)+B7*SIN(7.*PII)
     1+B9*SIN(9.*PII)+B11*SIN(11.*PII)+B13*SIN(13.*PII)+B15*SIN(15.*PII)
     2+B17*SIN(17.*PII)+B19*SIN(19.*PII)
       THH=TH+DC*DS*TK(I)
       ATH(I+1)=COS(THH)
       AF(I+1)=SIN(THH)
       FH(I+1)=B1*SIN(THH)+B3*SIN(3.*THH)+B5*SIN(5.*THH)+B7*SIN(7.*THH)
     1+B9*SIN(9.*THH)+B11*SIN(11.*THH)+B13*SIN(13.*THH)
     2+B15*SIN(15.*THH)+B17*SIN(17.*THH)+B19*SIN(19.*THH)
       I=I+1
       GO TO 11
 43    PHO=PI+(1.0/6.0)*DS*(OK(1)+2.0*(OK(2)+OK(3))+OK(4))
       THO=TH+(1.0/6.0)*DS*(TK(1)+2.0*(TK(2)+TK(3))+TK(4))
       TOI=T+(1.0/6.0)*DS*(THK(1)+2.0*(THK(2)+THK(3))+THK(4))
       PI=PHO
       TH=THO
       T=TOI

C     RECTANGULAR COORDINATE SYSTEM
C   RX=TRAIL
       EX=DS*ATH(I)*AO(I)
       EY=DS*AF(I)*AO(I)
       EZ=DS*AT(I)
       DKITE=TH*57.296
       RX=RX+EX
C      RY=SIDETRAIL
       RY=RY+EY
C      RZ=DEPTH
```

```
      RZ=RZ+EZ
      DPH=PI*57.29
      TXZ=SQRT((T**2*COS(TH)**2)/(1.-COS(PI)**2*SIN(TH)**2))
      TYZ=SQRT((T**2*SIN(PI)**2)/(1.-COS(PI)**2*SIN(TH)**2))
      TXX=TXZ*COS(PI)
      TYY=TYZ*SIN(TH)
      TZZ=TYZ*COS(TH)

      LBM=LBM+1
      NSM=LSM*LS-LBM
      SCOPE=SC*DS

       IF(K.EQ.KM.AND.LIZ.EQ.1) GO TO 22
C CONTROL FOR SAVING 100 FOOT INCREMENT VALUES
      IF(NSM) 22,22,16
 22    CONTINUE
      IF(SCOPE.EQ.10.0) GO TO 10
C  STORE BODY COORDINATE SYSTEM VALUES
      IC=IC+1
      SCO(IC)=SCOPE
      ST(IC)=T

      SRX(IC)=RX
      SRY(IC)=RY
      SRZ(IC)=RZ
      SDPH(IC)=DPH


      SDKITE(IC)=DKITE


      STXX(IC)=-TXX
      STYY(IC)=-TYY
      STZZ(IC)=-TZZ
 10   LSM=LSM+1

 16    CONTINUE
      IEND=IC
C END OF TOWLINE LOOP
C  CALL RECSYS TO PRINT RESULTS

      CALL RECSYS
      RETURN
      END
      SUBROUTINE TURN
C  TURN RATE CASE
C
      COMMON AA(3,3),AF(5),AO(5),AS(3,3),AT(5),ATH(5),C(3)
      COMMON CDKITE(90),CDPH(90),CRX(90),CRY(90),CRZ(90),CT(90)
      COMMON CTXX(90),CTYY(90),CTZZ(90),W(1001)
      COMMON LLL(3),MM(3),RR,SCO(90),SDKITE(90),SDPH(90)
      COMMON SRX(90),SRY(90),SRZ(90),ST(90),STX(90),STXX(90)
```

```
      COMMON STY(90),STYY(90),STZZ(90),SXB(90),THK(5),TK(5),OK(5)
      COMMON CN,CF,UD2,US,USKNOT,XNU,WW,WA,DIARAY,LS,KM,BUOY
      COMMON RD,RHO,RN,RO,RX,RY,RZ,SID,SIDDEG,UD,UDDEP,TRAD,MPRT
      COMMON RDO,PPH,UBOD,IEND,BX,BY,BZ,RS,CNN,FLONG,DS,MBX,BXX
      DIMENSION FR(4),FH(4)
      REAL K1,K2
C BEGIN TOWLINE CALCULATIONS
      KT=0
      LIZ=0
C  INITIAL GUESS FOR TURN CASE
      RS=US/SID
      RD=RS
      RDO=RS
 1000 CONTINUE
      SI=0.0
C
C  CALL DROGUE TO SET DROGUE DRAG
        LL DROGUE(BX,BY,BZ,DIARAY,FLONG,CF,RO,UD2,MBX,BXX)

C     PRINT CONTROL
      RX=0.0
      RY=0.0
      RZ=0.0
      SCOPE=0.0
      LBM=0
      LSM=0
      UD=UBOD
      UD2=UD*UD
      IC=0
      TT=BX*BX+BY*BY+BZ*BZ
      T=SQRT(TT)
      PPH=BZ/((BX*BX+BY*BY)**0.5)
      PI=ATAN(PPH)
      TTH=-BY/BX
      TH=ATAN(TTH)
      DTH=TH*57.296
      DPH=PI*57.29
C
      IF (LIZ) 76,76,74
 74   CONTINUE

C STORE LOWER END CONDITION VALUES
      IC=IC+1
      SCO(IC)=SCOPE
      ST(IC)=T
      SRX(IC)=RX
      SRZ(IC)=RZ
      SRY(IC)=RY
      SDPH(IC)=DPH
      SDKITE(IC)=DTH
      STXX(IC)=BX
      STYY(IC)=BY
```

```
      STZZ(IC)=BZ
   76 SC=0.0
C  LOOP TO SOLVE TOWLINE EQUATIONS

      DO 16 K=1,KM
      SC=SC+1.0
      I=1
      AT(I)=SIN(PI)
      AO(I)=COS(PI)
      AF(I)=SIN(TH)
      ATH(I)=COS(TH)


C     WT IS WEIGHT MINUS BUOYANCY OF EACH SEGMENT
      WT=W(K)-BUOY*DS
      IF(WA.GT.0.0) WT=(WA-BUOY)*DS

      B1=.8755
      B3=-.1518
      B5=-.028298
      B7=-.00503798
      B9=-.00506455
      B11=-.00190368
      B13=.00172655
      B15=.002913
      B17=-.0039122
      B19=-.00423226
      UD2=UD*UD
      RT=RO*UD2*DIARAY/12.

      FH(1)=B1*SIN(TH)+B3*SIN(3.*TH)+B5*SIN(5.*TH)+B7*SIN(7.*TH)
     1+B9*SIN(9.*TH)+B11*SIN(11.*TH)+B13*SIN(13.*TH)
     2+B15*SIN(15.*TH)+B17*SIN(17.*TH)+B19*SIN(19.*TH)

      FR(1)=B1*SIN(PI)+B3*SIN(3.*PI)+B5*SIN(5.*PI)+B7*SIN(7.*PI)
     1+B9*SIN(9.*PI)+B11*SIN(11.*PI)+B13*SIN(13.*PI)+B15*SIN(15.*PI)
     2+B17*SIN(17.*PI)+B19*SIN(19.*PI)

11     CONTINUE
      FH(I)=FH(I)*RT*CNN*DS
      FR(I)=FR(I)*RT*CN*DS
      FG=RT*AO(I)*3.1416*CF
C
C CYLINDRICAL COORDINATE SYSTEM

      RDD=DS*RD*SID*SID
      UM=WA/32.2
      AM=0.785*((DIARAY/12.)**2.0)
      CFF=UM*RDD
      CF1=(UM+RHO*AM)*RDD
      CF2=(UM+RHO*AM)*RDD
C     ETA/PHI    ROTATION
```

```
      TK(I)=(-FH(I)+(CF2+T*AO(I)*AO(I)/RD)*ATH(I))/T*AO(I)
      OK(I)=(WT*AO(I)-FR(I)-CF1*AT(I)*AF(I))/T
      THK(I)=FG+WT*AT(I)+CFF*AF(I)*AO(I)

C   RUNGE KUTTA INTEGRATION SCHEME
      IQ=I-3
      IF(IQ) 41,42,43
41    DC=.5
      GO TO 44
42    DC=1.0
44    PII=PI+DS*DC*OK(I)
      AO(I+1)=COS(PII)
      AT(I+1)=SIN(PII)
      FR(I+1)=B1*SIN(PII)+B3*SIN(3.*PII)+B5*SIN(5.*PII)+B7*SIN(7.*PII)
     1+B9*SIN(9.*PII)+B11*SIN(11.*PII)+B13*SIN(13.*PII)+B15*SIN(15.*PII)
     2+B17*SIN(17.*PII)+B19*SIN(19.*PII)
      THH=TH+DC*DS*TK(I)
      ATH(I+1)=COS(THH)
      AF(I+1)=SIN(THH)
      FH(I+1)=B1*SIN(THH)+B3*SIN(3.*THH)+B5*SIN(5.*THH)+B7*SIN(7.*THH)
     1+B9*SIN(9.*THH)+B11*SIN(11.*THH)+B13*SIN(13.*THH)
     2+B15*SIN(15.*THH)+B17*SIN(17.*THH)+B19*SIN(19.*THH)
      I=I+1
      GO TO 11
43    PHO=PI+(1.0/6.0)*DS*(OK(1)+2.0*(OK(2)+OK(3))+OK(4))
      THO=TH+(1.0/6.0)*DS*(TK(1)+2.0*(TK(2)+TK(3))+TK(4))
      TOI=T+(1.0/6.0)*DS*(THK(1)+2.0*(THK(2)+THK(3))+THK(4))
      PI=PHO
      TH=THO
      T=TOI
C   CYLINDRICAL COORDINATE SYSTEM

      ESI=DS*ATH(I)*AO(I)/RD
      ERD=-DS*AF(I)*AO(I)
      EZ=DS*AT(I)

      SI=SI+ESI
      RD=RD+ERD
      XX=RX
      YY=RY
      RX=RD*SIN(SI)
      RY=RDO-RD*COS(SI)
      RZ=RZ+EZ
      EX=RX-XX
      EY=RY-YY
      DPH=PI*57.296
      UD=RD*SID

      PSI=ATAN(EY/EX)
      DKITE=PSI*57.296
```

```
      TXZ=SQRT((T**2*COS(TH)**2)/(1.-COS(PI)**2*SIN(TH)**2))
      TYZ=SQRT((T**2*SIN(PI)**2)/(1.-COS(PI)**2*SIN(TH)**2))
      TXX=TXZ*COS(PI)
      TYY=TYZ*SIN(TH)
      TZZ=TYZ*COS(TH)

      IF (LIZ) 16,16,81
 81   LBM=LBM+1
      NSM=LSM*LS-LBM
      SCOPE=SC*DS

       IF(K.EQ.KM.AND.LIZ.EQ.1) GO TO 22
C CONTROL FOR SAVING 100 FOOT INCREMENT VALUES
      IF(NSM) 22,22,16
 22    CONTINUE
      IF(SCOPE.EQ.10.0) GO TO 10
C  STORE BODY COORDINATE SYSTEM VALUES
      IC=IC+1
      SCO(IC)=SCOPE
      ST(IC)=T

      SRX(IC)=RX
      SRY(IC)=RY
      SRZ(IC)=RZ
      SDPH(IC)=DPH


      SDKITE(IC)=DKITE


      STXX(IC)=-TXX
      STYY(IC)=-TYY
      STZZ(IC)=-TZZ
 10   LSM=LSM+1

 16    CONTINUE
      IEND=IC
C END OF TOWLINE LOOP
C ADJUSTMENT TO BODY TURN RADIUS


      RDP=RS*RDO/RD
      KT=KT+1
      IF(KT.GE.20)  GO TO 86
      IF(ABS(RS-RD).LE.10.) GO TO 200
      IF(KT.EQ.10)  GO TO 34
      RD=RDP
      RDO=RDP
      GO TO 35
   86 PRINT 89
   89 FORMAT(*    EXECUTION ERROR-FAILS TO CONVERGE    *)
      STOP
```

```
   34 RD=(RD+RDP)/2.
   35 CONTINUE
C  ADJUST BODY TURN RATE
      UBOD=RD*SID

      GO TO 1000

  200 IF(LIZ) 87,87,27
 87    LIZ=1
       RD=RDP
       RDO=RDP

       GO TO 1000
C  CALL CYLSYS TO PRINT RESULTS
 27    CALL CYLSYS
       RETURN
       END
       SUBROUTINE DROGUE(BX,BY,BZ,DIARAY,FLONG,CF,RO,UD2,MBX,BXX)
C    DROGUE END CONDITIONS (BX,BY,BZ)
       U=SQRT(UD2)/1.688
       Q=RO*UD2
       GO TO (1,2,3,4) MBX
C  MBX=1, VARIABLE DRAG
C  MBX=2, CONSTANT DRAG, HOERNER
C  MBX=3, NUSC FORMULATION, 15 FEET OF ROPE AS DROGUE
C  MBX=4, USER INPUT USED FOR BX, POSITIVE VALUE
C
C  BX USING VARIABLE DRAG DROGUE
C  CONE HALF ANGLE = 30 DEG AT 1 KNOT, 15 DEG AT 5 KNOT, 0 DEG AT 10 KN
1      IF(U.LE.10.) CDS=.9826-.1367*U+.004111*U*U
       IF(U.GT.10.0) CDS=0.026
       BX=-Q*CDS
       GO TO 5
C  BX FROM HOERNER REPORT
2      CFB=4.*FLONG*CF*12./DIARAY
       CDB=0.029/(CFB**0.5)
       SBASE=3.1416/4.*(DIARAY/12.)**2.0
       BX=-Q*CDB*SBASE
       GO TO 5
C
C  BX FROM NUSC REPORT
3      BX=-RO*UD2*0.2618*DIARAY*CF*15.0
       GO TO 5
C  BX FROM USER INPUT BXX
4      BX=-BXX
C
5      CONTINUE
       BY=0.
       BZ=0.
       RETURN
       END
       SUBROUTINE WEIGHT(WT,WTOT,DS,FLONG)
```

```
C  PRODUCES WEIGHT LISTING WT(X) OF MAST ARRAY
      DIMENSION WT(500),TR(8),S(76)
      DATA TR/24.4,49.0,96.5,121.1,168.5,192.9,72.101,145.0/
      DATA S/3.1,5.1,7.7,9.9,11.111,14.2,16.5,18.9,20.111,27.8,29.8,
     131.7,33.7,35.7,37.7,39.6,41.6,43.5,45.5,51.9,53.9,55.9,57.9,59.9,
     261.101,63.101,65.101,67.101,76.6,78.7,80.9,82.111,84.101,86.9,89.1
     3,91.3,93.5,99.8,101.8,103.7,105.8,107.8,109.7,111.7,113.7,115.8,
     4117.8,124.8,126.101,128.8,130.8,132.6,134.5,136.3,138.2,140.1,
     5144.2,148.7,150.7,152.7,154.8,156.9,158.9,160.9,163.0,165.1,
     6171.8,173.111,176.2,178.5,180.8,182.111,185.2,187.6,189.9,194.9/
      WTOT=0.0
C  CORRECT FOR ELONGATION OF ARRAY UNDER TOW
C  FROM 196.5 (AS MEASURED) TO 200 FEET
      DO 5 I=1,76
      IF(I.LE.8) TR(I)=TR(I)*200./196.5
5     S(I)=S(I)*200./196.5
      LM=IFIX(FLONG/DS)
      DO 10 I=1,LM+1
      WT(I)=0.0
 10   CONTINUE
C UNIFORM WEIGHT
C KEVLAR LINE, 0.020 #/FT AND HOSE, 0.43 #/FT
      W=0.020*DS+0.43*DS
      DO 20 I=1,LM
 20   WT(I)=WT(I)+W
      EEND=AMOD(FLONG,DS)
      WT(LM+1)=WT(LM+1)+EEND*(0.02+0.43)
C TRANSDUCER WIRE 0.132 #/FT
      W=0.132*DS
      J=6
      LM=IFIX(FOOT(TR(J))/DS)
      EEND=AMOD(FOOT(TR(J)),DS)
      DO 30 I=1,LM
 30   WT(I)=WT(I)+W
      WT(LM+1)=WT(LM+1)+EEND*0.132
C PINGER WIRE 0.024 #/FT
      W=0.024*DS
      J=8
      LM=IFIX(FOOT(TR(J))/DS)
      EEND=AMOD(FOOT(TR(J)),DS)
      DO 60 I=1,LM
 60   WT(I)=WT(I)+W
      WT(LM+1)=WT(LM+1)+EEND*0.024
C OIL 1.254 #/FT
      W=1.254*DS
      LM=IFIX(FLONG/DS)
      EEND=AMOD(FLONG,DS)
      DO 70 I=1,LM
 70   WT(I)=WT(I)+W
      WT(LM+1)=WT(LM+1)+EEND*1.254
C POINT WEIGHTS TRANSDUCER 1.287 #
      DO 80 J=1,6
```

```
      I=IFIX(FOOT(TR(J))/DS)
 80   WT(I)=WT(I)+1.287
C POINT WEIGHT PINGER 1.118#
      DO 90 J=7,8
      I=IFIX(FOOT(TR(J))/DS)
 90   WT(I)=WT(I)+1.118
C TAIL CONNECTOR 1.062#
      WT(LM+1)=WT(LM+1)+1.062
C SPACERS 0.543#
      DO 100 I=1,76
      J=IFIX(FOOT(S(I))/DS)
 100  WT(J)=WT(J)+0.543
C     BOY=(2.5/12.)**2.*3.1415*64.*DS/4.0
      DO 110 I=1,LM+1
C     X=DS*I
C     X1=DS*(I+1)
C     DIF=2.1815*DS-WT(I)
C     WRITE(13,22) X,WT(I),DIF,BOY
C     WRITE(13,22) X1,WT(I),DIF,BOY
110   WTOT=WTOT+WT(I)
      RETURN
      END
      REAL FUNCTION FOOT(X)
      A=AINT(X)
      CH=X-A
      IF (CH.EQ.0.101.OR.CH.EQ.0.111) CH=CH*10.
      CH=CH/1.20
      FOOT=A+CH
      RETURN
      END
```

APPENDIX B

PROGRAM SNAKE

DESCRIPTION

SNAKE is a frequency domain model of the hydroelastic response of a neutrally buoyant, flexible line array.

CAPABILITIES

The program computes the complex roots of the equations of motion modeling the first modes of vibration of a long, flexible line array that is clamped at the upstream end, free at the downstream end, and towed with uniform speed through water. For a given length-to-diameter ratio, the eigenvalues are computed for various nondimensional speeds, starting with zero. If the imaginary part of the eigenvalue goes negative, indicating a static or dynamic instability, the eigenvectors at the critical tow speed are computed.

INPUT

(1) Q2 - Ratio of towrope to midbody length

(2) QA - Ratio of tail length to nose length

(3) QE - Ratio of midbody length to diameter

(4) QD - Ratio of base diameter to midbody diameter

(5) XCT - Tangential drag coefficient

(6) XXX - Initial prediction of frequency of vibration for a given mode, and initial estimates of correction values.

OUTPUT

The real and imaginary roots of the modal equations are printed for a range of nondimensional tow speeds. If the imaginary part goes negative, indicating a static or dynamic instability in the zero through fourth modes, the program iterates to find the exact critical speed of instability. The eigenvectors are computed and printed for this speed. The tow speeds are then increased until the program reaches a user-input upper tow-speed limit or the equations diverge, or do not converge in a specified number of iterations.

MODEL THEORY

The theory is a fourth-order linear approximation of the hydroelastic equations of motion of a long, slender flexible line array of circular cross section immersed in an incompressible fluid and towed with a uniform velocity that is parallel to the longitudinal axis. A Predictor-Corrector method of analysis is employed to solve for the eigenvalues. The cylinder is free at the downstream end and clamped at the upstream end. Ellipsoidal sections are assumed for the nose and tail sections with the degree of eccentricity user selected. All motions are assumed to lie in the lateral plane. Stability conditions are found from solutions to linearized equations of motion resulting from small amplitude-motion assumptions.

INPUT DESCRIPTION

Two cards are required for input. The first contains the array physical parameters, and the second, the program run parameters. Because the program uses the Predictor-Corrector method to solve the towline equations, and no method is supplied to provide the initial estimates and correction values, these must be user supplied on the second card.

First card format (F5.3):

Column:

1 through 5 Q2 - Ratio of tow rope length to midbody length.

6 through 10 QA - Ratio tail length to nose length. The nose length is set in the program to be slightly greater than the midbody diameter. Therefore, the eccentricity is approximately zero.

11 through 15 QE - Ratio of length to diameter.

16 through 20 QD - Ratio of drogue diameter to midbody diameter.

21 through 25 XCT - Tangential drag coefficient = 4 CD.

Second card format (4I2, IX, 9F5.3):

Column:

1 through 2 Mode - Mode of calculation--zero through fourth mode--used only for program output with no effect on calculations.

3 through 4 Key - Print control index; 1 for maximum.

5 through 6 IAX - Number of points investigated on imaginary axis; 1 for zero mode, 0 otherwise.

7 through 8 IUP - Direction of analysis along imaginary axis for zero mode; 1 for upward, -1 for downward analysis; for first, second, third and fourth modes, use IUP = 1.

10 through 15 U - Starting nondimensional speed; usually zero, but for zero and first order may be necessary to increase to 1 or 2.

16 through 20 UM - Maximum velocity calculated.

21 through 25 DU - Initial estimate of velocity increment (typically 0.5).

26 through 35 OM - Initial upper estimate at starting velocity of solution frequency (complex).

36 through 45 OMI - Initial lower estimate at starting velocity of eigenvalue solution (complex).

46 through 55 001 - Initial estimate of correction increment. Real value should have same sign as the slope of the Argand curve at starting tow speed (complex), typically -0.5, 0.1.

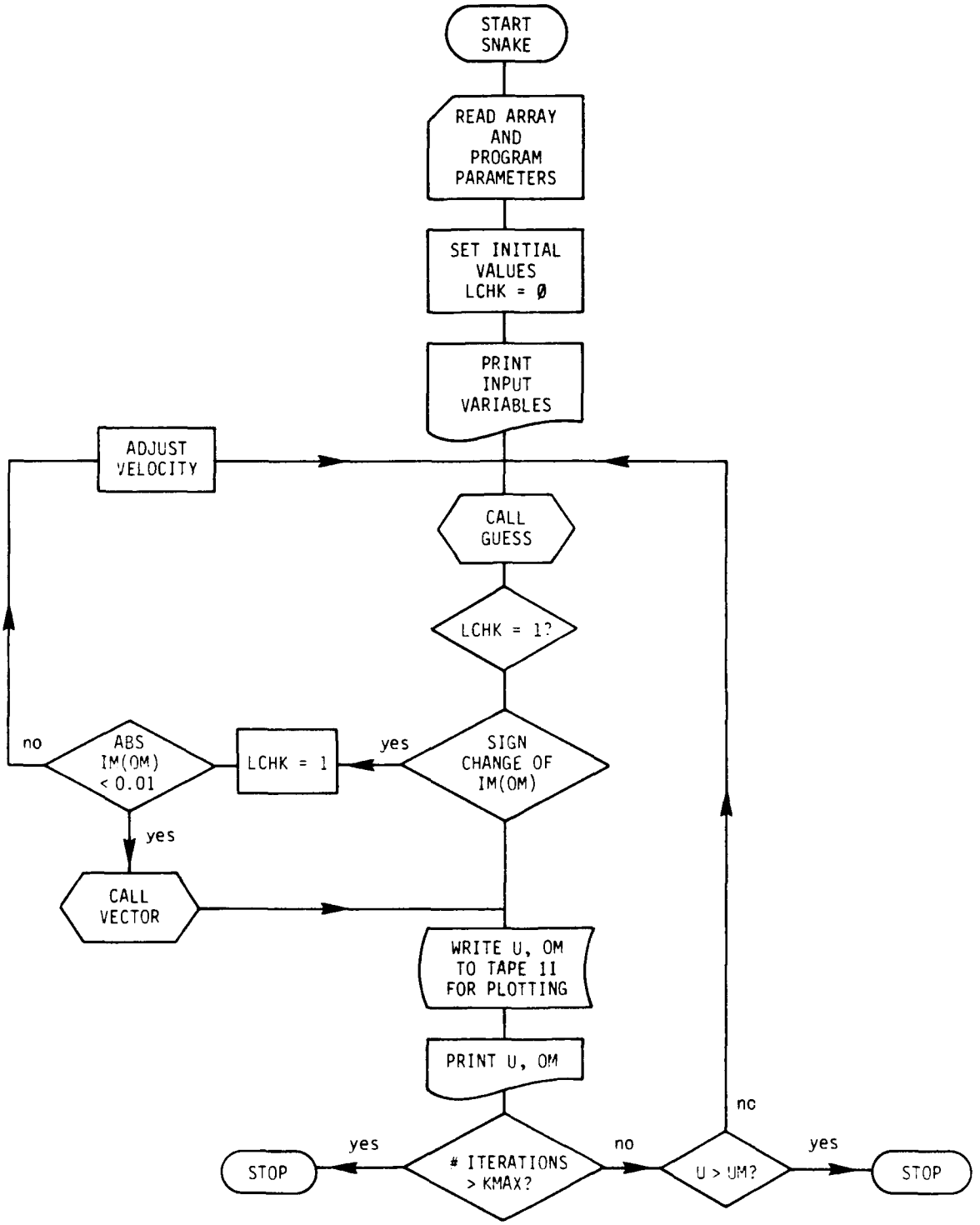
START SNAKE
READ ARRAY AND PROGRAM PARAMETERS
SET INITIAL VALUES LCHK = Ø
PRINT INPUT VARIABLES
ADJUST VELOCITY
CALL GUESS
LCHK = 1?
SIGN CHANGE OF IM(OM)
yes
LCHK = 1
no
ABS IM(OM) < 0.01
yes
CALL VECTOR
WRITE U, OM TO TAPE 11 FOR PLOTTING
PRINT U, OM
nc
ITERATIONS > KMAX?
yes
STOP
no
U > UM?
yes
STOP

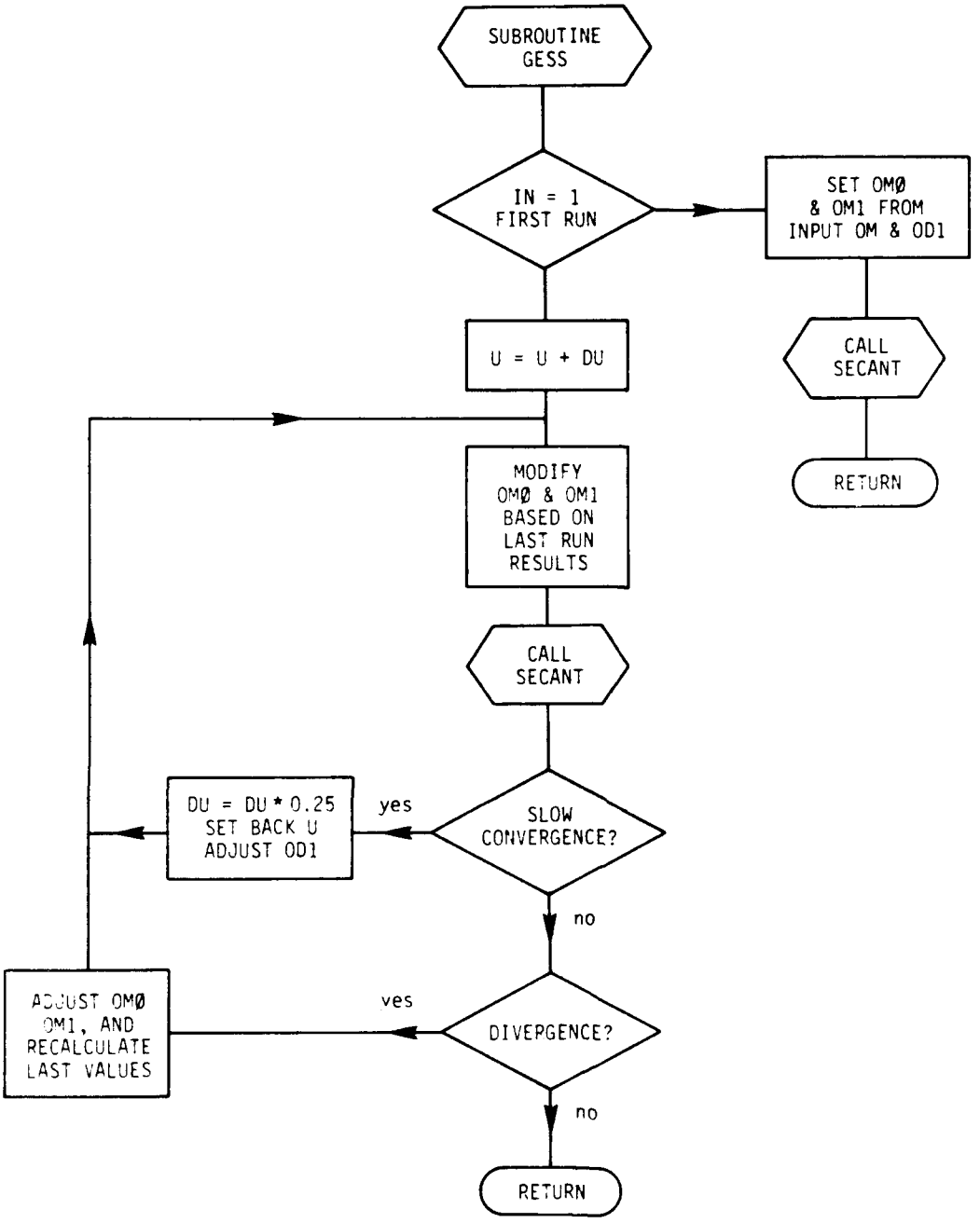
SUBROUTINE
GESS
IN = 1
FIRST RUN
SET OMØ
& OM1 FROM
INPUT OM & OD1
CALL
SECANT
RETURN
U = U + DU
MODIFY
OMØ & OM1
BASED ON
LAST RUN
RESULTS
CALL
SECANT
SLOW
CONVERGENCE?
yes
DU = DU * 0.25
SET BACK U
ADJUST OD1
no
DIVERGENCE?
yes
ADJUST OMØ
OM1, AND
RECALCULATE
LAST VALUES
no
RETURN

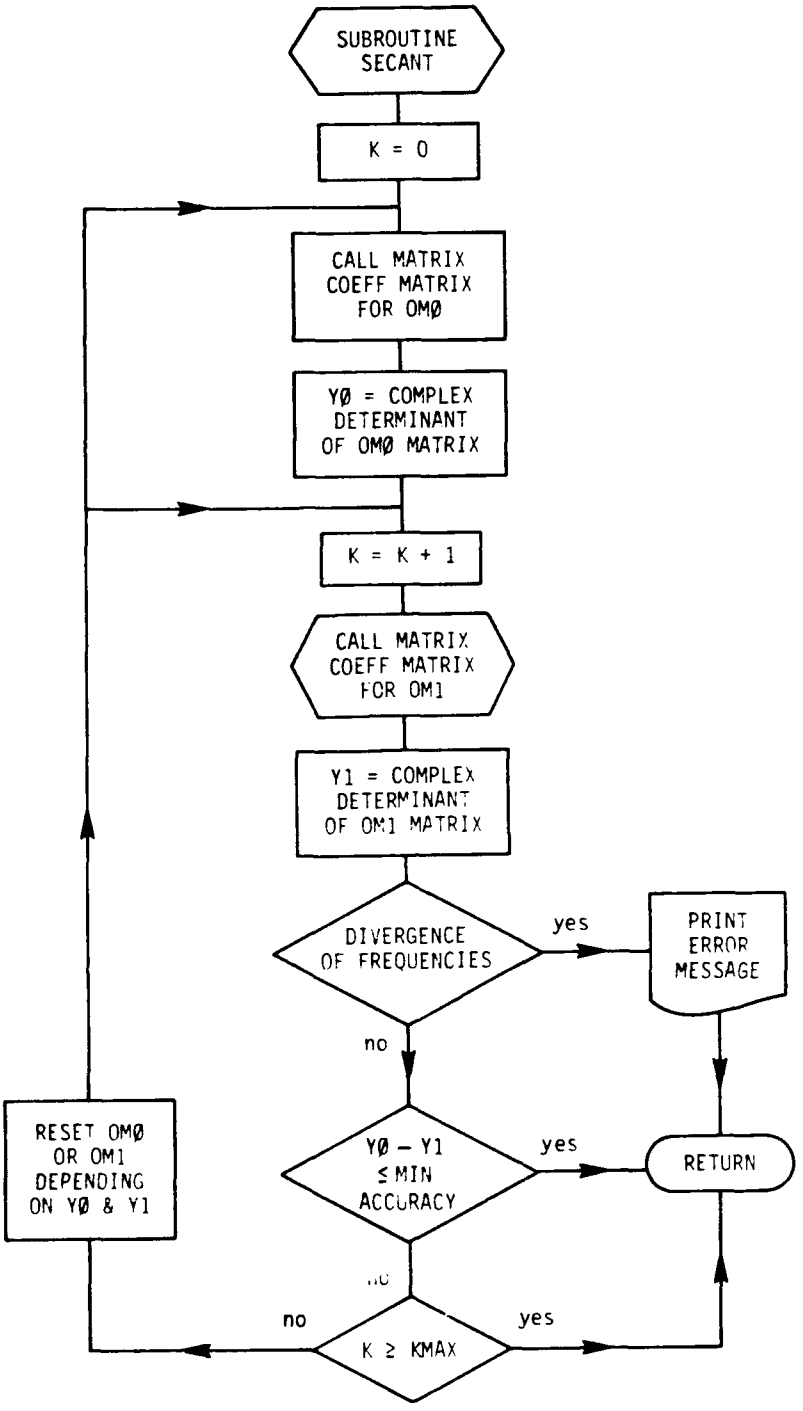
SUBROUTINE SECANT
K = 0
CALL MATRIX COEFF MATRIX FOR OMØ
YØ = COMPLEX DETERMINANT OF OMØ MATRIX
K = K + 1
CALL MATRIX COEFF MATRIX FOR OM1
Y1 = COMPLEX DETERMINANT OF OM1 MATRIX
DIVERGENCE OF FREQUENCIES
yes
PRINT ERROR MESSAGE
no
RESET OMØ OR OM1 DEPENDING ON YØ & Y1
YØ – Y1 ≤ MIN ACCURACY
yes
RETURN
no
K ≥ KMAX
no
yes

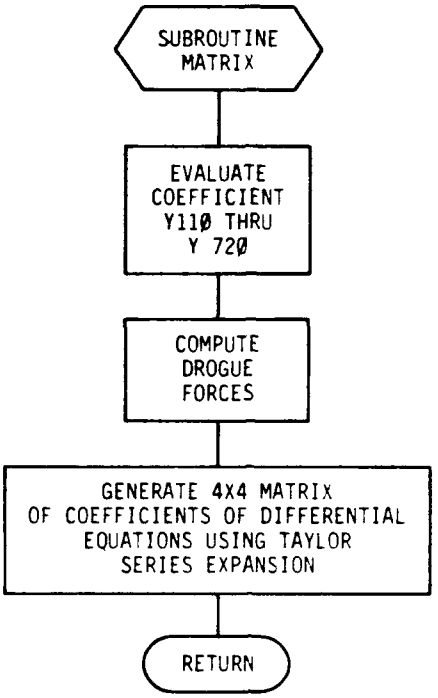
SUBROUTINE
MATRIX
EVALUATE
COEFFICIENT
Y11Ø THRU
Y 72Ø
COMPUTE
DROGUE
FORCES
GENERATE 4X4 MATRIX
OF COEFFICIENTS OF DIFFERENTIAL
EQUATIONS USING TAYLOR
SERIES EXPANSION
RETURN

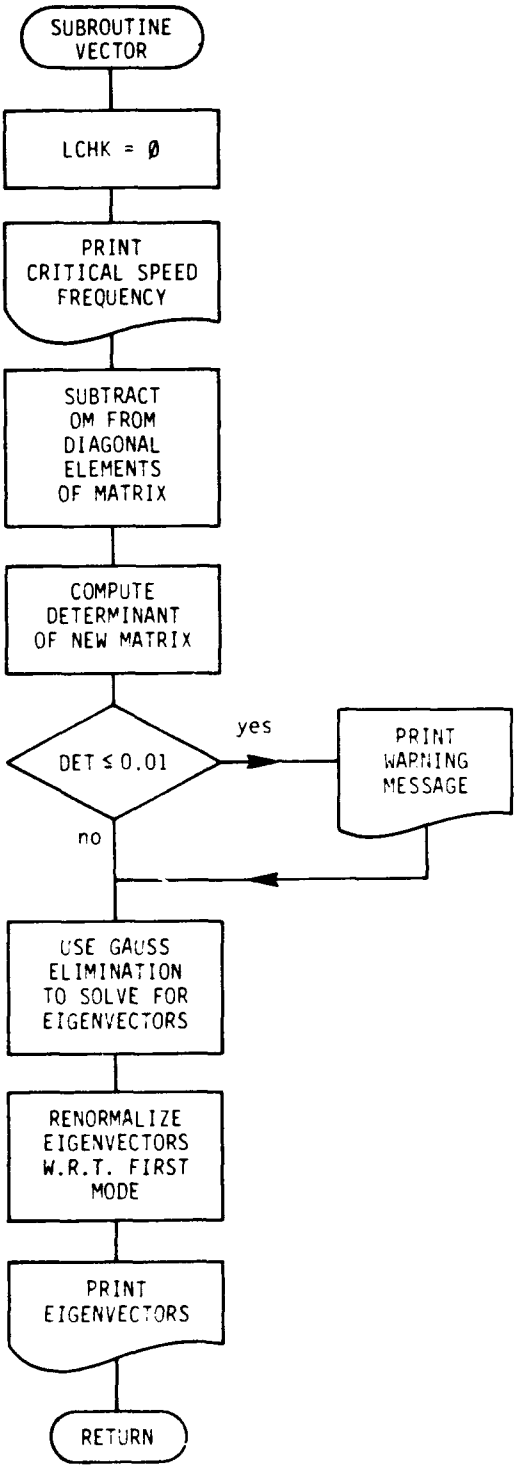
SUBROUTINE VECTOR
LCHK = Ø
PRINT CRITICAL SPEED FREQUENCY
SUBTRACT OM FROM DIAGONAL ELEMENTS OF MATRIX
COMPUTE DETERMINANT OF NEW MATRIX
DET ≤ 0.01
yes
PRINT WAPNING MESSAGE
no
USE GAUSS ELIMINATION TO SOLVE FOR EIGENVECTORS
RENORMALIZE EIGENVECTORS W.R.T. FIRST MODE
PRINT EIGENVECTORS
RETURN

```
      PROGRAM SNAKE (INPUT,OUTPUT,TAPE5=INPUT,TAPE6=OUTPUT,TAPE11)
      IMPLICIT COMPLEX(O,A,C,Y)
      COMMON Q1,Q2,QE,QA,QD,XCN,XCT
      DIMENSION A(4,4)
      REAL NEWU,OLDU
C
C  SNAKE IS A PREDICTOR-CORRECTOR ROUTINE TO SOLVE THE
C  FREQUENCY DOMAIN DIFFERENTIAL EQUATIONS MODELLING THE
C  THE HYDROELASTIC RESPONSE OF A FLEXIBLE CYLINDER OF
C  NEUTRAL BUOYNACY IN AXIAL FLOW
C
C  PROGRAM REVISED, JAMES OSSE  FALL 1981
C
C
C   DEFINE ARRAY PHYSICAL PARAMETERS
C   Q1= RATIO NOSE LENGTH TO MID BODY  (LAMDA 1)
C   Q2= RATIO TOW ROPE LENGTH TO MID BODY  (GAMMA)
C   QA= RATIO OF TAIL LENGTH TO NOSE LENGTH  (ALPHA)
C   QD= RATIO OF BASE DIAMETER (AT TAIL) TO MID BODY DIAMETER
C   QE= RATIO MID BODY LENGTH TO DIAMETER (EPSILON)
C   XCN= NORMAL COMPONENT OF DRAG COEFFICIENT
C   XCT= TANGENTIAL COMPONENT OF DRAG COEFFICIENT
C
C   DEFINE PROGRAM PARAMETERS
C   KEY= PRINT CONTROL INDEX        1 FOR MAXIMUM
C   IAX= UMBER OF POINTS INVESTIGATED ON IM-AXIS, INITIALLY 0 OR 1
C   IUP= 1 FOR UPWARDS ANALYSIS OF IMAGINARY BRANCH(-1 DOWNWARDS)
C   KM= MAXIMUM NUMBER OF ITTERATIONS ALLOWED AROUND DIVERGENT POINT
C   IFEND= NUMBER OF POINTS CALCULATED
C   U= VELOCITY
C   OM= INITIAL ESTIMATE OF OMEGA, GENERALLY GREATER
C   OM1= LOWER ESTIMATE OF OMEGA, DIRECTION OF OMEGA FOR INCREASED U
C   OD1= DELTA OMEGA AFTER FIRST ITTERATION, SHOULD CAUSE OM TO
C     GO IN DIRECTION OF ARGAND CURVE
C   DM= REQUIRED ITTERATIVE CONVERGENCE ACCURACY
C   UM= MAXIMUM VELOCITY CALCULATED TO IN PROGRAM
C   Q3= RATIO TAIL LENGTH TO MID BODY LENGTH (LAMDA 2)
C   DU= DELTA VELOCITY
C
      READ (5,500) Q2,QA,QE,QD,XCT
 500  FORMAT(5F5.3)
      READ(5,501) MODE,KEY,IAX,IUP,U,UM,DU,OM,OM1,OD1
 501  FORMAT(4I2,1X,9F5.2)
C  PARAMETERS
C  SET Q1, ECCENTRICITY OF NOSE/TAIL TO NEARLY ZERO FOR SMALL Q1
C   MAKES NOSE SPHERICAL INSTEAD OF ELLIPTICAL
      Q1=1.0/SQRT(QE*QE*4.)+0.02/QE
      XCN=XCT
      KM=12
      IFEND=125
      SU=0.0
      DUO=DU
```

```
      N=4
      DM=0.001
      Q3=Q1*QA
      X=1.
      NEWU=0.
      EIMO=10.
      OLDU=0.0
      LCHK=0
      IT=0
      WRITE(6,200) Q1,Q3,Q2,QE,QD,XCN,XCT
 200  FORMAT(1H1,10X,*    ARRAY CHARACTERISTICS*,//
     110X,*RATIO NOSE LENGTH TO MID BODY*,5X,F9.4,
     1/,10X,*RATIO TAIL LENGTH TO MID BODY*,5X,F9.4,/
     2,10X,*RATIO TOW ROPE LENGTH TO MID BODY*,1X,F9.4,/
     2,10X,*RATIO MID BODY LENGTH TO DIAMETER*,1X,F9.4,/
     3,10X,*RATIO DROGUE TO MID BODY DIAMETER*,1X,F9.4,/
     3,10X,*NORMAL DRAG COEFFICIENT*,11X,F9.4,/,10X,
     4,*TANGENTIAL DRAG COEFFICIENT*,7X,F9.4,//)
      WRITE(6,100)MODE,KEY,IAX,IUP,UM,DU,DM,OD1,MODE,OM,OM1
 100  FORMAT(10X,*    PROGRAM RUN PARAMETERS*,//10X,*MODE = *,I3,
     1*   KEY = *,I3,/10X,
     1*NUMBER OF POINTS INVESTIGATED ON IM AXIS*,I4,/
     210X,*1 FOR UPWARDS ANALYSIS OF IM AXIS, -1 DOWNWARDS*,I4/
     610X,*MAXIMUM VELOCITY CALCULATED TO *,F6.2,* IN STEPS OF *,F6.2
     3,/10X,*REQUIRED ITTERATIVE ACCURACY  *,F10.4,/
     410X,*DELTA OMEGA AFTER FIRST ITTERATION  *,2F10.4/
     1,10X,*UPPER ESTIMATED VALUE OF MODE *,I2,* AT ZERO VELOCITY *,
     22F10.4,/,10X,*LOWER ESTIMATED VALUE AT ZERO VELOCITY *,2F10.4,//)
      PRINT 110
110   FORMAT(43X,*REAL*,4X,*IMAGINARY*/)
C  MAIN LOOP IN PROGRAM
      DO 1 IN=1,IFEND
      CALL GESS
     1(OM1,OM,OD1,OD2,U,DU,DM,IN,N,K2,K1,K,IAX,IUP,KM,KEY,A,LCHK)
      EIGIM=-AIMAG(OM1)
C  CHECK FOR ZERO CROSSING OF REAL AXIS FROM SIGN CHANGE OF IM(OM1)
C
C  LCHK RESET TO ZERO IN VECTOR
C
      IF(ABS(EIGIM).LT.0.01.AND.U.NE.0)
     1CALL VECTOR(MODE,U,OM1,LCHK,EIMO,IT,DU,DUO,A,SU,QE)
      EIMN=SIGN(X,EIGIM)
      IF((EIMO+EIMN).EQ.0.OR.LCHK.EQ.1)GO TO 400
 470  EIMO=SIGN(X,EIGIM)
      OLDU=U
      EIGIM=SIGN(SQRT(ABS(EIGIM)),EIGIM)
      EIGRE=REAL(OM1)
      EIGRE=SQRT(ABS(EIGRE))
C  WRITE TO TAPE11 FOR PLOTTING
      WRITE(11,20)U,OM1
 20   FORMAT(3F10.4)
C  WRITE TO OUTPUT
```

```
      WRITE(6,10) U,OM1,K
10    FORMAT(10X,* VELOCITY = *,F7.3,4X,*OMEGA =*,2(2X,F8.3),
     1* IN *,I2,* ITTERATIONS*)
      IF((K.GE.KM+1).OR.((U-UM)*DU.GT.0.00))GO TO 1000
      GO TO 1
 400  IF(OLDU.EQ.0.0) GO TO 470
      IF(U.GT.UM) GO TO 1000
      IF((U-SU).LE.DU) GO TO 470
      LCHK=1
      DU=0.0
      IT=IT+1
      IF(IT.GT.10) GO TO 404
      IF(ABS(EIMO+EIMN).EQ.2.0) OLDU=NEWU-(OLDU-NEWU)
      NEWU=(U+OLDU)/2
      UOLD=OLDU
      OLDU=U
      U=NEWU
      EIMO=SIGN(X,EIGIM)
      PRINT 401,OLDU,EIGIM,EIMN,EIMO,NEWU,UOLD,LCHK,IT
 401  FORMAT(* VEL=*,F7.3,* EIGIM=*,F7.3,* EIMN=*,F7.3,* EIMO=*,F7.3,
     1* NEWU=*,F7.3,* OLDU=*,F7.3,* LCHK=*,I3,* IT=*,I3)
      GO TO 1
 404  WRITE(6,406)
 406  FORMAT (* ZERO CROSSING DOES NOT CONVERGE IN 10 ITTERATIONS*)
      IT=0
      DU=DUO
      LCHK=0
 1    CONTINUE
 1000 CONTINUE
      STOP
      END
      SUBROUTINE GESS
     1(OM1,OM,D1,D,U,DU,RM,IN,N,I2,I1,I,IAX,IUP,IM,KEY,A,LCHK)
C
C   VARIBLE NAME CHANGE FROM MAIN PROGRAM AS FOLLOWS:
C   D1=OD1  D=OD2  RM=DM  I2=K2  I1=K1  I=K  IM=KM
C
C REQUIRED SUBROUTINE SECANT(A,X1,X0,U,DN,KM,L,M,N,K,KEY)AND N<20***
C OM1 = (IN-1)-TH FREQUENCY (REQUIRED INITIALLY (IN=1)) --> (IN)-TH
C OM = (IN-2)-TH FREQUENCY. AT IN=1,CHOSEN CLOSE TO EXPECTED
C ROOT GENERALLY BECOMES THE (IN-1)-TH EXCEPT NEAR DISCONTINUITIES
C D1=(IN-1)-TH FREQUENCY INCREMENT PREDICTED (REQUIRED INITIALLY)
C D=(IN-2)-TH REAL FREQUENCY INCREMENT (NOT REQUIRED INITIALLY).
C DU=(IN-2)-TH VELOCITY INCREMENT, BECOMES THE IN-TH.
C U= (IN-1)-THE VELOCITY, BECOMING THE IN-TH (REQUIRED INITIALLY).
C RM=GENERAL ACCURACY (MINIMUM DU=100*RM).
C IN=NUMBER OF POINTS CALCULATED SO FAR (LOOP IN MAIN PROGRAM).
C I2=(IN-3)-TH SECANT ITERATIONS (NOT REQUIRED AT IN=1).
C I1 =(IN-2)-TH SECANT ITERATIONS (NOT REQUIRED AT IN=1)
C I=(IN-1)-TH SECANT ITERATIONS (NOT REQUIRED AT IN=1)
C IAX=NUMBER OF POINTS INVESTIGATED ON IM-AXIS (INITIALLY 0 OR 1).
C IUP = 1 FOR UPEARDS ANALYSIS OF IMAGINARY BRANCH (-1 DOWNWARDS).
```

```
C IM=MAXIMUM SECANT ITERATIONS (I=IM+1 IN CASE OF DIVERGENCE.)
C KEY=1,0,-1 IF INTERMEDIATE CALCULATIONS ARE TO BE PRINTED OUT, OR
C > 0 IF REGULAR VARIABLE STEPS IN VELOCITY ARE  RNQURRED (DU MAY
C BE DOUBLED IF U IS AN INTEGER MULTIPLE OF 2*DU AND I*I1*[I2<9),
C = 0 FOR NON NECESSARY REGULAR INTEGER STEPPED VALUES OF U.
C < 0 IF DU IS TO REMAIN CONSTANT. (ALMOST ACHIEVED BY I=2,I1>4)
      DIMENSION A(4,4),L(10),M(10)
      COMPLEX A,OM1,OM0,OM,D1,D,GI
C
      DD1=0
      J1=1+(1/IN)*(IM-1)
C INITIAL VELOCITY.  INITIAL CHARACTERISTICS KEPT FOR NEXT STEP.
C   FIRST RUN THRU GO TO 81, J=12
      IF(IN.EQ.1.OR.LCHK.EQ.1) GO TO 81
      GI=(0.00,1.00)
      J=0
 1000 R0=REAL(OM)
      IF(I.LT.IM) GO TO 1
C SPECIAL CASES OF DIVERGENCE.
      IF (IN.LE.3) GO TO 101
      IF((I1.EQ.1) .AND. (I2.EQ.1))GO TO 3
      IF(IAX) 101,10,11
C SPECIAL CASES OF CONVERGENCE.
  1   IF(KEY.LT.0) I=2
      IF(IN.LE.3) GO TO 50
      JAX=IAX+5
      GO TO (12,4,4,4,2,7,4,4,4),JAX
  2   R1=REAL(OM1)
      IF((R1.GT.RM*10. ).AND.(R0.LT.RM*10.  )) GO TO 12
      IF((R1.LT.RM*10. ). AND.(R0.GT.RM*10. )) GO TO 10
      IF( (R1+RM .LT. R0/2.) .AND. (I1.GT.1) ) I=MIN0(I,4)
      IF(R1+RM .LT. R0/4.) I=MAX0(2,I-I1)
      IF((I.LE.4+4/IN).OR.(ABS(DU/4.00).LT.100*RM)) GO TO 4
C SLOW CONVERGENCE . DIVISION OF STEP BY 4.
  3   U=U-0.7500*DU
      DU=DU/4.00
      D=(5*D+3*D1)/32
      D1=(5*D1+3*D)/32+(I/IM)*(D1-D)/8.00
      OM1=OM+D1
      I1=4
      I2=2
      GO TO 80
C SPECIAL PROCEDURE TO FACE TOO QUICK VARIATIONS OF FREQUENCY.
  4   IF (KEY.LT.0) GO TO 6
      IF(IN.EQ.4) GO TO 64
      IF(IAX.EQ.0) GO TO 5
      F=(OM1-OM)/D
      IF((ABS(F).LT.0.5).AND.(I.LE.2)) J=-1
      I=I-J
      IF(IAX.GT.4) GO TO 5
C SECOND, THIRD, FOURTH POINTS ON OR OFF IM-AXIS.
      D=(D+OM1-OM)/2.00
```

```
      I=MIN0(I,2)
      GO TO 6
 5    IF (I.GE.3)GO TO 6
      IF (I*I1*I2.LE.8) GO TO 64
      IF(I.EQ.1) GO TO 65
      GO TO 6
 64   KU=(U+RM/5.00)/DU
      IF(KEY.EQ.0)KU=0
      IF(KU-(KU/2)*2 .EQ. 0) GO TO 66
 65   J=I-2-(4/IN)*MIN0(I-3,2)
      GO TO 67
 66   J=I/2 - (I/4)*(IN/4)
      IF((I*I1.EQ.1).AND.(KU-(KU/4)*4 .EQ. 0))J=1
 67   I=I-J
C PREDICTED STEP FACTOR. NEW CHARACTERISTICS
 6    DDB=2.00**(2-I)
      IDUM=ABS(DU/(101*RM))
      IF((IDUM+1)*DDB.LT.0.900) DDB=2.00**(2/(IDUM+1) - 2)
      DU=DU*DDB
      F=(OM1-OM0)/D1
      IF(F.GT.0.) J1=-1
      DD1=(OM1-OM-D1)/2.00
      D1 =(3*(OM1-OM)-D + (OM1-OM-D)*DDB)*DDB/2.00
      D  =(3*(OM1-OM)-D - (OM1-OM-D)*DDB)*DDB/2.00
      DD1=DD1*D1/D
      I2=I1-1+1/I1
      I1=I+J
 7    U=U+DU
      OM1=OM1+D1+DD1
      IF(IAX.NE.0) IAX=IAX+1
      GO TO 80
C FIRST POINT OFF RE-AXIS (TO BE RECALCULATED)
 10   IAX=1
      H1=REAL(D1)
      IF(((R0+3.00*H1).GT.0.00) .AND. (I.EQ.IM)) GO TO 11
      D1  =GI*CABS(D)*IUP
      OM1=OM-R0
      GO TO 51
C FIRST POINT OFF IM-AXIS (TO BE RECALCULATED)
 11   IAX=-4
      D1=(CABS(D) + D1/2.00)*1.500
      IF(R0.GT.10.00*RM) D1=(GI*CABS(D)*IUP+H1)*0.7500
      OM1=OM
      GO TO 52
C SECOND POINT OFF IM-AXIS (TO BE PREDICTED)
 12   IAX=-3
      D1=CABS(OM1-OM)
 50   U=U+DU
      IF(IN.NE.3) GO TO 52
      IAX=5*IAX
      D1=OM1-OM
 51   D=D1
```

```
 52   OM1=OM1+D1
      I2=2
      I1=2
      IF(IN.GT.3) J1=1+IABS(IAX+1)
      DD1=0
 80   OM=OM1-D1-DD1
      R1=REAL(OM1)
      R0=REAL(OM)
C INVESTIGATION OF A NEGATIVE PREDICTION BEYOND IM-AXIS.
      IF((R1.LT.10.00*RM) .AND. (IAX .EQ.0)) GO TO 10
 81   OM0=OM+D1+DD1-J1*D1/IM
      IF(IN.GT.1) J1=I
      CALL SECANT(A,OM1,OM0,U,RM,IM,N,I,KEY)
      IF(I*J1 .GE. IM*IM) I=IM+1
      IF((I.LT.IM) .OR. (ABS(DU).LT.199*RM) .OR. (IN.LT.4)) GO TO 100
      IF((IAX-1)*(IAX+4))91, 90, 100
 90   D1=(D*(1-IAX)+H1*(4+IAX))/5
      D=D1
      IAX=-IAX+1
 91   IF(IAX.EQ.0) GO TO 100
      WRITE(6,99) U
 99   FORMAT(* -GESS- VELOCITY SET BACK TO*,F9.6,*-3/4(DU) AND DU=DU/4
     1*/)
      GO TO 3
 101  I=IM+1
 100  IF(I.EQ.IM) GO TO 1000
      RETURN
      END
      SUBROUTINE SECANT(A,X1,X0,UE,DM,KM,N,K,KEY)
C  VARIABLE NAME CHANGE FROM CALL STATEMENT AS FOLLOWS:
C   X1=OM1  X0=OM0  UE=U   KM=IM  K=I
      DIMENSION A(4,4)
      COMPLEX A,X0,X1,X2,Y1,Y0,CDET,X
      X=X1
      K=0
      IF(CABS(X0).LT.DM.OR.CABS(X1-X0).LT.DM) X0=X0+(1.00,1.00)*DM
C  MATRIX CALL RETURNS FILLED MATRIX A AS FUNCTION OF U
C  FOR HIGH ESTIMATE OF OMEGA, OM0
 4    CALL MATRIX(A,UE,X0,N)
      M=N
C   DETERMINANT OF MATRIX A
      Y0=CDET(A,M)
      Z0=CABS(Y0)
 1    K=K+1
C   FOR LOW ESTIMATE OF OMEGA, OM1
      CALL MATRIX(A,UE,X1,N)
C   DETERMINANT OF MATRIX A
      Y1=CDET(A,M)
      Z1=CABS(Y1)
      X2=(X1*Y0-X0*Y1)/(Y0-Y1)
      RX=REAL(X2)
      YR0=Y0
```

```
      W0=YR0*Y1
      W1=(YR0-Y0)*Y1/DM
      IF((W0.LE.0.).AND.(W1.LT.-W0)) Z0=10.*Z0
      IF(((1-1/K)*Z1.GT.Z0). OR. (K.GE.KM))GO TO 3
      IF(IABS(KEY).NE.1) GO TO 5
      WRITE(6,10) UE,X0,Y0,X1,Y1,X2
 10   FORMAT(* V=*,F6.2,* OM0=*,2F9.3,* DET OF OM0=*,2F9.3,* OM1=*,2F9.3,
     1* DET OF OM1=*,2F9.3,* X2=*,2F9.3/)
 5    CX=-AIMAG(X2)
      IF(ABS(CX).LT.DM) X2=RX
      IF((CABS(1.00-X1/X2).LT.DM).OR.(CABS(X2-X1).LT.DM)) GO TO 2
      IF(RX+DM) 6,6,7
 6    Z0=X1-X0
      X0=X2-RX
      X1=X0-(0.00,1.00)*RX
      IF(Z0.GT.2.*DM)X0=X0-RX
      GO TO 4
 7    X0=X1
      X1=X2
      IF(ABS(RX).LT.DM) X1=X1-RX
      Z0=Z1
      Y0=Y1
      GO TO 1
 3    WRITE (6,11)K,KM,UE,X0,Y0,X1,Y1,X2
 11   FORMAT(*0-SECANT- INTERRUPTED BECAUSE OF DIVERGENCE OF FREQUENCY A
     1FTER K=*,I2,* ITERATIONS IF K<KMAX=*,I2,* .LAST ITERATION TRACE
     2  BACK:*/* V=*,F9.6,2(*   X=*,2F10.3,* Y=*,2F10.3),*   X2=*,
     32F10.3/)
      K=KM
 2    X0=X
      X1=X2
      RETURN
      END
      SUBROUTINE MATRIX (A,U,OMEGA,M)
C
      IMPLICIT COMPLEX(O,A,B,C,Z)
      COMMON Q1,Q2,QE,QA,QD,XCN,XCT
      DIMENSION A(4,4),B(85,4),C(85,4)
      O=(0.00,1.00)
      Z=OMEGA
      Z2=Z*Z
      PI=3.141592653500
      Q11=Q1*Q1
      QEE=QE*QE
      QAA=QA*QA
C
C Q1 IS THE RATIO OF LENGTH OF NOSE SECTION/LENGTH OF MAIN BODY
C Q2 IS THE RATIO OF LENGTH OF TOW-ROPE/LENGTH OF MAIN BODY
C QA IS THE RATIO OF LENGTH OF  TAIL SECTION/LENGTH OF NOSE SECTION
C QE IS THE RATIO OF LENGTH OF MAIN BODY/DIAMETER OF CYLINDER
      YE=SQRT(1.00-1.00/(4.00*Q11*QEE))
C YE IS THE ECCENTRICITY OF THE ELLIPSOID
```

```
C  YE GOES TO ZERO FOR SPHERICAL NOSE
      YEE=YE*YE
      YEI=1.00/YE
      YEL=ALOG((1.00+YE)/(1.00-YE))
      YEX=YE/(1.00-YEE)
      YEXX=YEE/(1.00-YEE)
      YEEI=1.00/YEE
      XK1=-YE*(0.500*YEI*YEL-1.00)/(0.500*YEL-YEX)
      XK2=-(0.500*YEL-YEX)/(0.500*YEL-YEX*(1.00-2.00*YEE))
      XL3=-YEE*(1.500*YEI*YEL-3.00-YEXX)/(1.500*(2.00*YEI-YE)*YEL-6.00+
     *  YEXX)
C
C DIMENSIONLESS PARAMETERS OF I,S
C   BOUNDARY CONDITIONS OF NOSE AND TAIL
C
C  SAME AS I120 THRU I720 AS SHOWN IN YU'S  THESIS PG. B1
      Y110=PI*Q1/4.00
      Y120=0.500*Q1*(QA*SQRT(1.00-QAA)+ASIN(QA))
      Y210=2.00*Q1/3.00
      Y220=QA*Q1*(1.00-QAA/3.00)
      Y310=2.00*Q1*XK2/3.00
      Y320=QA*Q1*(1.00-QAA/3.00)*XK2
      XXK1=1.00+XK1
      XXK2=1.00+XK2
      XXK12=XXK1*XXK2
      XXK11=XXK1*XXK1
C   ECCENTRICITY OF TAIL
      XYAE=YE*QA
      XXA=XK1-(1.00+XK1)*XL3
      XXB=YEE+2.00*XXK1*XL3
      YEEZ=(1.00-YEE)/YEE
      TE1=ALOG(1.00-YEE)
      TE2=ALOG(1.00-YEE*QAA)
      TT1=(XXA-XXB)*YEEI
      Y410=XXK12*YEEI*(1.00+YEEZ*TE1)/2.00
      Y420=XXK12*YEEI*(QAA+YEEZ*TE2)/2.00
      Y510=Q11*XL3/4.00
      Y520=Q11*QAA*XL3*(2.00-QAA)/4.00
      Y610=Q1*(XXA-2.00*XXB/3.00+XXB*YEEI+(XXA-TT1-XXB*YEEI*YEEI)*0.500*
     1  YE*YEL)*YEEI
      Y620=Q1*(XXB*QAA*QA/3.00+(XXA-XXB+XXB*YEEI)*QA+(XXA-TT1-XXB*YEEI*
     1  YEEI)*0.500*YE*ALOG((1.00+XYAE)/(1.00-XYAE)))*YEEI
      Y710=0.500*YEEI*(XXK11-YEE+YEEZ*XXK11*TE1)
      Y720=0.500*YEEI*(QAA*(XXK11-YEE)+YEEZ*XXK11*TE2)
      SMAX=PI/(4.00*QEE)
      SBASE=PI*(1.00-QAA)/(4.00*QEE)
      XCDF=QE*XCT*(1.00+Y110+Y120)+2.00*(.710+Y720)
C     XCD=0.02900*(1.00-QAA)**1.5/SQRT(XCDF)
      XCD=0.029*(QD)**3.0/SQRT(XCDF)
C  XCD = 0.029 * (BASE DIA/MID BODY DIA)**3.0 /SQRT(XCDF) EQN. #30
C
      U2=U*U
```

```
      UX1=U*SQRT(2.00)
      UX2=U/SQRT(2.00)
C
C COEFFICIENTS OF DIFFERENTIAL EQUATIONS C*S
C   SAME AS COEFFICIENTS G0 THRU G10 IN YU'S THESIS
C  THE FOLLOWING COEFFICIENTS C5 THRU C8 ARE THE ORIGINAL COEFFICIENTS
C     C5=U2*0.500*((Q1+Q2)*(QE*XCT*(1.00+Y110+Y120)+2.00*(Y710+Y720)+
C    1  SBASE*XCD/SMAX)/Q2-QE*XCN*Y110-2.00*Y410)+UX2*(-Y610+Y310)*O*Z-
C    2  0.500*Y510*Z2
C     C6=-0.500*U2*(QE*XCT*(1.00+Y110+Y120)+2.00*(Y710+Y720)+SBASE*XCD
C    1  /SMAX)/Q2+UX2*(-0.500*QE*XCN*Y110-Y410)*O*Z+0.500*(Y210-Y310)*Z2
C     C7=U2*0.500*Q1*(QE*XCT*(1.00+Y110+Y120)+2.00*(Y710+Y720)+SBASE
C    1  *XCD/SMAX)*(Q1+Q2)/Q2
C     C8=-U2*0.500*Q1*(QE*XCT*(1.00+Y110+Y120)+2.00*(Y710+Y720)+SBASE*
C    1  XCD/SMAX)/Q2
C
C  P IS TOW ROPE TENSION
C  PN IS NORMAL COMPONENT OF TOW ROPE FORCE
C  PL IS LONGITUDINAL COMPONENT
      P=(QE*XCT*(1.00+Y110+Y120)+2.00*(Y710+Y720)+SBASE*XCD/SMAX)
      PN=P/Q2
      PL=P*(Q1+Q2)/Q2
      C1=U2*(1.00-0.500*(QE*XCT*(0.500+Y120)+2.00*Y720+SBASE*XCD/SMAX))
      C2=U2*0.500*QE*XCT
      C3=0.500*QE*XCN*U2+UX1*O*Z
      C4=-Z2+0.500*UX2*QE*XCN*O*Z
      C5=U2*0.5*(PL-QE*XCN*Y110-2.00*Y410)+UX2*(-Y610+Y310)*O*Z-
     2  0.500*Y510*Z2
      C6=-0.5*U2*PN+UX2*(-0.500*QE*XCN*Y110-Y410)*O*Z+0.500*(Y210-Y310)
     1*Z2
      C7=0.5*U2*Q1*PL
      C8=-0.5*PN*U2
      C9=U2*(0.500*QE*XCN*Y120-Y420)+UX2*(Y320-Y620)*O*Z-0.500*Y520*Z2
      C10=UX2*(0.500*QE*XCN*Y120-Y420)*O*Z-0.500*(Y220+Y320)*Z2
C  SET UP 4X4 IDENTITY MATRIX
      DO 91 I=1,4
      DO 92 J=1,4
 92   C(I,J)=(0.00,0.00)
 91   C(I,I)=(1.00,0.00)
C MM IS THE ORDER OF POWER SERIES
      MM=70
      DO 93 N=5,MM
      J=N-1
      CX1=-(C1-0.500*C2)/(J*(J-1))
      CX2=-(C2*(J-4)+C3)/(J*(J-1)*(J-2))
      CX3=-C4/(J*(J-1)*(J-2)*(J-3))
      DO 94 I=1,4
      C(N,I)=CX1*C(N-2,I)+CX2*C(N-3,I)+CX3*C(N-4,I)
 94   CONTINUE
 93   CONTINUE
C   SET UP MATRIX A, LOOKS LIKE:
C          1          2          3          4
```

```
C       ------------------------------------
C  1       C6          C5        0,0        -6,0
C  2       C8          C7       -2,0         0,0
C  3      0,0         0,0        2,0         6,0
C  4      C10       C9+C10    2C9+C10     3C9+C10-6
C
       A(1,1)=C6
       A(1,2)=C5
       A(1,3)=(0.00,0.00)
       A(1,4)=(-6.00,0.00)
       A(2,1)=C8
       A(2,2)=C7
       A(2,3)=(-2.00,0.00)
       A(2,4)=(0.00,0.00)
       A(3,1)=(0.00,0.00)
       A(3,2)=(0.00,0.00)
       A(3,3)=(2.00,0.00)
       A(3,4)=(6.00,0.00)
       A(4,1)=C10
       A(4,2)=C9+C10
       A(4,3)=2.00*C9+C10
       A(4,4)=3.00*C9+C10-6.00
C  SUMS B(5,1) THRU B(70,1) INTO A(3,1)
       DO 81 N=5,MM
       B(N,1)=(N-1)*(N-2)*C(N,1)
 81    A(3,1)=A(3,1)+B(N,1)
C    SUMS B(5,2) THRU B(70,2) INTO A(3,2)
       DO 99 N=5,MM
       B(N,2)=(N-1)*(N-2)*C(N,2)
 99    A(3,2)=A(3,2)+B(N,2)
       DO 96 N=5,MM
       B(N,3)=(N-1)*(N-2)*C(N,3)
 96    A(3,3)=A(3,3)+B(N,3)
       DO 71 N=5,MM
       B(N,4)=(N-1)*(N-2)*C(N,4)
 71    A(3,4)=A(3,4)+B(N,4)
C    SUBTRACTS  B(5,1) THRU B(70,1) FROM A(4,1)
       DO 72 N=5,MM
       B(N,1)=((N-1)*(N-2)*(N-3)-C9*(N-1)-C10)*C(N,1)
 72    A(4,1)=A(4,1)-B(N,1)
C    SUBTRACTS B(5,2) THRU B(70,2) FROM A(4,2)
       DO 73 N=5,MM
       B(N,2)=((N-1)*(N-2)*(N-3)-C9*(N-1)-C10)*C(N,2)
 73    A(4,2)=A(4,2)-B(N,2)
       DO 74 N=5,MM
       B(N,3)=((N-1)*(N-2)*(N-3)-C9*(N-1)-C10)*C(N,3)
 74    A(4,3)=A(4,3)-B(N,3)
       DO 75 N=5,MM
       B(N,4)=((N-1)*(N-2)*(N-3)-C9*(N-1)-C10)*C(N,4)
 75    A(4,4)=A(4,4)-B(N,4)
       RETURN
       END
```

```
      COMPLEX FUNCTION CDET(A,N)
      COMPLEX A,PIVOT,HOLD
      INTEGER END, ROW, COL, PIVROW, PIVCOL
      DIMENSION A(4,4),L(10),M(10)
C DETERMINANT OF THE BOUNDARY CONDITION
C
      END =N-1
      CDET=(1.00,0.00)
      DO 10 I=1,N
      L(I)=I
 10   M(I)=I
      DO 100 LMNT=1,END
      PIVOT=(0.00,0.00)
      DO 20 I=LMNT,N
      ROW=L(I)
      DO 20 J=LMNT,N
      COL=M(J)
      IF(CABS(PIVOT).GE.CABS(A(ROW,COL))) GO TO 20
      PIVROW=I
      PIVCOL=J
      PIVOT = A(ROW,COL)
 20   CONTINUE
      IF (PIVROW.EQ.LMNT) GO TO 22
      CDET=-CDET
      KEEP=L(PIVROW)
      L(PIVROW)=L(LMNT)
      L(LMNT)=KEEP
 22   IF(PIVCOL.EQ.LMNT) GO TO 26
      CDET=-CDET
      KEEP=M(PIVCOL)
      M(PIVCOL)=M(LMNT)
      M(LMNT)=KEEP
 26   CDET=CDET*PIVOT
      IF(CABS(PIVOT).EQ.0.00) GO TO 333
      JAUG=LMNT+1
      PIVROW=L(LMNT)
      PIVCOL=M(LMNT)
      DO 100 I=JAUG,N
      ROW=L(I)
      HOLD=A(ROW,PIVCOL)/PIVOT
      DO 100 J=JAUG,N
      COL=M(J)
 100  A(ROW,COL)=A(ROW,COL)-HOLD*A(PIVROW,COL)
      CDET=CDET*A(ROW,COL)
 333  RETURN
      END
      SUBROUTINE VECTOR(MODE,U,OM1,LCHK,EIMO,IT,DU,DUO,A,SU,QE)
      DIMENSION A(4,4),Y(4)
      COMPLEX OM1,A,S,Y,M,DUM,DET,CDET
      DU=DUO
      LCHK=0
      SU=U
```

```
      IT = 0
      EIMO=10.
      PRINT 400,U,OM1,IT
 400  FORMAT(* U=*,F10.5,* OM1=*,2F10.5,* IN *,I3,* ITTERATIONS*)
C  PRINT DIMENSIONAL VEL AND OMEGA
      DIA=2.5/12.0
      EI=7.8125
      DMASS=2*1.99*3.1416*DIA*DIA/4.0
      DIML=QE*DIA
      DIMOM=REAL(OM1)/(DIML*DIML*(DMASS/EI)**0.5)
      DIMU=U/(DIML*(DMASS/EI/2.0)**0.5)
      DIMOMHZ=DIMOM/6.28
      PRINT 700,DIMU,DIMOM,DIMOMHZ
700   FORMAT(*DIM. VELOCITY =*,F9.3,* KNOTS *,
     1*DIM. FREQUENCY =*,F9.3,*RPS, OR*,F9.3,*HZ*)
      WRITE(6,500)
 500  FORMAT(* COMPLEX MATRIX A(4,4) LOOKS LIKE:*)
      WRITE(6,600) ((A(I,J),J=1,4),I=1,4)
 600  FORMAT (1H ,8E15.6/)
C   SUBTRACT EIGENVALUES FROM DIAGONAL ELEMENTS
      N=4
      DO 10 I=1,N
 10   A(I,I)=A(I,I)-OM1
C  COMPUTE DETERMINANT . SINGULAR IF ZERO, NO UNIQUE SOLUTION
      DET=CDET(A,N)
      IF(ABS(REAL(DET)).GT.0.1) GO TO 20
      WRITE(6,310) DET
 310  FORMAT(* CAUTION , DETERMINANT VALUE IS *, 2E15.7)
 20   CONTINUE
C  BEGIN GAUSS ELIMINATION SCHEME
C  TAKEN FROM MCCRACKEN AND DORN "NUMERICAL METHODS AND FORTRAN PROGR."
C  NORMALIZE W.R.T. FOURTH COLUMN
C  Y IS EIGENVECTOR
      Y(N)=(1.,1.)
      N1=N-1
      K=1
 30   I=K+1
C  REARRANGE ROWS TO REDUCE ROUNDOFF ERROR
C  FIND MAXIMUM ELEMENT
      L=K
 60   IF(CABS(A(I,K)).GT.CABS(A(L,K))) L=I
      IF (I.EQ.N ) GO TO 50
      I=I+1
      GO TO 60
 50   IF(L.EQ.K) GO TO 82
C  INTERCHANGE A(K,J) AND A(L,J)
      J=K
 70   DUM=A(K,J)
      A(K,J)=A(L,J)
      A(L,J)=DUM
      IF(J.EQ.N1) GO TO 80
      J=J+1
```

```
      GO TO 70
C  RESET I TO ORIGINAL VALUE
80    DUM=A(K,N)
      A(K,N)=A(L,N)
      A(L,N)=DUM
 82   I=K+1
C  CONTINUE WITH GAUSS ELIMINATION
C  DEFINE MULTIPLIER
 85   M=A(I,K)/A(K,K)
      A(I,K)=(0.0,0.0)
      J=K+1
 90   A(I,J)=A(I,J)-M*A(K,J)
      IF(J.EQ.N) GO TO 100
      J=J+1
      GO TO 90
 100  IF(I.EQ.N) GO TO 110
      I=I+1
      GO TO 85
 110  IF(K.EQ.N-1) GO TO 150
      K=K+1
      GO TO 30
C  BACK SUBSTITUTE
150   I=N-1
 160  J=I+1
      S=(0.,0.)
 170  S=S+A(I,J)*Y(J)
      IF(J.EQ.N) GO TO 180
      J=J+1
      GO TO 170
 180  Y(I)=(A(I,N)-S)/A(I,I)
      IF(I.EQ.1) GO TO 200
      I=I-1
      GO TO 160
C  RENORMALIZE EIGENVECTORS SO THAT FIRST MODE  Y(1) =1.00
200   AMP=0.0
      M=(1.,1.)/Y(1)
      DO 210 I=1,N
      Y(I)=M*Y(I)
 210  AMP=AMP+REAL(Y(I))
C
C  PRINT EIGENVECTORS
      WRITE(6,300) MODE,OM1,(Y(I),I=1,N),AMP
 300  FORMAT(* EIGENVECTORS ASSOCIATED WITH MODE*,I3,* AT FREQUENCY *,
     12F10.5,* RADIANS PER SECOND  ARE AS FOLLOWS*/,4(2E15.6/),/
     2*  WITH A TOTAL AMPLITUDE OF *,E15.6)
      RETURN
      END
```

APPENDIX C

ARRAY DATA RUNS

EVENT DESCRIPTION
SHIPS SPEED 2.000 KNOTS
TURN RATE 0 DEGREES/SEC

ARRAY DIAMETER 2.500 INCHES
ARRAY LENGTH 200.000 FEET
CN= 1.2000 CNN= 1.2000 CF= .0027

BUOYANCY PER FOOT OF ARRAY 2.1816 POUNDS PER FOOT
TOTAL BUOYANCY OF ARRAY 436.3194 POUNDS

500 DISTRIBUTED WEIGHT SEGMENTS ARE GENERATED FROM ARRAY DATA
AVERAGE WEIGHT PER FOOT OF ARRAY 2.1161 POUNDS PER FOOT
TOTAL WEIGHT OF ARRAY 423.2182 POUNDS

POSITIVE NET BUOYANCY IS LIGHT ARRAY, NEGATIVE IS HEAVY ARRAY
AVERAGE NET BUOYANCY PER FOOT OF ARRAY .0655 POUNDS PER FOOT (LIGHT)
TOTAL NET BUOYANCY OF ARRAY 13.1012 POUNDS (LIGHT)

COORDINATE ORIGIN AT TOW VEHICLE

SCOPE (FEET)	TENSION (POUNDS)	TRAIL (FEET)	DEPTH (FEET)	SIDE TRAIL (FEET)	TOWLINE ANGLE (DEGREES)	KITE ANGLE (DEGREES)
0	4.998	0	0	0	-6.467	0
.400	4.881	-3.988	-.291	0	-1.458	0
4.000	4.805	-7.967	-.684	0	-6.048	0
8.000	4.715	-11.950	-1.050	0	-6.686	0
12.000	4.603	-15.934	-1.404	0	-4.391	0
16.000	4.512	-19.918	-1.775	0	-5.080	0
20.000	4.407	-23.902	-2.104	0	-2.430	0
24.000	4.320	-27.893	-2.368	0	-2.154	0
28.000	4.231	-31.878	-2.683	0	-3.635	0
32.000	4.141	-35.864	-3.013	0	-3.944	0
36.000	4.051	-39.850	-3.338	0	-4.215	0
40.000	3.962	-43.839	-3.628	0	-4.170	0
44.000	3.874	-47.828	-3.914	0	-4.086	0
48.000	3.779	-51.820	-4.143	0	-.148	0
52.000	3.698	-55.807	-4.399	0	-4.408	0
56.000	3.613	-59.801	-4.609	0	-4.329	0
60.000	3.529	-63.795	-4.809	0	-4.176	0
64.000	3.444	-67.787	-5.053	0	-4.382	0
68.000	3.349	-71.779	-5.288	0	-.623	0
72.000	3.265	-75.773	-5.490	0	-.425	0
76.000	3.177	-79.760	-5.745	0	-2.625	0
80.000	3.092	-83.751	-5.990	0	-2.831	0
84.000	3.006	-87.743	-6.222	0	-2.946	0
88.000	2.921	-91.736	-6.454	0	-3.076	0
92.000	2.837	-95.729	-6.662	0	-2.957	0
96.000	2.753	-99.723	-6.859	0	-2.723	0
100.000	2.669	-103.711	-7.049	0	-5.068	0
104.000	2.583	-107.700	-7.329	0	-5.967	0
108.000	2.481	-111.686	-7.647	0	-1.960	0
112.000	2.395	-115.677	-7.884	0	-2.288	0
116.000	2.309	-119.668	-8.114	0	-2.609	0
120.000	2.216	-123.646	-8.518	0	-6.239	0
124.000	2.129	-127.629	-8.774	0	-8.889	0
128.000	2.000	-131.604	-9.188	0	.174	0
132.000	1.918	-135.598	-9.346	0	.984	0
136.000	1.841	-139.593	-9.479	0	-5.430	0
140.000	1.756	-143.586	-9.655	0	-5.151	0
144.000	1.671	-147.581	-9.783	0	-4.101	0
148.000	1.578	-151.559	-9.881	0	-7.080	0
152.000	1.480	-155.548	-10.124	0	1.143	0
156.000	1.395	-159.539	-10.307	0	1.470	0
160.000	1.310	-163.530	-10.485	0	1.830	0
164.000	1.225	-167.521	-10.662	0	2.143	0
168.000	1.138	-171.509	-10.866	0	1.532	0
172.000	1.030	-175.470	-10.852	0	-9.845	0
176.000	.900	-179.433	-11.307	0	8.138	0
180.000	.810	-183.413	-11.376	0	-9.370	0
184.000	.690	-187.379	-11.756	0	-3.004	0
188.000	.583	-191.348	-11.874	0	-.035	0
192.000	.455	-195.288	-12.098	0	-9.819	0
196.000	.313	-199.814	-12.493	0	-9.771	0
200.000	.300	-199.208	-12.561	0	0	0

EVENT DESCRIPTION
SHIPS SPEED 3.000 KNOTS
TURN RATE 0 DEGREES/SEC

ARRAY DIAMETER 2.500 INCHES
ARRAY LENGTH 200.000 FEET
CN= 1.2000 CNN= 1.2000 CF= .0027

BUOYANCY PER FOOT OF ARRAY 2.1816 POUNDS PER FOOT
TOTAL BUOYANCY OF ARRAY 436.3194 POUNDS

500 DISTRIBUTED WEIGHT SEGMENTS ARE GENERATED FROM ARRAY DATA
AVERAGE WEIGHT PER FOOT OF ARRAY 2.1161 POUNDS PER FOOT
TOTAL WEIGHT OF ARRAY 423.2162 POUNDS

POSITIVE NET BUOYANCY IS LIGHT ARRAY, NEGATIVE IS HEAVY ARRAY
AVERAGE NET BUOYANCY PER FOOT OF ARRAY .0655 POUNDS PER FOOT (LIGHT)
TOTAL NET BUOYANCY OF ARRAY 13.1012 POUNDS (LIGHT)

COORDINATE ORIGIN AT TOW VEHICLE

SCOPE (FEET)	TENSION (POUNDS)	TRAIL (FEET)	DEPTH (FEET)	SIDE TRAIL (FEET)	TOWLINE ANGLE (DEGREES)	KITE ANGLE (DEGREES)
0	10.039	0	0	0	-3.676	0
.400	9.836	-3.996	-.178	0	-1.270	0
4.000	9.660	-7.989	-.409	0	-3.467	0
8.000	9.474	-11.983	-.623	0	-3.757	0
12.000	9.278	-15.978	-.828	0	-2.608	0
16.000	9.089	-19.972	-1.039	0	-2.876	0
20.000	8.895	-23.967	-1.226	0	-1.548	0
24.000	8.711	-27.964	-1.382	0	-1.470	0
28.000	8.527	-31.959	-1.585	0	-2.147	0
32.000	8.341	-35.955	-1.751	0	-2.259	0
36.000	8.156	-39.951	-1.922	0	-2.344	0
40.000	7.971	-43.947	-2.094	0	-2.310	0
44.000	7.786	-47.944	-2.253	0	-2.255	0
48.000	7.597	-51.942	-2.382	0	-.331	0
52.000	7.417	-55.938	-2.526	0	-2.322	0
56.000	7.235	-59.936	-2.640	0	-2.302	0
60.000	7.053	-63.934	-2.751	0	-2.264	0
64.000	6.870	-67.932	-2.886	0	-2.380	0
68.000	6.681	-71.929	-3.017	0	-.529	0
72.000	6.499	-75.927	-3.135	0	-.493	0
76.000	6.315	-79.924	-3.279	0	-1.480	0
80.000	6.132	-83.921	-3.413	0	-1.580	0
84.000	5.950	-87.919	-3.541	0	-1.640	0
88.000	5.767	-91.916	-3.670	0	-1.719	0
92.000	5.584	-95.914	-3.788	0	-1.717	0
96.000	5.402	-99.912	-3.907	0	-1.714	0
100.000	5.220	-103.909	-4.029	0	-2.865	0
104.000	5.037	-107.905	-4.192	0	-3.345	0
108.000	4.844	-111.900	-4.375	0	-1.301	0
112.000	4.661	-115.897	-4.517	0	-1.541	0
116.000	4.477	-119.894	-4.667	0	-1.925	0
120.000	4.289	-123.886	-4.915	0	-3.710	0
124.000	4.106	-127.880	-5.090	0	-5.121	0
128.000	3.899	-131.872	-5.319	0	-.012	0
132.000	3.717	-135.870	-5.406	0	.398	0
136.000	3.540	-139.869	-5.485	0	-2.910	0
140.000	3.357	-143.867	-5.583	0	-2.767	0
144.000	3.174	-147.865	-5.656	0	-2.278	0
148.000	2.989	-151.859	-5.728	0	-3.926	0
152.000	2.799	-155.855	-5.867	0	.415	0
156.000	2.616	-159.853	-5.976	0	.588	0
160.000	2.433	-163.850	-6.084	0	.774	0
164.000	2.250	-167.847	-6.194	0	.904	0
168.000	2.065	-171.843	-6.325	0	.467	0
172.000	1.878	-175.832	-6.322	0	-6.240	0
176.000	1.688	-179.819	-6.592	0	4.066	0
180.000	1.484	-183.813	-6.660	0	-5.627	0
184.000	1.283	-187.802	-6.888	0	-1.068	0
188.000	1.092	-191.792	-6.949	0	.600	0
192.000	.892	-195.775	-7.087	0	-5.909	0
196.000	.695	-199.355	-7.324	0	-4.360	0
200.000	.676	-199.754	-7.355	0	0	0

EVENT DESCRIPTION
SHIPS SPEED 4.000 KNOTS
TURN RATE 0 DEGREES/SEC

ARRAY DIAMETER 2.500 INCHES
ARRAY LENGTH 200.000 FEET
CN= 1.2000 CNN= 1.2000 CF= .0027

BUOYANCY PER FOOT OF ARRAY 2.1816 POUNDS PER FOOT
TOTAL BUOYANCY OF ARRAY 436.3194 POUNDS

500 DISTRIBUTED WEIGHT SEGMENTS ARE GENERATED FROM ARRAY DATA
AVERAGE WEIGHT PER FOOT OF ARRAY 2.1161 POUNDS PER FOOT
TOTAL WEIGHT OF ARRAY 423.2182 POUNDS

POSITIVE NET BUOYANCY IS LIGHT ARRAY, NEGATIVE IS HEAVY ARRAY
AVERAGE NET BUOYANCY PER FOOT OF ARRAY .0655 POUNDS PER FOOT (LIGHT)
TOTAL NET BUOYANCY OF ARRAY 13.1012 POUNDS (LIGHT)

COORDINATE ORIGIN AT TOW VEHICLE

SCOPE (FEET)	TENSION (POUNDS)	TRAIL (FEET)	DEPTH (FEET)	SIDE TRAIL (FEET)	TOWLINE ANGLE (DEGREES)	KITE ANGLE (DEGREES)
0	17.417	0	0	0	-2.282	0
.400	17.082	-3.998	-.114	0	-.919	0
4.000	16.764	-7.996	-.259	0	-2.151	0
8.000	16.440	-11.993	-.393	0	-2.305	0
12.000	16.109	-15.991	-.521	0	-1.637	0
16.000	15.785	-19.989	-.651	0	-1.768	0
20.000	15.456	-23.987	-.766	0	-1.000	0
24.000	15.133	-27.986	-.864	0	-.967	0
28.000	14.811	-31.984	-.977	0	-1.337	0
32.000	14.487	-35.983	-1.090	0	-1.367	0
36.000	14.164	-39.981	-1.200	0	-1.422	0
40.000	13.841	-43.980	-1.298	0	-1.388	0
44.000	13.518	-47.979	-1.394	0	-1.361	0
48.000	13.192	-51.978	-1.474	0	-.260	0
52.000	12.872	-55.976	-1.561	0	-1.377	0
56.000	12.551	-59.976	-1.629	0	-1.373	0
60.000	12.229	-63.975	-1.697	0	-1.361	0
64.000	11.907	-67.974	-1.779	0	-1.431	0
68.000	11.582	-71.973	-1.858	0	-.373	0
72.000	11.260	-75.973	-1.932	0	-.366	0
76.000	10.938	-79.971	-2.019	0	-.907	0
80.000	10.616	-83.970	-2.101	0	-.966	0
84.000	10.294	-87.970	-2.178	0	-1.006	0
88.000	9.973	-91.969	-2.257	0	-1.060	0
92.000	9.651	-95.968	-2.331	0	-1.081	0
96.000	9.329	-99.967	-2.407	0	-1.116	0
100.000	9.008	-103.966	-2.487	0	-1.773	0
104.000	8.686	-107.964	-2.590	0	-2.062	0
108.000	8.358	-111.962	-2.704	0	-.891	0
112.000	8.036	-115.961	-2.797	0	-1.075	0
116.000	7.713	-119.960	-2.900	0	-1.384	0
120.000	7.388	-123.956	-3.081	0	-2.367	0
124.000	7.066	-127.954	-3.180	0	-3.148	0
128.000	6.730	-131.951	-3.318	0	-.044	0
132.000	6.409	-135.950	-3.371	0	.186	0
136.000	6.090	-139.950	-3.420	0	-1.736	0
140.000	5.768	-143.949	-3.481	0	-1.667	0
144.000	5.446	-147.948	-3.529	0	-1.434	0
148.000	5.124	-151.948	-3.581	0	-2.366	0
152.000	4.797	-155.945	-3.667	0	.160	0
156.000	4.476	-159.944	-3.736	0	.252	0
160.000	4.154	-163.943	-3.805	0	.345	0
164.000	3.831	-167.942	-3.877	0	.393	0
168.000	3.508	-171.940	-3.962	0	.137	0
172.000	3.189	-175.937	-3.959	0	-4.242	0
176.000	2.850	-179.931	-4.134	0	2.154	0
180.000	2.528	-183.929	-4.194	0	-3.613	0
184.000	2.196	-187.925	-4.342	0	-.452	0
188.000	1.870	-191.921	-4.388	0	.152	0
192.000	1.541	-195.918	-4.486	0	-3.150	0
196.000	1.234	-199.508	-4.639	0	-2.454	0
200.000	1.201	-199.908	-4.656	0	0	0

EVENT DESCRIPTION
SHIPS SPEED 5.000 KNOTS
TURN RATE 0 DEGREES/SEC

ARRAY DIAMETER 2.500 INCHES
ARRAY LENGTH 200.000 FEET
CN= 1.2000 CNN= 1.2000 CF= .0027

BUOYANCY PER FOOT OF ARRAY 2.1616 POUNDS PER FOOT
TOTAL BUOYANCY OF ARRAY 436.3194 POUNDS

500 DISTRIBUTED WEIGHT SEGMENTS ARE GENERATED FROM ARRAY DATA
AVERAGE WEIGHT PER FOOT OF ARRAY 2.1161 POUNDS PER FOOT
TOTAL WEIGHT OF ARRAY 423.2182 POUNDS

POSITIVE NET BUOYANCY IS LIGHT ARRAY, NEGATIVE IS HEAVY ARRAY
AVERAGE NET BUOYANCY PER FOOT OF ARRAY .0655 POUNDS PER FOOT (LIGHT)
TOTAL NET BUOYANCY OF ARRAY 13.1012 POUNDS (LIGHT)

COORDINATE ORIGIN AT TOW VEHICLE

SCOPE (FEET)	TENSION (POUNDS)	TRAIL (FEET)	DEPTH (FEET)	SIDE TRAIL (FEET)	TOWLINE ANGLE (DEGREES)	KITE ANGLE (DEGREES)
0	27.027	0	0	0	-1.518	0
.400	26.516	-3.999	-.077	0	-.645	0
4.000	26.018	-7.998	-.174	0	-1.429	0
8.000	25.515	-11.997	-.263	0	-1.523	0
12.000	25.008	-15.996	-.348	0	-1.090	0
16.000	24.505	-19.995	-.434	0	-1.169	0
20.000	23.999	-23.994	-.510	0	-.673	0
24.000	23.496	-27.994	-.575	0	-.654	0
28.000	22.995	-31.993	-.650	0	-.887	0
32.000	22.492	-35.992	-.724	0	-.916	0
36.000	21.990	-39.992	-.797	0	-.934	0
40.000	21.487	-43.991	-.861	0	-.917	0
44.000	20.985	-47.991	-.924	0	-.892	0
48.000	20.481	-51.990	-.976	0	-.185	0
52.000	19.981	-55.990	-1.033	0	-.898	0
56.000	19.480	-59.989	-1.078	0	-.896	0
60.000	18.979	-63.989	-1.123	0	-.891	0
64.000	18.477	-67.989	-1.177	0	-.937	0
68.000	17.974	-71.988	-1.229	0	-.258	0
72.000	17.472	-75.988	-1.278	0	-.257	0
76.000	16.971	-79.987	-1.335	0	-.599	0
80.000	16.469	-83.987	-1.389	0	-.638	0
84.000	15.968	-87.987	-1.440	0	-.668	0
88.000	15.466	-91.986	-1.492	0	-.704	0
92.000	14.965	-95.986	-1.541	0	-.723	0
96.000	14.464	-99.986	-1.592	0	-.756	0
100.000	13.963	-103.985	-1.647	0	-1.179	0
104.000	13.461	-107.984	-1.716	0	-1.370	0
108.000	12.956	-111.984	-1.793	0	-.620	0
112.000	12.454	-115.983	-1.856	0	-.755	0
116.000	11.952	-119.982	-1.927	0	-.979	0
120.000	11.448	-123.981	-2.037	0	-1.591	0
124.000	10.947	-127.980	-2.119	0	-2.076	0
128.000	10.436	-131.978	-2.209	0	-.039	0
132.000	9.935	-135.978	-2.244	0	.107	0
136.000	9.436	-139.978	-2.277	0	-1.134	0
140.000	8.934	-143.978	-2.317	0	-1.095	0
144.000	8.433	-147.977	-2.350	0	-.962	0
148.000	7.931	-151.976	-2.387	0	-1.549	0
152.000	7.427	-155.976	-2.444	0	.080	0
156.000	6.925	-159.975	-2.490	0	.136	0
160.000	6.424	-163.975	-2.536	0	.189	0
164.000	5.922	-167.974	-2.585	0	.208	0
168.000	5.420	-171.974	-2.643	0	.031	0
172.000	4.922	-175.972	-2.645	0	-2.961	0
176.000	4.408	-179.970	-2.764	0	1.310	0
180.000	3.908	-183.969	-2.811	0	-2.445	0
184.000	3.399	-187.967	-2.912	0	-.291	0
188.000	2.895	-191.965	-2.950	0	-.094	0
192.000	2.389	-195.963	-3.021	0	-2.063	0
196.000	1.927	-199.559	-3.134	0	-1.571	0
200.000	1.876	-199.959	-3.144	0	0	0

EVENT DESCRIPTION
SHIPS SPEED 10.000 KNOTS
TURN RATE 0 DEGREES/SEC

ARRAY DIAMETER 2.500 INCHES
ARRAY LENGTH 200.000 FEET
CN= 1.2000 CNN= 1.2000 CF= .0027

BUOYANCY PER FOOT OF ARRAY 2.1816 POUNDS PER FOOT
TOTAL BUOYANCY OF ARRAY 436.3194 POUNDS

500 DISTRIBUTED WEIGHT SEGMENTS ARE GENERATED FROM ARRAY DATA
AVERAGE WEIGHT PER FOOT OF ARRAY 2.1161 POUNDS PER FOOT
TOTAL WEIGHT OF ARRAY 423.2182 POUNDS

POSITIVE NET BUOYANCY IS LIGHT ARRAY, NEGATIVE IS HEAVY ARRAY
AVERAGE NET BUOYANCY PER FOOT OF ARRAY .0655 POUNDS PER FOOT (LIGHT)
TOTAL NET BUOYANCY OF ARRAY 13.1012 POUNDS (LIGHT)

COORDINATE ORIGIN AT TOW VEHICLE

SCOPE (FEET)	TENSION (POUNDS)	TRAIL (FEET)	DEPTH (FEET)	SIDE TRAIL (FEET)	TOWLINE ANGLE (DEGREES)	KITE ANGLE (DEGREES)
0	107.614	0	0	0	-.391	0
.400	105.610	-4.000	-.020	0	-.173	0
4.000	103.609	-8.000	-.045	0	-.367	0
8.000	101.607	-12.000	-.068	0	-.390	0
12.000	99.603	-16.000	-.090	0	-.281	0
16.000	97.601	-20.000	-.112	0	-.299	0
20.000	95.598	-24.000	-.131	0	-.174	0
24.000	93.596	-28.000	-.148	0	-.170	0
28.000	91.594	-32.000	-.167	0	-.228	0
32.000	89.592	-35.999	-.186	0	-.234	0
36.000	87.590	-39.999	-.205	0	-.238	0
40.000	85.588	-43.999	-.221	0	-.233	0
44.000	83.586	-47.999	-.237	0	-.227	0
48.000	81.584	-51.999	-.250	0	-.050	0
52.000	79.583	-55.999	-.265	0	-.227	0
56.000	77.581	-59.999	-.276	0	-.227	0
60.000	75.579	-63.999	-.288	0	-.227	0
64.000	73.577	-67.999	-.301	0	-.238	0
68.000	71.575	-71.999	-.315	0	-.068	0
72.000	69.573	-75.999	-.327	0	-.069	0
76.000	67.571	-79.999	-.342	0	-.153	0
80.000	65.570	-83.999	-.356	0	-.163	0
84.000	63.568	-87.999	-.369	0	-.171	0
88.000	61.566	-91.999	-.382	0	-.181	0
92.000	59.564	-95.999	-.395	0	-.187	0
96.000	57.563	-99.999	-.408	0	-.198	0
100.000	55.561	-103.999	-.422	0	-.304	0
104.000	53.559	-107.999	-.440	0	-.353	0
108.000	51.556	-111.999	-.460	0	-.186	0
112.000	49.554	-115.999	-.477	0	-.204	0
116.000	47.552	-119.999	-.496	0	-.265	0
120.000	45.550	-123.998	-.525	0	-.413	0
124.000	43.548	-127.999	-.546	0	-.530	0
128.000	41.544	-131.999	-.569	0	-.012	0
132.000	39.543	-135.999	-.578	0	.024	0
136.000	37.541	-139.999	-.587	0	-.288	0
140.000	35.540	-143.999	-.597	0	-.279	0
144.000	33.538	-147.998	-.606	0	-.250	0
148.000	31.536	-151.998	-.616	0	-.394	0
152.000	29.534	-155.998	-.630	0	.015	0
156.000	27.532	-159.998	-.642	0	.028	0
160.000	25.530	-163.998	-.654	0	.040	0
164.000	23.528	-167.998	-.667	0	.041	0
168.000	21.526	-171.998	-.683	0	-.011	0
172.000	19.526	-175.998	-.685	0	-.798	0
176.000	17.521	-179.998	-.716	0	.310	0
180.000	15.519	-183.998	-.730	0	-.641	0
184.000	13.515	-187.998	-.757	0	-.082	0
188.000	11.513	-191.998	-.769	0	-.084	0
192.000	9.510	-195.998	-.790	0	-.564	0
196.000	7.708	-199.597	-.823	0	-.393	0
200.000	7.506	-199.997	-.826	0	0	0

EVENT DESCRIPTION
SHIPS SPEED 20.000 KNOTS
TURN RATE 0 DEGREES/SEC

ARRAY DIAMETER 2.500 INCHES
ARRAY LENGTH 200.000 FEET
CN= 1.2000 CNN= 1.2000 CF= .0027

BUOYANCY PER FOOT OF ARRAY 2.1818 POUNDS PER FOOT
TOTAL BUOYANCY OF ARRAY 436.3194 POUNDS

500 DISTRIBUTED WEIGHT SEGMENTS ARE GENERATED FROM ARRAY DATA
AVERAGE WEIGHT PER FOOT OF ARRAY 2.1181 POUNDS PER FOOT
TOTAL WEIGHT OF ARRAY 423.2182 POUNDS

POSITIVE NET BUOYANCY IS LIGHT ARRAY, NEGATIVE IS HEAVY ARRAY
AVERAGE NET BUOYANCY PER FOOT OF ARRAY .0655 POUNDS PER FOOT (LIGHT)
TOTAL NET BUOYANCY OF ARRAY 13.1012 POUNDS (LIGHT)

COORDINATE ORIGIN AT TOW VEHICLE

SCOPE (FEET)	TENSION (POUNDS)	TRAIL (FEET)	DEPTH (FEET)	SIDE TRAIL (FEET)	TOWLINE ANGLE (DEGREES)	KITE ANGLE (DEGREES)
0	430.331	0	0	0	-.098	0
.400	422.324	-4.000	-.005	0	-.043	0
4.000	414.318	-8.000	-.011	0	-.092	0
8.000	406.312	-12.000	-.017	0	-.098	0
12.000	398.306	-16.000	-.022	0	-.070	0
16.000	390.299	-20.000	-.028	0	-.075	0
20.000	382.293	-24.000	-.033	0	-.044	0
24.000	374.287	-28.000	-.037	0	-.043	0
28.000	366.281	-32.000	-.042	0	-.057	0
32.000	358.275	-36.000	-.047	0	-.059	0
36.000	350.269	-40.000	-.051	0	-.060	0
40.000	342.262	-44.000	-.055	0	-.058	0
44.000	334.256	-48.000	-.059	0	-.057	0
48.000	326.250	-52.000	-.063	0	-.012	0
52.000	318.244	-56.000	-.066	0	-.057	0
56.000	310.238	-60.000	-.069	0	-.057	0
60.000	302.232	-64.000	-.072	0	-.057	0
64.000	294.226	-68.000	-.075	0	-.060	0
68.000	286.220	-72.000	-.079	0	-.017	0
72.000	278.214	-76.000	-.082	0	-.017	0
76.000	270.208	-80.000	-.086	0	-.038	0
80.000	262.202	-84.000	-.089	0	-.041	0
84.000	254.195	-88.000	-.092	0	-.043	0
88.000	246.189	-92.000	-.096	0	-.045	0
92.000	238.183	-96.000	-.099	0	-.047	0
96.000	230.177	-100.000	-.102	0	-.050	0
100.000	222.171	-104.000	-.106	0	-.076	0
104.000	214.165	-108.000	-.110	0	-.088	0
108.000	206.159	-112.000	-.115	0	-.042	0
112.000	198.153	-116.000	-.119	0	-.051	0
116.000	190.147	-120.000	-.124	0	-.067	0
120.000	182.140	-124.000	-.131	0	-.104	0
124.000	174.134	-128.000	-.137	0	-.133	0
128.000	166.128	-132.000	-.143	0	-.003	0
132.000	158.122	-136.000	-.145	0	.006	0
136.000	150.116	-140.000	-.147	0	-.072	0
140.000	142.110	-144.000	-.150	0	-.070	0
144.000	134.104	-148.000	-.152	0	-.063	0
148.000	126.098	-152.000	-.154	0	-.099	0
152.000	118.091	-156.000	-.158	0	.004	0
156.000	110.085	-160.000	-.161	0	.007	0
160.000	102.079	-164.000	-.164	0	.010	0
164.000	94.073	-168.000	-.167	0	.010	0
168.000	86.067	-172.000	-.171	0	-.003	0
172.000	78.061	-176.000	-.172	0	-.201	0
176.000	70.054	-180.000	-.180	0	.077	0
180.000	62.048	-184.000	-.183	0	-.161	0
184.000	54.042	-188.000	-.190	0	.021	0
188.000	46.036	-192.000	-.193	0	-.022	0
192.000	38.029	-196.000	-.198	0	-.142	0
196.000	30.823	-199.600	-.207	0	-.098	0
200.000	30.022	-200.000	-.207	0	0	0

EVENT DESCRIPTION
SHIPS SPEED 25.000 KNOTS
TURN RATE 0 DEGREES/SEC

ARRAY DIAMETER 2.500 INCHES
ARRAY LENGTH 200.000 FEET
CN= 1.2000 CNN= 1.2000 CF= .0027

BUOYANCY PER FOOT OF ARRAY 2.1816 POUNDS PER FOOT
TOTAL BUOYANCY OF ARRAY 436.3194 POUNDS

500 DISTRIBUTED WEIGHT SEGMENTS ARE GENERATED FROM ARRAY DATA
AVERAGE WEIGHT PER FOOT OF ARRAY 2.1161 POUNDS PER FOOT
TOTAL WEIGHT OF ARRAY 423.2182 POUNDS

POSITIVE NET BUOYANCY IS LIGHT ARRAY, NEGATIVE IS HEAVY ARRAY
AVERAGE NET BUOYANCY PER FOOT OF ARRAY .0655 POUNDS PER FOOT (LIGHT)
TOTAL NET BUOYANCY OF ARRAY 13.1012 POUNDS (LIGHT)

COORDINATE ORIGIN AT TOW VEHICLE

SCOPE (FEET)	TENSION (POUNDS)	TRAIL (FEET)	DEPTH (FEET)	SIDE TRAIL (FEET)	TOWLINE ANGLE (DEGREES)	KITE ANGLE (DEGREES)
0	672.384	0	0	0	-.063	0
.400	659.874	-4.000	-.003	0	-.028	0
4.000	647.365	-8.000	-.007	0	-.059	0
8.000	634.855	-12.000	-.011	0	-.063	0
12.000	622.346	-16.000	-.014	0	-.045	0
16.000	609.836	-20.000	-.018	0	-.048	0
20.000	597.327	-24.000	-.021	0	-.028	0
24.000	584.817	-28.000	-.024	0	-.027	0
28.000	572.308	-32.000	-.027	0	-.036	0
32.000	559.798	-36.000	-.030	0	-.037	0
36.000	547.289	-40.000	-.033	0	-.038	0
40.000	534.779	-44.000	-.035	0	-.037	0
44.000	522.270	-48.000	-.038	0	-.036	0
48.000	509.760	-52.000	-.040	0	-.008	0
52.000	497.251	-56.000	-.042	0	-.036	0
56.000	484.742	-60.000	-.044	0	-.036	0
60.000	472.232	-64.000	-.046	0	-.036	0
64.000	459.723	-68.000	-.048	0	-.038	0
68.000	447.213	-72.000	-.050	0	-.011	0
72.000	434.704	-76.000	-.052	0	-.011	0
76.000	422.195	-80.000	-.055	0	-.025	0
80.000	409.685	-84.000	-.057	0	-.026	0
84.000	397.176	-88.000	-.059	0	-.027	0
88.000	384.666	-92.000	-.061	0	-.029	0
92.000	372.157	-96.000	-.063	0	-.030	0
96.000	359.648	-100.000	-.065	0	-.032	0
100.000	347.138	-104.000	-.068	0	-.049	0
104.000	334.629	-108.000	-.071	0	-.057	0
108.000	322.119	-112.000	-.074	0	-.027	0
112.000	309.610	-116.000	-.076	0	-.033	0
116.000	297.100	-120.000	-.080	0	-.043	0
120.000	284.591	-124.000	-.084	0	-.066	0
124.000	272.081	-128.000	-.088	0	-.085	0
128.000	259.572	-132.000	-.091	0	-.002	0
132.000	247.062	-136.000	-.093	0	.004	0
136.000	234.553	-140.000	-.094	0	-.046	0
140.000	222.043	-144.000	-.096	0	-.045	0
144.000	209.534	-148.000	-.097	0	-.040	0
148.000	197.025	-152.000	-.099	0	-.063	0
152.000	184.515	-156.000	-.101	0	.002	0
156.000	172.006	-160.000	-.103	0	.004	0
160.000	159.496	-164.000	-.105	0	.006	0
164.000	146.987	-168.000	-.107	0	.006	0
168.000	134.477	-172.000	-.109	0	-.002	0
172.000	121.968	-176.000	-.110	0	-.128	0
176.000	109.458	-180.000	-.115	0	.049	0
180.000	96.949	-184.000	-.117	0	-.103	0
184.000	84.439	-188.000	-.121	0	-.013	0
188.000	71.930	-192.000	-.123	0	-.014	0
192.000	59.420	-196.000	-.127	0	-.091	0
196.000	48.161	-199.600	-.132	0	-.063	0
200.000	46.910	-200.000	-.133	0	0	0